The Fire Performance of Post-Tensioned Timber Buildings

By

Reuben Shaun Costello

Supervised by Professor Andrew Buchanan

Supervisory Committee:

Dr Anthony K. Abu

Professor Peter Moss

A thesis submitted in partial fulfilment of the requirements for the degree of

Master of Engineering in Fire Engineering

Department of Civil and Natural Resources Engineering

University of Canterbury

Private Bag 4800

Christchurch, New Zealand

December 2013

Abstract

Post-tensioned timber buildings utilise a new construction technique developed largely as part of research undertaken at the University of Canterbury. Timber buildings are constructed using an engineered timber product, such as laminated veneer lumber (LVL), and then stressed with post-tensioned unbonded high-strength steel tendons. The tendons apply a compressive stress to timber members to create a ductile moment resisting connection between adjacent timber members. The major benefit of post-tensioned timber buildings is a significantly improved structural performance.

As timber is a combustible material there is a perceived high fire risk in timber buildings. While timber buildings can be designed to perform very well in fire, a design guide for the fire safety design of post-tensioned timber buildings has not been previously developed. Furthermore, previous research has found that post-tensioned timber box beams may be susceptible to shear failure in fire conditions.

This research investigated the fire performance of post-tensioned timber buildings. A design strategy for the fire performance of post-tensioned timber buildings was developed in conjunction with a simplified calculation method for determining the fire resistance of post-tensioned timber structural members. The fire performance and failure behaviour of post-tensioned timber box beam was also specifically investigated, with special focus given to the shear performance of box beams. A full scale furnace test of a LVL post-tensioned LVL box beam was conducted at the Building Research Association of New Zealand (BRANZ). Four further full scale tests of LVL box beams were conducted at ambient temperature at the University of Canterbury structural laboratory.

Through this research two distinct strategies for the fire design of post-tensioned timber structures were developed. The first strategy is to rely on the residual timber of the members only. The second strategy considers specific fire protection of the post-tensioning system, which can then be used to contribute to the fire resistance of the member. The results of the full scale tests showed good agreement with the proposed the simplified calculation method. It was also determined that shear failure does not need to be specifically considered other than performing strength checks as for other design actions.

Acknowledgements

Firstly, I would like to thank my supervisors, Professor Andy Buchanan, Dr Tony Abu and Professor Peter Moss, for the support and guidance they provided throughout my research. Their expertise and approachability made this project enjoyable as well as a valuable learning experience. Also, thank you to the other members of the Fire Engineering academic staff for their challenging lecturers during the MEFE programme.

I would also like to thank the Structural Timber Innovation Company for funding this research project and providing me with direct financial support during my MEFE course. Furthermore, the support the NZFS Commission provides to the Fire Engineering programme is greatly appreciated.

Thank you to my fellow Fire Engineering students, especially James O'Neill, for their support and friendship during the course. The camaraderie between the students helped me immensely enjoy my time back at UC.

A special thank you must go to Grant Dunlop. Without his practical knowledge and willingness to get things done my testing would simply not have happened. The attitude Grant brings to a research project contributes significantly to its success.

I was fortunate enough to be able to call upon the knowledge of a number of practicing engineers who have designed Pres-Lam buildings, for which I thank them. Learning from their design experience was invaluable and directly contributed to sections of this thesis. These engineers, the companies they worked for and the buildings they contributed to the design of are:

- Paul Martini, Aurecon – NMIT
- Darin Millar, Holmes Fire – EXPAN
- Stanley Chung, Opus – Carterton Events Centre
- Michael Huynh, Holmes Fire – CoCA
- Andrew Chapman, Kirk Roberts – Merritt
- Andrew Brown, Opus – Trimble
- Chris Watson, Ruamoko Solutions – St Elmo Courts

I would also like to thank my family for the endless encouragement they have provided throughout my studies. This is especially true for my parents Peter and Deirdri who I know will always be there for me.

Finally, I cannot express my gratitude enough to my partner Katelyn for her support and company during what has been a rather busy time.

Table of Contents

List of Figures

List of Tables

Nomenclature

A	Cross sectional area (mm^2)
A_s	Shear area (mm^2)
c	Char depth (mm)
d	Depth (mm)
d_{test}	k_{24} test depth (mm)
D	Depth of beam (mm)
e	Eccentricity (mm)
E	Elastic modulus (GPa)
E_d	Design action effect
f_b	Characteristic bending stress (MPa)
f_c	Characteristic compression stress (MPa)
f_s	Characteristic shear stress (MPa)
G	Shear modulus (MPa)
G	Permanent actions (kPa)
I	Second moment of area (mm^4)
I_{cc}	Local second moment of area (mm^4)
k_1	Duration of load factor
k_4	Parallel support factor
k_5	Grid system factor
k_8	Stability factor
k_{24}	Size factor
l	Lateral action (kPa)
L	Span of beam (m)
M^*	Design bending moment (kNm)
M_q	Bending moment demand at midspan (kNm)

M_{PT}	Bending moment due to post-tensioning (kNm)
M_n	Bending capacity (kNm)
N^*	Design axial force (kN)
N_n	Axial capacity (kNm)
F_{PT}	Post-tensioning force (kN)
q	Applied loads (kPa)
Q	First moment of area (mm^3)
Q	Imposed actions (kPa)
R_d	Design capacity
t	Thickness (mm)
T	Time (min)
V^*	Design shear force (kN)
V_n	Shear capacity (kNm)
$V^*_{inclined}$	Shear demand in inclined region (kN)
w	Uniformly distributed load (kN/m)
w	Width (mm)
W	Width of section (mm)
W_{trib}	Tributary width (m)
$\bar{y}$	Neutral axis depth (mm)
Z	Section modulus (mm^3)

Greek

β	Char rate (mm/min)
γ	Zero strength layer (mm)
δ	Deflection (mm)
Δ	Change in
$\sigma_{f,c}$	Compressive stress at centroid of top flange (MPa)

$\sigma_{f,t}$	Tensile stress at centroid of bottom flange (MPa)
$\sigma_{f,c,max}$	Compressive bending stress at extreme fibre of top flange (MPa)
$\sigma_{f,t,max}$	Tensile bending stress at extreme fibre of bottom flange (MPa)
ψ_l	Long-term load factor
φ	Strength reduction factor

Subscripts

c	Compression
f	Flange of beam
f, bot	Bottom flange of beam
f, top	Top flange of beam
i	Time step i
$inclined$	Inclined region of tendon
n	Nominal strength
PT	Post-tensioning
q	Uniformly distributed load
t	Tension
V	Shear
w	Web of beam
x	Individual section of beam
0	Initial conditions

1 Introduction

1.1 Background

Timber is an organic material that has been widely used as a construction material throughout human history. This is largely due to its high stiffness and strength-to-weight ratio and the relative simplicity with which it can be used (SP Technical Research Institute of Sweden, 2010). Timber is also widely regarded as a sustainable material, especially when compared to other construction materials such as steel and concrete. These factors have led to an increased use of timber in recent years.

There are vast plantations of Radiata Pine in New Zealand that are sustainably managed to produce timber for use as a construction material. As well as exporting large volumes of unprocessed logs timber is widely used within New Zealand in light timber framing and heavy timber structures. The heavy timber structures are often constructed using engineered timber products, such as glued laminated timber (glulam), laminated veneer lumber (LVL) and cross-laminated timber (CLT) (Buchanan, 2007).

Timber is a combustible material and has been used as a fuel source since the dawn of human civilization. This has led to a wide held belief by the general public that timber is not a safe building material to use in many buildings, although it is extensively accepted for use in residential housing. This has led to the use of timber as a building material being heavily restricted by many standards and building regulations throughout the world (O'Neill, 2008). Despite these restrictions timber structures can be designed to perform very well in fires (Spearpoint, 2008). This is discussed further in Chapter 2.

A significant field of research relating to timber structures involves a new construction technique which utilises post-tensioned timber members. Buildings utilising post-tensioned timber members are often referred to as Pres-Lam buildings. As this is a very new construction technique little research has been conducted into the fire performance of post-tensioned timber structures. The starting point of this project was the research conducted by Spellman et al. (2012). This research aimed to further the limited knowledge of the fire performance of post-tensioned timber buildings and encourage the use of timber as a construction material.

1.2 STIC

The Structural Innovation Timber Company (STIC) is a New Zealand registered company that developed and commercialised new technologies between 2008 and 2013 with the aim of increasing the use of structural timber in the building and construction market. The seven shareholders of STIC were Carter Holt Harvey Ltd, Nelson Pine Industries Ltd, Wesbeam Pty Ltd, Building Research Association New Zealand Inc, NZ Pine Manufacturers Association, Auckland Uniservices Ltd (University of Auckland) and University of Canterbury. Forest and Wood Products Australia and Foundation for Research Science and Technology also provided substantial financial backing of STIC.

The research and development programme supported by STIC were carried out in three parallel research areas under the supervision of Chief Executive Dr Robert Finch and Research Director Professor Andy Buchanan (STIC, 2009).

The three research areas are:

1. Single storey timber roofs and portal frames, conducted at the University of Auckland under the management of Professor Pierre Quenneville.
2. Timber floors for multi-storey timber buildings, conducted at University of Technology, Sydney under the management of Professor Keith Crews.
3. Timber frames for multi-storey timber buildings, conducted at the University of Canterbury under the management of Associate Professor Stefano Pampanin.

The research conducted for this thesis was part of the third research area, i.e. timber frames for multi-storey timber buildings. Significant financial support was received from STIC for the purpose of carrying out this research.

1.3 Objectives

The objectives of this research were:

1. To develop a design strategy for the fire performance of post-tensioned timber buildings.
2. To develop a simplified calculation method for the fire resistance of post-tensioned timber box beams.
3. To investigate the fire performance and failure behaviour of post-tensioned timber box beams.

1.4 Methodology

A fire safety strategy for post-tensioned timber buildings was developed using existing knowledge of fire performance of timber structures and by examining post-tensioned timber structures that have already been built. A spreadsheet model based on fundamental structural mechanics was then generated to predict the behaviour of LVL box beams with and without post-tensioning. A proposed simplified calculation method was developed based on the spreadsheet model. The fire safety strategy and simplified calculation method were then combined to produce the fire sections of a design guide for post-tensioned timber structures (STIC, 2013). The fire performance and failure behaviour of post-tensioned timber box beams was investigated by testing full scale timber box beams in both ambient conditions and in a furnace. The behaviour of the beams was predicted using the spreadsheet model. The results obtained and observations made were used to refine the design guide.

1.5 Outline of Thesis

Chapter 1 of this thesis gives an introduction to the research that has been conducted and outlines the objectives and methodology used in the research project. Fire safety in timber buildings, including New Zealand Building Code requirements and the fire performance of timber, is discussed in Chapter 2. Post-tensioned timber structures are examined in Chapter 3. The types of post-tensioned timber structures, the fire performance of these structures and an examination of post-tensioned timber buildings that have already been built are incorporated in this Chapter. Also included in Chapter 3 are two proposed design strategies for the design for fire resistance of post-tensioned timber structures. The simplified calculation method used to determine the fire resistance of post-tensioned timber structures is detailed in Chapter 4. Chapter 5 details the experimental furnace test of an LVL box beam and Chapter 6 details the experimental testing of LVL box beams conducted at ambient temperatures. A discussion of key points of the thesis is provided in Chapter 7. Conclusions and recommendations for future research can be found in Chapter 8.

2 Fire Safety in Timber Buildings

This Chapter provides an overview of background information and design considerations that are used in the fire safety design of timber buildings. Section 2.1 provides an overview of fire safety design with a special focus on the New Zealand Building Code requirements and Fire Resistance Ratings. Key aspects of fire safety design that are especially relevant to timber buildings, including construction fire safety and early fire hazard, are discussed in Section 2.2. The fire performance of timber is reviewed in Section 2.3 and includes brief discussions on hazards that are especially relevant for timber buildings.

2.1 Fire Safety Design

2.1.1 New Zealand Building Code Requirements

All new buildings in New Zealand must comply with the current New Zealand Building Code (NZBC), which sets out performance standards for new buildings. The NZBC is divided into two preliminary clauses and 35 technical clauses that each deal with separate building characteristics such as durability, structural stability and access. Clause C: Protection from Fire details how a building must perform for fire safety.

The NZBC is a "performance-based code" so concentrates on the required performance of buildings, rather than specifying materials or construction techniques. This is achieved by designating mandatory objectives, functional requirements and performance criteria for each clause that new buildings must meet.

There are three objectives given in Clause C: Protection from Fire (Department of Building and Housing, 2012b). The objectives are to:

a) safeguard people from an unacceptable risk of injury or illness caused by fire,
b) protect other property from damage caused by fire, and
c) facilitate firefighting and rescue operations.

All three of these objectives must be met in order for compliance with Clause C: Protection from Fire to be achieved. These objectives can be met using either a Compliance Document or an Alternative Solution. Alternative Solutions are used where compliance with the NZBC cannot be demonstrated with a Compliance Document, which includes both Acceptable Solutions, C/AS1 – C/AS6 and a Verification Method, C/VM2. Compliance with the NZBC for fire safety will be demonstrated, i.e. compliance with Clause C is achieved, if the objectives outlined above are met.

2.1.2 Design Parameters for Fire Safety

Specific fire safety designs must consider and incorporate a wide range of parameters in order to comply with the NZBC. Spearpoint (2008) suggests that the following parameters should be included in the fire safety design of a new building:

- Building characteristics
- Occupant characteristics
- Prevention of ignition
- Control of fire growth and smoke spread
- Limit fire spread within the building
- Prevent fire spread to other buildings
- Allow rapid egress of occupants
- Facilitate fire service operations
- Prevent structural collapse
- Minimise damage to building and its contents

2.1.3 Fire Resistance Ratings

A key element of demonstrating compliance with the NZBC is demonstrating that building elements are able to achieve an appropriate Fire Resistance Rating (FRR). FRR is the minimum fire resistance of a building element when "*determined in the standard test for fire resistance, or in accordance with a specific calculation method verified by experimental data from standard fire resistance tests"* (Department of Building and Housing, 2012a). The ISO 834 fire resistance test (ISO, 1975) is used as the standard test for fire resistance as it allows the fire resistance of construction elements to be easily compared. The only facility in New Zealand able to complete full scale tests in accordance with ISO 834 is located at the Building Research Association of New Zealand (BRANZ), and is shown in Figure 2.1.

Figure 2.1 Professor Andy Buchanan at the BRANZ ISO 834 test facility

There are three criteria that comprise an FRR; Structural Adequacy, Integrity and Insulation. Structural Adequacy corresponds to the time that an element can continue to resist its applied actions. Integrity is the time that a fire separation can prevent the passage of flame or hot gases. Insulation is the time that an element can control heat transfer through the element so that the temperature on the side not exposed to fire is within defined limits. All times are given in minutes.

Not all building elements need to achieve all three criteria. However, all three criteria are always presented in the specific order of Structural Adequacy, Integrity then Insulation. The relevant failure criteria for a range of building elements are detailed in Table 2.1. For example, a partition requiring a 30 minute FRR for integrity and insulation but not requiring a structural adequacy rating would be shown as –/30/30.

Table 2.1 Failure criteria for building elements (Buchanan, 2001)

Element	Structural Adequacy	Integrity	Insulation
Partition		X	X
Door		X	X
Load-bearing wall	X	X	X
Floor/ceiling	X	X	X
Beam	X		
Column	X		
Fire-resistant glazing		X	

The magnitude of the FRR is based largely on the objective of the fire safety design, which is not necessarily the objective required by the NZBC as the building owner or insurer may require a higher FRR. Buchanan (2001) outlines four possible criteria that are considered when determining an appropriate FRR:

1. Time for occupants to escape from building
2. Time for fire-fighters to carry out rescue activities
3. Time for fire-fighters to surround and contain the fire
4. The duration of a burnout of the fire compartment with no intervention

The Acceptable Solutions in the NZBC states two requirements for the FRR to apply to building elements; Life Rating and Property Rating. The Life Rating is based on the time required for occupants to move to a safe place whereas the Property Rating is based on the protection of other property. The magnitude of the ratings depends on the use of the building being considered, e.g. higher rating are required for buildings being used for crowd activities or high level storage and lower ratings are required for buildings design for offices and low level storage. Through the Life Rating, the first criteria stated by Buchanan is explicitly considered in the NZBC Acceptable Solutions. Each of the other three criteria are implicitly considered.

All four of the criteria suggested by Buchanan are explicitly considered by the NZBC in the Verification Method, C/VM2. This is achieved by giving a method for calculating the FRR for the full burnout of a firecell, which takes into account the dimensions of the firecell, Fire Load Energy Density (FLED), ventilation area and construction materials. By considering the full burnout of a firecell the occupant's safety and fire-fighter operations are taken into account in the fire safety design of a building.

Design for full burnout of a firecell in a timber building is not explicitly considered in the NZBC but may be an important design issue due to the combustibility of timber. However, this author believes that the potential risk of the primary structural elements of a timber building catastrophically failing during full burnout can be effectively mitigated. This can be achieved through the design of timber members that are large enough to resist full burnout, with passive protection if required, or most effectively, through the installation of an automatic fire sprinkler system. Further details on automatic fire sprinkler systems are presented in Section 2.1.4.

2.1.4 Automatic Fire Sprinklers

An automatic fire sprinkler system is the most reliable general fire protection system available (Spearpoint, 2008) and are widely used in buildings. These systems work by pre-wetting fuel surrounding a fire so that the spread and growth of the fire is limited. This reduces the products of fire, i.e. smoke and heat, and also prevents additional materials being consumed by the fire, thus limiting the damage caused. While most automatic fire sprinkler systems are designed only to limit spread and growth of a fire, with extinguishment to be completed by firefighters, in reality many systems exceed the design and extinguish the fire, thus further limiting damage caused by the fire.

The major benefit of automatic fire sprinkler systems in the fire safety design of a building is that the NZBC allows the required FRR for building elements to be reduced by 50% when an automatic fire sprinkler system is installed. Furthermore, the maximum FRR for a sprinklered firecell is 240/240/240 under the NZBC. It is difficult to quantitatively justify a partial reduction in the FRR as an automatic fire sprinkler system is likely to either control a fire totally or fail so will not reduce fire severity at all. Two arguments to justify this reduction are described by Buchanan (2001).

2.1.5 Fire Design for Structural Adequacy

Prevention of structural collapse during fire is quantified through the structural adequacy criteria of FRR. In order to determine whether a member is able to carry its applied loads within deflection limits for the required time, hence meet the structural adequacy criteria, the applied loads need to be defined. There are two types of loads that need to be considered. These are:

- Gravity actions, e.g. self-weight and snow, and;
- Lateral actions, e.g. wind and earthquake.

The gravity actions are given in AS/NZS 1170.1:2002 (Standards New Zealand, 2002b), which is represented in Equation 2.1. A long-term load factor, ψ_l, is included to reduce the magnitude of the imposed action so that it represents the quasi-permanent value of the imposed action, rather than the full design value. A value of $\psi_l = 0.4$ is used for the long-term load factor for all floors except when used for storage, when $\psi_l = 0.6$ is used.

$$q = G + \psi_l Q \qquad 2.1$$

Where: q = Applied loads (kPa)
G = Permanent actions (kPa)
ψ_l = Long-term load factor
Q = Imposed actions (kPa)

In addition to the gravity actions, Section 2.2.3 of B1/VM1, the Compliance Document for NZBC Clause B1: Structure (Department of Building and Housing, 2011) requires that the structure can be designed to resist a lateral force during a fire. This lateral action, which is calculated as the maximum of a nominal 0.5 kPa face load and 2.5% of the vertical load, as shown in Equation 2.2, is included to ensure that a structure exposed to fire will not collapse in a "normal" wind during a fire or prior to repair or demolition.

$$l = \max\{0.5\ kPa, 0.025(G + \psi_l Q)\} \qquad 2.2$$

Where: l = Lateral action (kPa)
G = Permanent actions (kPa)
ψ_l = Long-term load factor
Q = Imposed actions (kPa)

2.2 Fire Safety Design of Timber Buildings

As outlined in Section 1.1, timber is a combustible material hence it may be perceived to be an unsafe building material due to fire safety concerns. The combustibility of timber is demonstrated in Figure 2.2, which shows an LVL box beam burning following the completion of a full scale ISO 834 furnace test. The combustibility of timber must be addressed during the fire safety design of timber buildings to ensure that they are designed to perform well in fires and meet the NZBC requirements.

Figure 2.2 LVL box beam burning (Spellman, 2012)

Timber buildings can be designed to perform as well as or better than buildings constructed from other materials, i.e. steel or concrete. The fire safety design process for timber buildings is very similar to that for buildings constructed from steel or concrete. The design parameters outlined in Section 2.1.2, such as occupant density, egress routes, fire and smoke spread and fire service operations, must be considered for all buildings.

In addition to the standard design parameters there are three key fire safety design considerations that are especially relevant for timber buildings and require explicit detailing. These key elements are construction fire safety, early fire hazard and structural adequacy.

2.2.1 Construction Fire Safety

Construction site fire safety is very important. Many fires have occurred on timber building construction sites in countries such as Canada, USA and UK, bringing multi-storey timber buildings into disrepute. However, this is a particular problem for light timber frame buildings which are much more susceptible than the heavy timber construction used in post-tensioned timber buildings.

STIC (2012a) has provided simple guidelines for improving the safety on construction sites. These recommendations include provision of active systems for detection, alarm and fire suppression, and early installation of passive protection systems such as gypsum board lining materials. Tight security is also recommended on construction sites because many construction fires are deliberate arson attacks.

2.2.2 Early Fire Hazard

Fire safety in the initial stages of a fire depends on the early fire hazard. As timber is a combustible material its use as a surface lining creates a significant risk for rapid fire growth and thus poses a serious hazard to life safety in the early stages of fire development. The NZBC restricts the area of exposed combustible surfaces in buildings, especially in regions used for sleeping occupancies, crowd assembly or routes used for egress as occupants are unlikely to have completed egress before significant fire development has occurred.

The surface finish requirements under the NZBC may present a problem to the fire safety design of timber buildings. However, additional protection methods can be used to mitigate the hazard of rapid fire development on timber or other combustible surfaces. Gypsum plasterboard and fire resistant coatings can be used to improve the fire performance of timber surface finishes. Also, buildings where automatic fire sprinkler systems are installed are subject to less onerous surface finishes requirements. The sprinkler system may provide sufficient protection so that the use of some exposed timber products is allowed.

Under the NZBC structural timber elements, including columns, beams, portals and shear walls no more than 3.0 m wide, are exempt from surface finish requirements. This exemption is based on the relatively small surface area of these structural elements, which mitigates the risk of fire rapidly propagating across the room of origin and creating a significant hazard early in the fire development.

Further guidance on the NZBC provisions for surface finishes and early fire spread in timber buildings is provided by STIC (2012b).

2.2.3 Structural Adequacy

The structural adequacy of buildings which use timber structural members must be carefully considered during the fire safety design as the members will char when exposed to fire, thus reducing their cross section so reducing the load carrying capacity of the member. The fire performance of timber is discussed in more detail in Section 2.3.

A simple process is followed to determine the structural adequacy of timber structures in fire conditions. The steps undertaken during this process are detailed below.

1. Determine the duration of the fire that the structure must resist, i.e. the FRR.
2. Calculate the char depth that will occur at the required FRR, inclusive of zero strength layer.
3. Calculate the residual cross section of the member by subtracting the char depth from the full cross section of the member that is exposed to fire.
4. Calculate the strength of the residual member.
5. Calculate the loading demand acting on the member for fire conditions.
6. Compare the strength of the residual member and the loading demand acting on the member for fire conditions.

If the strength is greater than or equal to the loading demand the member meets structural adequacy requirements. If not, the member does not meet structural adequacy requirements and a stronger section needs to be designed.

There are three approaches that can be used when designing a building for structural adequacy. These are:

1. Tabulated data method
2. 'Simple' calculation method
3. Advanced calculation method

The tabulated data method is the least sophisticated and correspondingly is the simplest to use. It can be easily adopted with little specialist knowledge. The advanced calculation method is the most complex and requires significant specialist knowledge and facilities, i.e. computer modelling software. The 'simple' calculation method fits in between the other two methods in terms of both complexity and knowledge required for use. The calculation method proposed in Chapter 4 is a 'simple' calculation method that can be used with only a moderate knowledge base.

2.3 Fire Performance of Timber

The fire performance of timber depends heavily on the size of the member. Light timber frames, which generally consist of 45 mm wide and 75 mm to 150 mm deep members, do not perform well when exposed to fire whereas heavy timber, which uses larger sections for beams, columns and other primary structural elements, has very good inherent fire resistance (Buchanan, 2007).

2.3.1 Light Timber Frames

The poor fire performance of light timber frames is caused by the high relative surface area of the members. Despite this, structures constructed using light timber framing can still perform well in fire if the timber members are sufficiently protected from exposure. This is most easily and commonly achieved using protective linings, such as gypsum plasterboard or calcium silicate board (Buchanan, 2001). The protective lining prevents the light timber frame from being exposed to fire and the fire resistance of the building is provided by the protective linings themselves. Light timber frame systems can be designed to achieve an FRR of up to 240 minutes (Winstone Wallboards, 2013).

2.3.2 Heavy Timber Construction

The good inherent fire resistance of heavy timber structures is largely due to the insulating char layer that forms. When exposed to a large enough heat source the temperature of timber will increase until approximately 300°C, at which point the timber will ignite and a char layer forms (Buchanan, 2001). This char layer, the front of which is approximated as a 300°C temperature isotherm, insulates the timber not exposed to fire.

The thermal penetration depth, which is the distance from the char layer to timber at ambient temperature, can conservatively assumed to be 35 mm for radiata pine (Janssens and White, 1994). This is demonstrated in Figure 2.3. However, the size of the thermal penetration depth may be as small as 25 mm (Lache, 1992) or as large as 50 mm (Mikkola, 1990). The properties of the timber, e.g. bending strength, modulus of elasticity etc., below the thermal penetration depth are unchanged and can continue to resist applied loads.

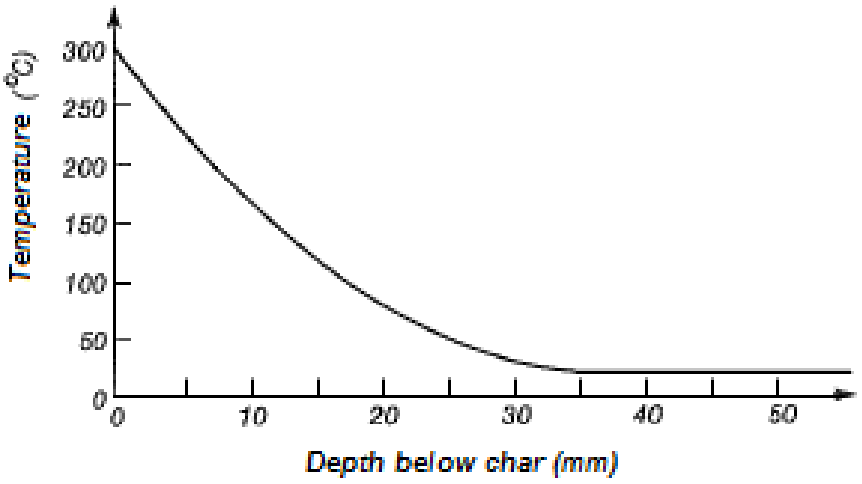

Figure 2.3 Temperature profile below the char layer (Buchanan, 2007)

If there is sufficient heat and oxygen to support combustion, the timber will burn resulting in loss of cross-section, i.e. the timber will "char away", until there is no unburned timber remaining. The rate at which this process occurs, known as the char rate, is slow and predictable and as such it takes a long time for the loss of cross-section to occur. This means that heavy timber members can continue to resist applied loads for a long time during a fire and hence heavy timber structures provide good inherent resistance without additional protection systems.

2.3.3 Char Rate of Heavy Timber

There have been many studies to investigate the charring behaviour of timber. Lane (2005) concluded that a char rate of 0.72 mm/min to calculate a reduced cross section, which allows for corner rounding and a heat-affected zone, is appropriate for radiata pine. Spellman (2012) suggested an additional zero strength layer of 7.0 mm, adopted from EN 1995-1-2:2004 (European Commission, 2004b), should also be included in addition to a char rate of 0.72 mm/min. Tsai (2010) measured an average charring rate of between 0.72 mm/min and 0.78 mm/min for a range of LVL radiata pine specimens. Frangi and Fontana (2003) measured a mean charring rate of 0.69 mm/min for a range of spruce specimens. However, they also state that an increased charring rate should be used for residual section sizes of less than 40 mm. NZ3603:1993 (Standards New Zealand) uses a char rate of 0.65 mm/min for radiata pine and all other species of a similar density. In addition to the one-dimensional char rate corner rounding must also be explicitly considered by assuming that radius of arris rounding is equal to the calculated char depth. EN 1995-1-2:2004 (European Commission, 2004b) uses either a one-dimensional char rate of 0.65 mm/min or a notional charring rate of 0.70 mm/min for LVL. A 7.0 mm zero strength layer is also included for both char rates.

The notional char rate implicitly includes corner rounding whereas this must be calculated separately if a one-dimensional char rate is used. Furthermore, possible fissures are also considered in the notional char rate. The difference between the two char rates is demonstrated in Figure 2.4 where $d_{\mathrm{char,n}}$ and $d_{\mathrm{char,0}}$ represent the notional and one-dimensional char depths, respectively.

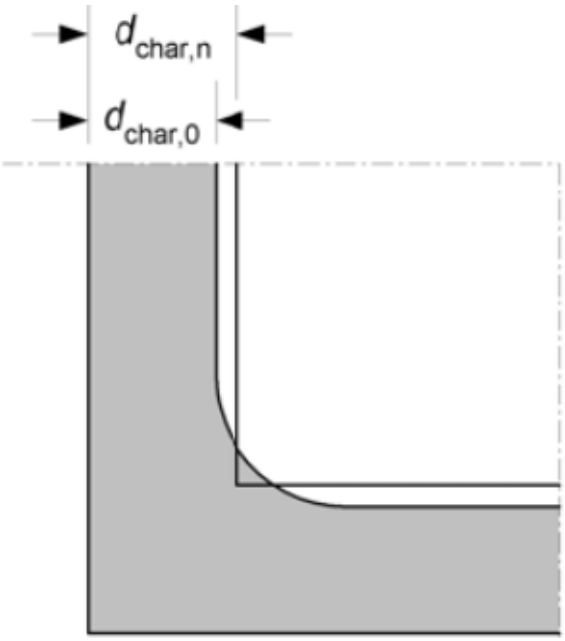

Figure 2.4 One-dimensional and notional char rate of timber (European Commission, 2004b)

The calculations made in this research project were based on the EN 1995-1-2:2004 notional char rate of 0.70 mm/min plus a 7.0 mm zero strength layer.

3 Post-Tensioned Timber Structures

This Chapter outlines the newly developed construction technique of post-tensioned timber with special focus on the fire performance of buildings constructed using this technique. An overview of post-tensioned timber buildings is presented in Section 3.1. The fire performance of these buildings is discussed in Section 3.2, which includes an overview of previous research conducted on the fire performance of post-tensioned timber buildings. Section 3.3 proposes two alternate design strategies for the fire safety design of post-tensioned timber buildings. Section 3.4 addresses additional issues that must be considered during the fire safety design process. Finally, in Section 3.5 the post-tensioned timber buildings that have been designed and built in New Zealand are described and the fire design of each structure is reviewed.

3.1 Post-Tensioned Timber Buildings

Post-tensioned timber buildings utilise a new construction technique developed largely as part of research undertaken at the University of Canterbury (Palermo et al., 2005, Newcombe, 2007, Buchanan et al., 2011). While this system was originally developed for use in concrete structures (Priestley et al., 1999) it has also been adopted for use in timber structures.

Post-tensioned timber buildings incorporate unbonded high-strength steel tendons that are stressed after construction of the individual timber members. The post-tensioned tendons, which are unbonded along the length of the member, apply a compressive stress to the timber member and create a ductile moment resisting connection between adjacent timber members, e.g. at a beam-column joint. Beams, columns and walls are all able to be post-tensioned so many of these ductile moment resisting connections can be easily incorporated throughout the building.

LVL, an engineered timber product, is the most commonly used material in post-tensioned timber buildings in New Zealand and Australia. This is largely based on the higher and more reliable strength of LVL compared to sawn timber and glue laminated timber (STIC, 2013). LVL is described in more detail in Section 5.3. CLT can also be used in post-tensioned timber buildings.

A representation of a single storey of a post-tensioned timber moment resisting frame with a straight tendon, creating four moment-resisting connections, is shown in Figure 3.1. Figure 3.2 shows a full scale test of a two bay post-tensioned timber moment resisting frame tested at the University of Canterbury.

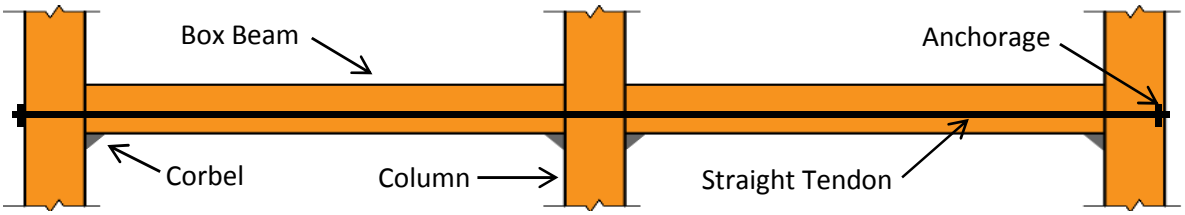

Figure 3.1 Moment resisting frame in post-tensioned timber building using straight tendons

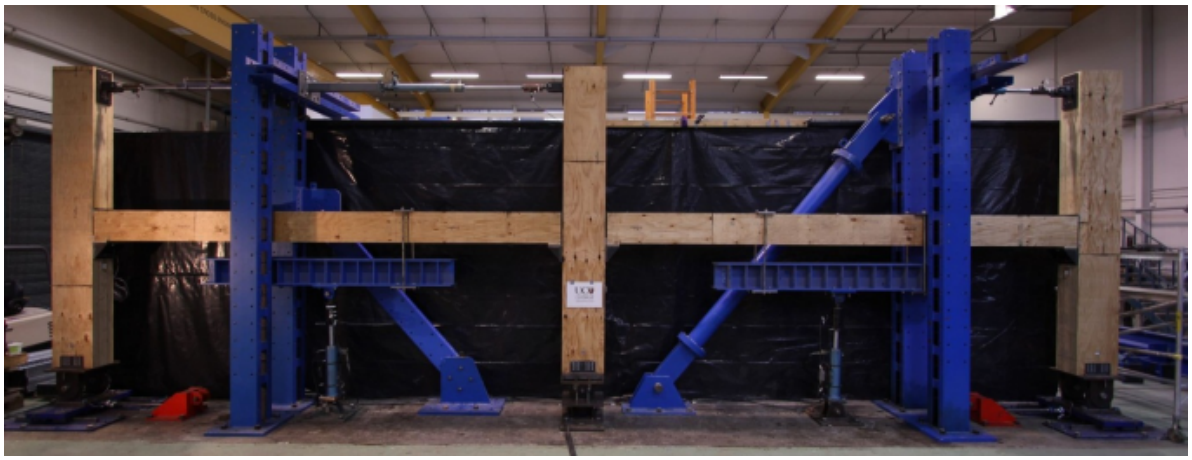

Figure 3.2 Two-bay post-tensioned timber test frame (van Beerschoten, 2013)

The major benefit of post-tensioned timber buildings is a significantly improved seismic performance with little or no residual damage to the structure following a large earthquake. This is achieved through the use of a post-tensioning system which allows “controlled rocking” (Pampanin, 2005) at ductile moment resisting connections under seismic loads. The “controlled rocking” enables the unbonded tendons to elastically elongate, and dissipate energy, as well as recentering the structure. Energy dissipation is also provided by yielding of specially designed short lengths of mild steel at each moment resisting connection. These connections are referred to as “hybrid” systems (Stanton et al., 1997). The dissipating devices are also shown in Figure 3.3.

Figure 3.3 Typical moment resisting beam-column joint in a post-tensioned timber building

The post-tensioning system also allows for more efficient structures to be designed in non-seismic regions. An eccentric tendon in a beam will create a hogging bending moment that resists gravity loads so increasing the flexural capacity of the member. The magnitude of the hogging bending moment created by the post-tensioning system is proportional to the distance between the centroids of the tendon and the beam, i.e. the tendon eccentricity.

Draped tendons, where the eccentricity of the tendon varies along the length of the beam, allows for a more efficient design. Figure 3.4 shows a two-bay frame with a draped tendon. The tendon eccentricity is largest at the mid-span of the beam, which corresponds to the maximum flexural demand, while the tendon eccentricity reduces in the region close to the column where the flexural demand is lower. In moment resisting frames, the tendon eccentricity may be negative, i.e. above the centroid of the beam, at the column face in order to resist the negative bending moment at this location.

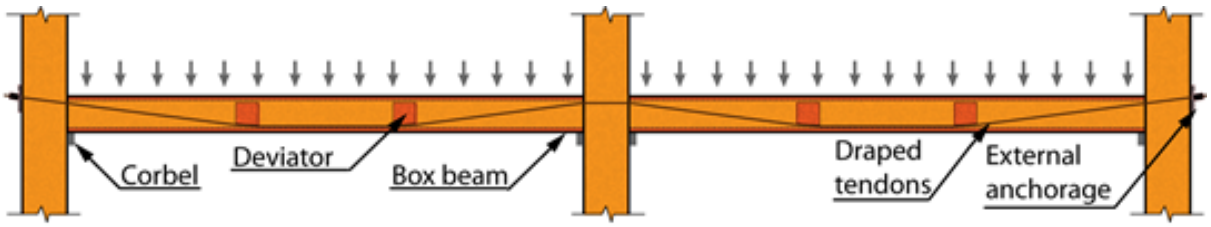

Figure 3.4 Moment resisting frame in post-tensioned timber building using draped tendons

Draped tendons provide an additional benefit in that the shear demand on the member is resisted along the length of the inclined tendon as a portion of the tendon force acts vertically. This is not the case for straight tendons however, as the tendon force does not act vertically. Highly-optimised box beams are especially susceptible to shear failure as the box members utilise relatively thin webs so there is relatively little shear capacity at the centroid of the beam, i.e. in the web, which corresponds to the location of maximum shear load. This is further amplified in fire conditions as the beam chars, further reducing the thickness of the webs, and therefore the shear capacity of the beam. This is further discussed in Section 3.2.

Post-tensioned beams are often incorporated in a moment resisting frame, rather than using simply supported beams. Utilising a moment resisting frame will create a negative moment in the beams close to the beam-column joints. The maximum bending demand on the beam at mid-span is correspondingly reduced but the end column will have to resist additional bending moments. The bending moment diagram for a simply supported beam and a continuous beam is shown in Figure 3.5.

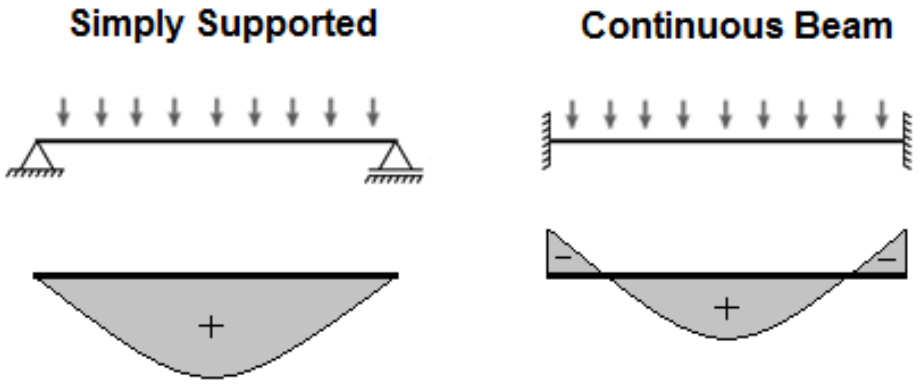

Figure 3.5 Bending moment diagram for a simply supported beam and a continuous beam

Timber structural members other than beams, i.e. columns and walls, are also able to incorporate post-tensioning to improve the efficiency of the structural design. The major difference between the post-tensioning systems used in columns and walls as opposed to that used in beams is that the post-tensioning system in columns and walls only improves the lateral load resistance of the member and does not improve the gravity load carrying capacity.

3.2 Fire Performance of Post-Tensioned Timber Buildings

There are many questions relating to the fire safety of these buildings. While a post-tensioned timber building may be designed as per a "normal" timber building without post-tensioning, i.e. the load carrying capacity of the post-tensioning system is not included in the fire safety design and the residual timber of the structural elements is used to resist the loads, there are potential benefits that can be obtained by considering the post-tensioning system that may lead to more efficient design of these buildings. Some of the key issues regarding the fire resistance of post-tensioned timber buildings that need addressing so that designers are informed and able to design better structures are listed below.

- Should the additional capacity of member provided by the post-tensioning system be considered in the fire safety design of post-tensioned timber buildings?
- What are the benefits of including the post-tensioning system in the fire resistance design and are these benefits significant? Also, what are the risks of using the post-tensioning system?
- Does a reduction in the post-tensioning force due to heating of the post-tensioning system need to be considered?
- Do second order effects, e.g. anchorage rotation and tendon elongation, need to be considered?
- Do dissipaters require fire protection?

3.2.1 Previous Research

Spellman (2012, Spellman et al., 2012) has conducted the only significant previous research into the fire-performance of post-tensioned timber buildings. The research largely focussed on post-tensioned box beams with the intent of developing design guidance for these members verified by full scale furnace tests of these beams. These furnace tests, conducted in accordance with ISO 834 (ISO, 1975), were the main effort of the research. The beams were designed to simulate the configuration of beams that may typically be used in multi-storey post-tensioned timber buildings. Spellman used his proposed calculation method, discussed below, to predict failure modes and times for each of the tests. The predicted and actual failure modes are summarised in Table 3.1 and Table 3.2 states the predicted and actual failure times for each test. Photographs of the beams following failure for each of the tests are shown in Figure 3.6.

(a) Beam following shear failure of the web in Test 1

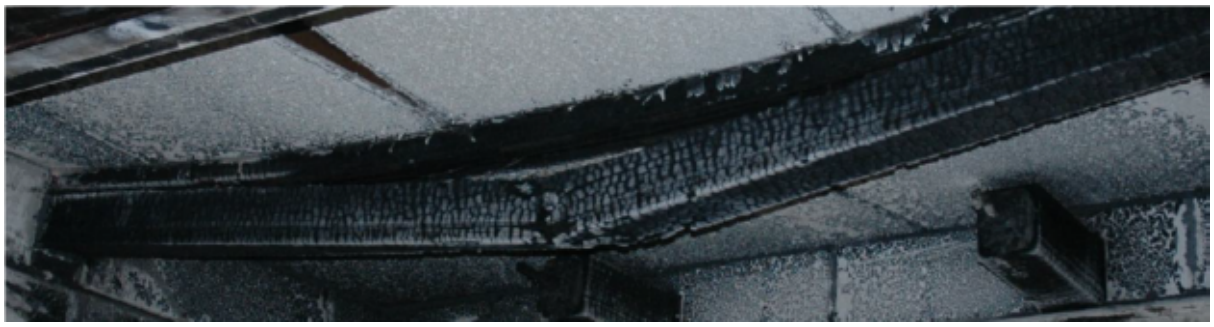

(b) Beam following failure in Test 2 showing detachment of the top flange, mid-span crushing of the bottom flange and buckling of the web

(c) Beam following failure in Test 3 showing detachment of the top flange and crushing of the bottom flange at the support and one third span

Figure 3.6 Beams following failure in Spellman's furnace tests (Spellman, 2012)

Table 3.1 Predicted and actual failure modes of full scale post-tensioned box beam furnace tests

Test	Predicted Failure Mode	Actual Failure Mode
1	Shear failure in bottom corner	Shear failure of the web
2	Mid-span combined bending and compression failure	Detachment of the top flange and web along the beam length in conjunction with mid-span crushing of the bottom flange and buckling of the web
3	End of beam combined bending and compression failure	Localised detachment of the top flange and web in conjunction with crushing of the bottom flange at the support and one third span

Table 3.2 Predicted and actual failure times of full scale post-tensioned box beam furnace tests

Test	Predicted Failure Time	Actual Failure Time
1	61 minutes	64 minutes
2	43 minutes. Revised to 37 minutes	22 minutes
3	53 minutes	56 minutes

The predicted failure modes did not match the actual failure modes observed. However, the predicted failure times were relatively close to the actual failure times in Tests 1 and 3. An unexpectedly early failure occurred in Test 2. Spellman states that this was because his original method did not sufficiently consider the interaction of bending and compression forces. His proposed methodology was revised to better consider this interaction, which resulted in a reduced predicted failure time of 37 minutes, rather than 43 minutes as originally predicted.

Spellman also investigated the performance of tendon anchorages in fire conditions and potential fire protection methods. This was achieved by testing five anchorages with different forms of fire protection concurrently with the full scale beam tests, shown in Figure 3.7. Again these were conducted in accordance with ISO 834 (ISO, 1975). A summary of the performance of the different anchorages is presented in Table 3.3. The columns headed 95% F_{PT} and 50% F_{PT} refer to the time taken for the tendon force to decrease to that percentage of the original tendon force.

Figure 3.7 Anchorage protection tests conducted concurrently with the full scale beam test (Spellman, 2012)

Table 3.3 Summary of anchorage protection tests

Protection Method	**T_{Plate} > 200°C**	**T_{Tendon} >200°C**	**95% F_{PT}**	**50% F_{PT}**
Unprotected	1 – 3 minutes	12 minutes	10 minutes	15 minutes
Intumescent paint	5 minutes	24 minutes	3 minutes	25 minutes
Kaowool blanket	35 minutes	38 minutes	52 minutes	63 minutes
Timber encasement	>64 minutes	>64 minutes	>64 minutes	>64 minutes
Gypsum plasterboard	>64 minutes	>64 minutes	35 minutes	>64 minutes

The anchorages that were encased by timber or gypsum performed the best in the tests. Spellman states that apparent poor performance of the intumescent paint and kaowool blanket protection methods does not rule out their successful use as a fire protection method for tendon anchorages but special consideration should be given any design using these protection methods. Spellman also suggested that further research into anchorage protection should be conducted. However, he demonstrated that two methods, timber encasement and gypsum plasterboard, are appropriate for use in practice. As such, this research project does not consider anchorage protection.

Spellman also proposed a design methodology for post-tensioned timber beams in fire conditions. This method is based on calculating the capacity of a post-tensioned timber box beam with a reduced residual cross-section, due to charring, and checking against demands. The contribution of the post-tensioning system is included in Spellman's method.

His proposed design method considers the heating of the post-tensioning system and second order effects, each of which changes the post-tensioning force. Heating of the post-tensioning system is considered by calculating a reduced elastic modulus and the thermal expansion of the tendon. The second order effects considered include rotation of the anchorages, additional axial compression of the beam, axial bowing of the beam due to the eccentric tendon and flexural deflection of the beam due to the eccentric tendon. The inclusion of these additional parameters significantly increases the complexity of the proposed design process. As a simpler alternative, this research project aimed to produce a simplified calculation method that, where appropriate, does not include the additional parameters that add to the complexity of the method.

Spellman observed that while post-tensioned box beams can be designed to achieve sufficient flexural capacity in fire conditions the shear capacity of these members may not be sufficient to avoid undesirable shear failure modes in fire-conditions. Spellman made the additional observation that shear stresses may be an issue at the interface between the web and the lower flange as charring occurs in two-directions at this point, so the shear area may be significantly lower at this position than elsewhere. This is demonstrated in Figure 3.8 where the thickness at the lower corner of the cross section is much less than the web thickness. Therefore, the maximum shear stress may occur in the bottom corners of the member, which may lead to shear failure at this location. As such, Spellman suggested that the location of the critical shear stress may be at either the bottom corners or at the centroid of the beam. Spellman recommended that further research of shear failure of post-tensioned box beams be completed in order to determine if it is a significant issue. This recommendation led to this research project being undertaken.

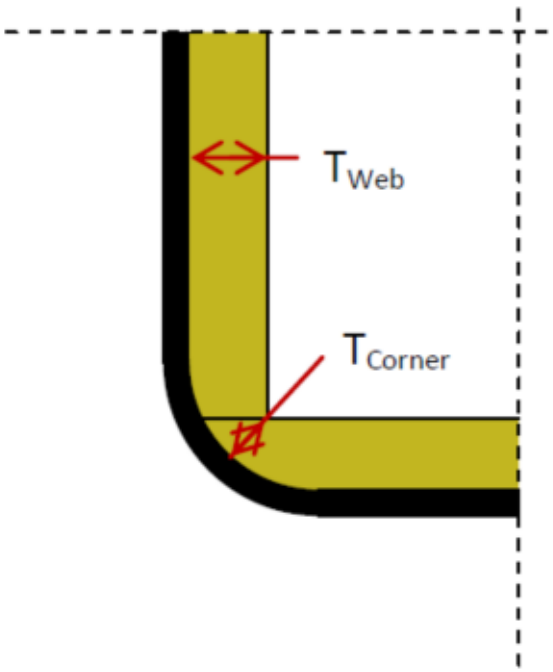

Figure 3.8 Beam cross section showing corner rounding (Spellman, 2012)

3.3 Design for Fire Resistance of Post-Tensioned Timber Structures

A design guide for post-tensioned timber buildings has been produced by STIC (2013). The proposed design guide includes an overall fire safety strategy for post-tensioned timber buildings and a simplified calculation method for the fire resistance of post-tensioned timber box beams.

Producing this design guide has three main benefits. These are:

1. Designers are more aware of issues that may compromise the fire safety design of a building if not properly addressed, such as proper fire stopping of gaps around structural connections.
2. Designers can incorporate the contribution of the post-tensioning system in the fire design calculations for the FRR of the building, which may lead to more efficient designs.
3. Designers are more confident in the fire performance of post-tensioned timber buildings as the proposed fire safety methodology has been verified by full scale fire resistance tests at BRANZ (Building Research Association of New Zealand) and simulated fire resistance tests at the University of Canterbury. These tests are described in more detail in Chapters 5 and 6.

Each of these three benefits increases the likelihood of uptake of post-tensioned timber building technology.

3.3.1 Design Strategies

Objective 1 of this thesis is to develop a design strategy for the fire performance of post-tensioned timber buildings. This thesis proposes that there are two alternative strategies that can be used when designing post-tensioned timber buildings for fire resistance. These are:

1. Residual timber only.
2. Fire protection of the post-tensioning system.

The first strategy relies solely on the residual timber members to resist the applied loads during a fire, so the steel post-tensioning components do not need to be protected.

The second strategy involves protecting all of the steel components used in the post-tensioning system, i.e. tendons, anchorages etc., so that the effect of the post-tensioning system can be considered when assessing the structural performance of the building in fire conditions. Fire protection of some elements may be inherently provided, e.g. internal tendons will be protected from fire exposure by the timber of the beam.

The designer must choose one of the two strategies early in the design process and use it as the basis of the entire design. The considerations that should be taken into account when making this decision are discussed below.

If the first strategy is used, i.e. the post-tensioning system is not specifically fire protected, the size of the members must be large enough such that the reduced loads in fire conditions can be resisted by the residual timber section only. The residual section size is easily calculated by reducing the total section size by the char depth on surfaces exposed to fire. Also, the connections between members, for example beam-column joints, must be designed to support the members without the aid of the post-tensioned system during a fire.

The use of this strategy means that there are no additional costs or specific detailing required associated with protecting the post-tensioning system. This results in a simpler design which requires less time to complete as well as reducing construction time due to reduced fire protection detailing.

As stated in Section 2.1, B1/VM1 (Department of Building and Housing, 2011) requires that the structure is able to resist a lateral load both during and after a fire. This requirement to consider lateral loading means that careful consideration must be given to the lateral load resistance of the whole building during and after the fire when the first strategy is used. This is especially important if the post-tensioning is an integral component of a lateral load resisting frame. However, as the fire will be contained within a single fire compartment on a single floor level in a multi-storey building, the residual lateral load resisting capacity of the structure on the floors unaffected by fire is likely to be sufficient so that lateral load resistance for the whole building is provided. This issue still needs to be checked carefully in the design process.

Using the second strategy, i.e. fire protecting the post-tensioning system, will prevent the temperature of the steel components from increasing significantly for the duration of the required fire resistance time. Thus the structural fire safety design can incorporate the contribution of post-tensioning, which could lead to smaller and more efficient members and thus a potentially more cost-effective design. The timber members must be sized to ensure that there is sufficient residual timber to resist the applied loads and the post-tensioning forces for the required fire resistance time.

There will be additional costs, for both construction and design, when the second strategy is used. The design process of the structural members is somewhat more complex, which will lead to an increased design cost. Also specific detailing for the fire protection of all steel components that are part of the post-tensioning system is required, resulting in increased design and construction costs. Furthermore, all potential gaps or holes that could provide a path for hot gases to migrate and come into contact with the post-tensioning system, such as around connections between timber members, need to be considered in the design such that this is not possible. This again may increase both design and construction costs. These additional costs may be outweighed by a more efficient design of the members themselves. Additional information regarding the fire design of structural detailing is given in Section 3.4. Table 3.4 details the advantages and disadvantages of the two design strategies.

Table 3.4 Advantages and disadvantages of the two design strategies

Design Strategy	Advantages	Disadvantages
1. Residual timber only	• No additional design steps for fire design • Faster construction • Reduced cost of protection	• Does not utilise existing post-tensioning capacity • Additional detailing of beam-column connections
2. Fire protection of post-tensioning system	• No reduction in post-tensioning during fire • Full lateral load resistance during fire • Friction due to post-tensioning system remains at beam-column joints	• Specific detailing required • Additional cost to protect the post-tensioning

3.4 Fire Design of Structural Detailing

As steel is a highly conductive material, any exposed steel components are sensitive to increases in temperature. This is particularly true for exposed steel used in the post-tensioning system. The yield strength of steel is greatly reduced when it exceeds a temperature of approximately 370°C, as demonstrated in Figure 3.9. As the temperature of steel exposed to fire is expected to be greater than this, the load carrying capacity of a post-tensioning system is negligible if the tendons are exposed to fire.

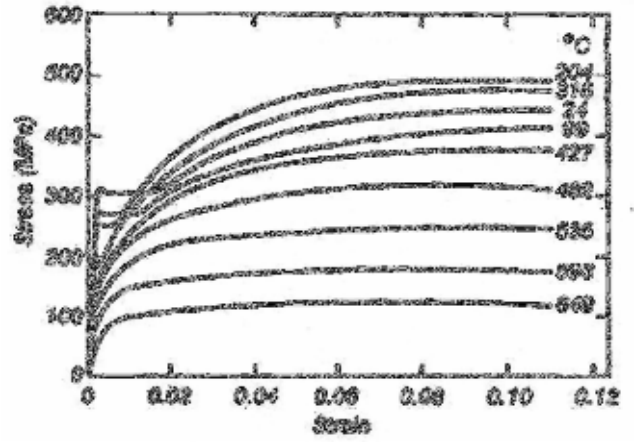

Figure 3.9 Stress-strain curve of structural steel at various temperatures (Harmathy, 1970)

Steel tendons inside the timber box members do not lose much strength in a fire because they are protected from elevated temperatures by the thermal insulating properties of the timber. The post-tensioning anchorages may need fire protection if they are within the building and likely to be exposed to fire.

3.4.1 Fire Resistance of Post-Tensioning

Design of fire resistance for post-tensioning will depend on the strategy selected above. If the post-tensioning requires fire resistance, this must include:

- Protection of tendons
- Protection of anchorages

If the tendons are protected from fire in a cavity within the beam or the wall, it is unlikely that additional fire protection is necessary because of the excellent insulating properties of the residual wood below the char layer. However, simple calculations can be performed to determine the maximum temperature reached inside the cavity. The proposed simplified calculation method detailed in Section 4, does not include this calculation.

If the post-tensioning is required to be protected from fire, it is essential to ensure that the anchorages also have the same fire resistance. In many cases these anchorages will be protected by other structures, or be outside the building envelope. In other cases it will be necessary to apply fire protection to the anchorage, using protective material such as intumescent paint. Some guidance is given by Spellman (2012). Early discussion with the Fire Engineer is essential to determine the most appropriate protection requirements corresponding to the fire design strategy for the building.

3.4.2 Fire Resistance of Brackets and Corbels

Timber beams are supported on brackets, joist hangers or corbels to resist gravity loads. The Fire Engineer must assess whether exposed steel brackets, joist hangers or corbels require fire resistance. Whether to protect an element from fire will often depend on the fire strategy used, i.e. if the post-tensioning system is protected from fire exposure or not.

Elements that provide support to primary structural members under gravity loads will always require protection if the post-tensioning system is not protected from fire exposure. However, if the post-tensioning system is protected from fire the friction between a beam and column that is produced by the post-tensioning force is likely to be sufficient to resist gravity demands at the supports. This is an additional benefit of protecting the post-tensioning system that the design may incorporate. If fire resistance of corbels and brackets is required it can usually be provided with protective material. An example of a steel corbel protected with intumescent paint is shown in Figure 3.10. It is worth noting however that limited research by Peng (2010) has found that intumescent coating on exposed steel connections provided little benefit to the fire resistance of the connection.

Figure 3.10 Steel corbel protected with intumescent paint (STIC, 2013)

Checks should be made on the size and residual bearing area of any corbels and timber seating details, such that adequate bearing remains after a fire event.

3.4.3 Fire Resistance of Dissipaters

External dissipaters which are part of the seismic structural system will not normally need to be protected from fire because it is not a design requirement of AS/NZS 1170.1:2002 (Standards New Zealand, 2002b) to design for a fire and an earthquake at the same moment. If the dissipaters are contributing to the gravity load resistance during normal building operation then special consideration will need to be given to the dissipaters to determine whether protection is required under reduced fire loading conditions.

3.4.4 Fire Protection of Service Holes

Service holes may be required in timber walls, floors or beams. Ardalany (2010, 2012) has researched the impact that service holes have on the performance of structural members in ambient conditions.

The fire resistance of these members for all timber buildings will also be affected by the presence of service holes. In addition to reducing the cross section, and so the ambient strength, of the member the service holes will increase the number of surfaces and the total surface area exposed to fire. This effectively increases the charring rate in the area around the service hole, which may lead to premature failure of the member. This can be prevented from occurring by specific detailing to prevent fire passing through the assembly in order to retain at least the same fire resistance as the penetrated element.

Service holes in the structural members of post-tensioned timber buildings introduce an additional complication as they may expose the tendon to fire, which would otherwise be protected by the surrounding timber of the structural member. This must be addressed by the designer if the post-tensioning system has been designed to contribute to the fire resistance of the member. Again, this will require specific detailing to prevent fire passing through the assembly in order to retain at least the same fire resistance as the penetrated element.

3.5 Current Pres–Lam Buildings

A number of post-tensioned timber buildings have been or are currently being built throughout New Zealand. A short description of seven of these buildings is provided below. Special consideration is given to the fire resistance of the post-tensioning system, as well as other key aspects of the fire safety design, including the presence of an automatic fire sprinkler system and the surface finishes used. Information about these buildings was obtained through discussions with the designers and a peer-reviewer as well as site visits. A summary of the fire safety designs of these post-tensioned timber buildings is presented in Table 3.5.

Table 3.5 Summary of fire design of post-tensioned timber buildings

Building	Automatic Sprinkler System?	Required structural adequacy	Post-tensioning system protected?
NMIT	Yes	30 minutes	No
EXPAN	No	15 minutes	No
Carterton Events Centre	Yes	60 minutes	No
CoCA	Yes	30 minutes	No
Merritt	No	60 minutes	No
Trimble	Yes	30 minutes	No
St Elmo Courts	Yes	30 minutes	No

3.5.1 NMIT building

The three-storey Nelson-Marlborough Institute of Technology (NMIT) building in Nelson, which opened in 2011, was the first building in the world that utilised post-tensioned timber technology. Post-tensioned coupled timber walls are used to resist lateral loads in both directions. The post-tensioning is provided by internal high strength steel bars that are connected to the building foundation.

The design used floors and interior fire rated partitions to create multiple firecells. An automatic fire sprinkler system compliant with NZS 4541:2007 (Standards New Zealand, 2007) is installed in this building. A 30 minute structural adequacy fire resistance was required for the structural elements used in this building.

The purpose of the post-tensioning system is to resist lateral loads so fire protection of the post-tensioning system, other than the inherent protection of the internal bars provided by the timber walls, is not needed to achieve the required FRR. However, as this was the first Pres-Lam building in the world to be built and there was no fire design guidance available to the designer, it was decided to take a conservative approach and intumescent paint was used to protect any anchorages that were not inherently protected by the timber member.

Plywood panels were used to line some ceilings. This did not meet the NZBC surface finish requirements. An alternative solution was proposed where conventional sprinkler heads, which spray water upwards towards the ceiling, were used to mitigate the risk of rapid fire spread across the plywood panels. A smoke control system was also installed in this building to provide sufficient egress time for occupants prior to the environment becoming untenable in a fire (P. Martini, Per. Com.)

(a) NMIT building construction (b) Completed NMIT building

Figure 3.11 NMIT building (STIC, 2013)

3.5.2 University of Canterbury EXPAN building

The University of Canterbury EXPAN building, shown in Figure 3.12, is a former research test structure that was converted into a small office building in 2011. The two-storey structure uses post-tensioned moment resistant frame in one direction and post-tensioned walls in the other direction to resist lateral loads. The light weight of the completed building meant that external dissipaters are not required in this building.

The building was a single firecell with no interior fire rated partitions. An automatic fire sprinkler system is not installed in this building. A 15 minute structural adequacy fire resistance was required for the structural elements used in this building.

The residual timber of the primary structural elements is sufficient to resist the applied loads during a fire so protection of the post-tensioning system was not required. Furthermore, the corbels used to support the beam under gravity loads are also not protected but were still able to achieve the 15 minute structural adequacy fire resistance.

All surface finishes meet the requirements under the NZBC, with no special requirements to limit the area of timber surface finishes due to the small size of the building and that structural timber elements are exempt from surface finish requirements (D. Millar, Per. Com.).

(a) EXPAN building during construction

(b) Completed EXPAN building

Figure 3.12 University of Canterbury EXPAN building (STIC, 2013)

3.5.3 Carterton Events Centre

The Carterton Events centre is a multi-purpose community facility for approximately 400 people which was opened in 2011. The post-tensioning system design is very similar to that used in the NMIT building; post-tensioned walls with internal bars to resist lateral loads in both directions are used.

The building was a single firecell with no interior fire rated partitions. An automatic fire sprinkler system compliant with NZS 4541:2007 (Standards New Zealand, 2007) is installed in this building. A 60 minute structural adequacy fire resistance was required for the structural elements used in this building.

Similarly to the NMIT building, the post-tensioning system was not protected from fire exposure other than the inherent fire protection of the internal bars provided by the timber walls. The bottom anchorage was also protected from fire by 45 mm thick LVL inserts that capped the anchorage cavity. These caps were installed mainly for constructability and architectural reasons; however these caps do increase the inherent fire resistance of the post-tensioning system. The required FRR was achieved using the load-carrying capacity of the residual timber of the structural elements.

All surface finishes meet the requirements under the NZBC, with no special requirements to limit the area of timber surface finishes due to the installation of the automatic sprinkler system and that structural timber elements are exempt from surface finish requirements (S. Chung , Per. Com.).

(a) Post-tensioned wall being erected

(b) Interior of finished building

(c) Exterior of finished building

Figure 3.13 Carterton Events Centre (S. Chung, Per. Com.)

3.5.4 Massey University College of Creative Arts

The three-storey College of Creative Arts (CoCA) building at the Wellington Campus of Massey University opened in 2012. Post-tensioned concrete walls are used in one direction and a post-tensioned moment resisting timber frame in the other direction. Both the beams and columns of the moment resisting frame were post-tensioned. The tendons used in the beams are draped so they resist vertical loads as well as lateral loads.

The building was a single firecell with no interior fire rated partitions. An automatic fire sprinkler system compliant with NZS 4541:2007 (Standards New Zealand, 2007) is installed in this building.

A 30 minute structural adequacy fire resistance was required for the structural elements used in this building.

As the tendons are completely exposed, as shown in Figure 3.14 (a), they will lose strength very early in a fire, at which point they will no longer resist load. As such, the post-tensioning system does not contribute to the capacity of the frame during a fire so is not included in FRR calculations. Also, the post-tensioning system used in the walls and columns were not protected from fire exposure as the post-tensioning system is used only to resist lateral loads. The residual timber of the primary structural elements is used to carry loads during fire. The beams are supported throughout the fire by corbels that are protected with intumescent paint.

All surface finishes meet the requirements under the NZBC, with no special requirements to limit the area of timber surface finishes due to the installation of the automatic sprinkler system and structural timber elements are exempt from surface finish requirements. A smoke control system was installed in this building to provide sufficient egress time for occupants prior to the environment becoming untenable in a fire (M. Huynh, Per. Com.).

(a) Exposed draped tendons (b) CoCA building during construction

Figure 3.14 CoCA building (STIC, 2013)

3.5.5 Merritt Building

The Merritt building is a three-storey mixed-use office and retail building in the CBD of Christchurch currently under construction. A post-tensioned moment resisting frame resists lateral loads in one direction while a pre-cast tilt slab concrete wall resists lateral loads in the other direction. Internal straight tendons with an initial eccentricity of zero are used in the beams of the moment resisting frame.

The building used floors and interior fire rated partitions to create multiple firecells. An automatic fire sprinkler system is not installed in this building. A 60 minute structural adequacy fire resistance was required for the structural elements used in this building.

While the timber will protect the tendons from fire exposure the anchorages of the post-tensioning system are not protected from fire exposure so heat is able to propagate throughout the post-tensioning system. As such, the post-tensioning system will resist loads during the early stages of a fire but cannot be relied upon to contribute to the capacity of the frame for the entire fire duration. Furthermore, as the tendons are straight with no initial eccentricity the post-tensioning system will provide negligible contribution to the resistance of vertical loads even with full protection from fire exposure. The fire safety design of the Merritt building did not include a contribution from the post-tensioning system and instead relied solely on the capacity of the residual timber to resist the applied loads (A. Chapman, Per. Com.).

The corbels used to support the beams in ambient conditions are not protected from fire exposure so cannot be used during a fire to support the beams. However, an internal steel tube that extends approximately 300 mm into the beam from the column, which acts as a dowel, is used to support the beam under vertical loads during a fire. As the tube is internal, it is inherently protected from fire exposure by the residual timber of the beam and column.

All surface finishes meet the requirements under the NZBC, with no special requirements to limit the area of timber surface finishes due to structural timber elements being exempt from surface finish requirements. The concrete tilt slab wall on the southern boundary of the building prevents fire spread to adjoining buildings.

(a) Beam and column, including corbels, anchorage and dissipaters

(b) Merritt building nearing completion

Figure 3.15 Merritt Building

3.5.6 Trimble Building

The Trimble building in Christchurch is a large two storey office building currently under construction. Post-tensioned walls are used in one direction and post-tensioned moment resisting frames are used in the other direction to resist lateral loads. In the moment resisting frame, tendons are only present in the first floor and not at roof level. The tendons in the frame are internal and draped so provide resistance to vertical loads in ambient conditions as well as lateral loads.

The building was designed as a single firecell with no interior fire rated partitions. An automatic fire sprinkler system compliant with NZS 4541:2007 (Standards New Zealand, 2007) is installed in this building. A 30 minute structural adequacy fire resistance was required for the structural elements used in this building.

The anchorages of the post-tensioning system are not protected from fire exposure. This will result in the loss of the load-carrying ability of the post-tensioning system in a fire. The residual timber of the beams and columns are used to resist the applied loads during fire (A. Brown, Per. Com.). The corbels are protected from fire exposure as they are coated with intumescent paint so provide support to the beams for the 30 minute required fire resistance rating.

All surface finishes meet the requirements under the NZBC, with no special requirements to limit the area of timber surface finishes due to the installation of the automatic sprinkler system and that structural timber elements are exempt from surface finish requirements.

(a) Beam-column joint, including dissipaters and corbels protected with white intumescent paint

(b) Trimble building during construction

Figure 3.16 Trimble building

3.5.7 St Elmo Courts Building

The St Elmo Courts building is a six-storey mixed-use commercial and residential accommodation building currently under construction in the Christchurch CBD. The structure uses both base-isolation and Pres-Lam technology to achieve a very high level of safety in seismic loading. Concrete columns and timber beams are used to create two-way moment resisting frames. Internally draped tendons, which resist both vertical and lateral loads, are used in the beams and span through the columns.

The building uses floors and interior fire rated partitions to create multiple firecells. An automatic fire sprinkler system compliant with NZS 4541:2007 (Standards New Zealand, 2007) is installed in this building. A 30 minute structural adequacy fire resistance was required for the structural elements used in this building.

The post-tensioning system is not protected from fire exposure, so the anchorages are not protected. The residual timber of the beams is used to resist the applied loads during fire.

Despite being the only structural element that supports the beams during a fire the corbels are not protected from fire exposure. The corbels are not required to be protected as they are sufficiently thick, 28 mm, for the steel temperature to remain low enough so that the beams continue to be supported (C. Watson, Per. Com.). This is aided by the presence of an automatic fire sprinkler system which reduces the required fire resistance time so the time over which heat transfer to the corbels is considered is reduced. The secondary steel beams used to support the floors are however protected using intumescent paint.

All surface finishes meet the requirements under the NZBC, with no special requirements to limit the area of timber surface finishes due to the installation of the automatic sprinkler system and that structural timber elements are exempt from surface finish requirements.

(a) Exterior view during construction

(b) Beam-column joint, including unprotected corbel

(c) Protected secondary beams

Figure 3.17 St Elmo Courts building

4 Simplified Calculation Method

This Chapter proposes a simplified calculation method for determining the fire resistance of post-tensioned timber structural members. Box beams are considered in detail. An overview of the proposed method is given in Section 4.1. The simplified calculation method is presented in Sections 4.2 and 4.3 for both design strategies. Section 4.4 outlines design considerations for other post-tensioned structural members, including draped box beams and moment resisting frames.

4.1 Overview

A simplified calculation method to determine the fire resistance of post-tensioned box beams has been developed. This method, which is detailed below, is based largely on NZS3603:1993 (Standards New Zealand, 1993).

The purpose of the proposed method is to provide a simple and clear process that designers can use to calculate the fire resistance of post-tensioned timber members. Furthermore, this method presents a process that can be used to incorporate the benefits of the post-tensioning system during a fire. This may lead to more efficient structures being designed.

The simplified calculation method is based on completing a series of design calculations to ensure that the design capacity of the member is greater or equal to the design action effect on the member being considered. Equation 4.1, taken from AS/NZS 1170.0:2002 (Standards New Zealand, 2002a), is the general form of the inequality that must be satisfied for each design action.

$$E_d \leq R_d \qquad 4.1$$

Where: E_d = Design action effect on the member

R_d = Design capacity of the member

Equation 4.1 will be applied for the following eight actions:

1. Bending, i.e.

$$M^* \leq \varphi M_{n,i}$$

2. Shear, i.e.

$$V^* \leq \varphi V_{n,i}$$

3. Axial, i.e.

$$N^* \leq \varphi N_{n,i}$$

4. Compressive stress, i.e.

$$\sigma_{f,c,i} \leq f_{c,i}$$

5. Tensile stress, i.e.

$$\sigma_{f,t,i} \leq f_{t,i}$$

6. Compressive bending stress, i.e.

$$\sigma_{f,c,max,i} \leq f_{b,i}$$

7. Tensile bending stress, i.e.

$$\sigma_{f,t,max,i} \leq f_{b,i}$$

8. Combined axial and bending capacity, i.e.

$$\frac{N^*}{\emptyset N_n} + \frac{M^*}{\emptyset M_n} \leq 1.0$$

The calculation method described is based on a simply-supported post-tensioned timber box beam with a straight tendon profile, as shown in Figure 4.1. The tendon may be located either at the centroid of the beam or near the bottom of the beam cross section. Other structural concepts, such as beams with draped tendons, are considered in Section 4.4.

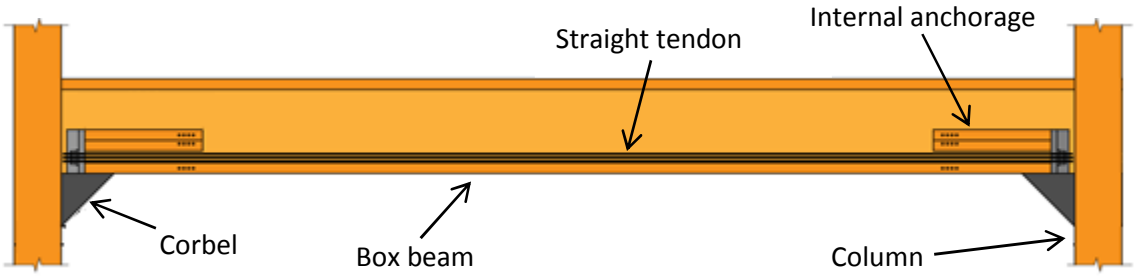

Figure 4.1 Post-tensioned box beam with a straight tendon (STIC, 2013)

Two approaches can be used when applying the proposed calculation method. The approaches differ in when the char depth is calculated. The two approaches calculate the char depth:

1. At the required FRR only; or
2. Across a range of timesteps.

The first approach, which is recommended to be used by designers, involves determining the required FRR for the building or firecell and calculating the residual section properties, and hence the residual strength of the member, at this FRR time only. The capacity of the member is then checked against demand to determine whether the member has a sufficient FRR.

The alternate approach is to calculate the section properties across a range of timesteps. A timestep of one minute is recommended. It is recommended that the time period considered includes the required FRR time and the predicted time to failure. The performance of the beam for the duration of the fire may also be determined when appropriate.

By calculating the capacity of the member across a range of timesteps the designer is able to determine the capacity of the member throughout the period of interest. Using these calculations a failure time can be predicted, as failure will occur when the capacity of the member becomes less than the demand on the member. The time at which this occurs, i.e. the failure time, can easily be found using this method. This is valuable for research purposes but will have less application for designers.

Both approaches use identical equations but the second approach is clearly more computationally intense. It is recommended that a spreadsheet is used throughout the design process for both approaches. However, a spreadsheet is required when using the second approach so that the calculations can be made at each time step.

As described in Section 3.3.1 there are two design strategies that can be used in the fire safety design for stability of post-tensioned timber buildings. The two design strategies are detailed separately in Sections 4.2 and 4.3. An example calculation, which details both design strategies, is presented in Appendix A.

4.2 Calculation Method for Strategy 1: Residual Timber Only

It is assumed that second order effects have a negligible effect on the performance of the beam so have not been considered in the proposed calculation method. Further explanation of this assumption is provided in Section 7.3. Lateral actions on the building are also not explicitly included in this calculation method but the design considerations for lateral actions are discussed in Section 3.3.1.

Three-sided exposure of the beam is assumed as the top surface of the beam is concealed from fire exposure by the floor of the level above. A char rate of 0.70 mm/min with an additional 7.0 mm zero strength layer is used, as recommended by EN 1995-1-2:2004 (European Commission, 2004b). This is shown in Equations 4.2 and 4.3. The use of this char rate includes an allowance for corner rounding (SP Technical Research Institute of Sweden, 2010) so corner rounding has not been explicitly considered in these calculations.

The zero strength layer used in EN 1995-1-2:2004 (European Commission, 2004b) linearly increases from 0 mm to a maximum value of 7 mm during the first 20 minutes of fire exposure. As the failure did not occur during the first 20 minutes of fire exposure during the full scale furnace test or in the calculations presented in Appendix A, the linear increase in zero strength layer is not included in this thesis for simplicity. The following calculation method can be modified to include the linear increase in zero strength layer if a failure time of less than 20 minutes is being considered.

$$\beta = 0.70 \frac{mm}{min} \qquad 4.2$$

$$\gamma = 7.0\ mm \qquad 4.3$$

Where: β = Char rate (mm/min)
γ = Zero strength layer (mm)

The char depth, c_i, at time T_i is calculated using Equation 4.4.

$$c_i = \beta T_i + \gamma \qquad 4.4$$

Where: c_i = Char depth at time i (mm)
T_i = Time i (min)

The residual section dimensions are calculated by reducing the initial section dimension by the char depth. The dimensions are illustrated in Figure 4.2. Equations 4.5 and 4.6 are used to calculate the residual thickness of the top and bottom flanges, $t_{f,top,i}$ and $t_{f,bot,i}$, respectively.

$$t_{f,top,i} = t_{f,top,0} \tag{4.5}$$

$$t_{f,bot,i} = t_{f,bot,0} - c_i \tag{4.6}$$

Where:
$t_{f,top,i}$ = Residual thickness of top flange at time i (mm)
$t_{f,top,0}$ = Initial thickness of top flange (mm)
$t_{f,bot,i}$ = Residual thickness of bottom flange at time i (mm)
$t_{f,bot,0}$ = Initial thickness of bottom flange (mm)

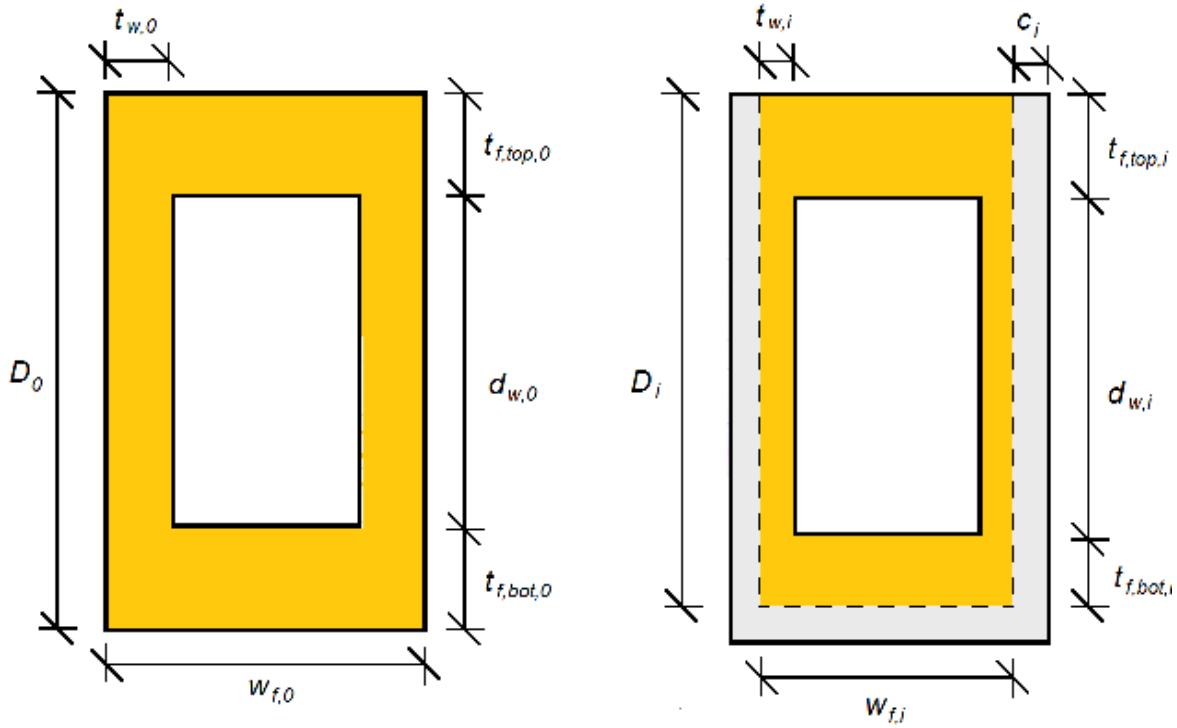

(a) Full section dimensions (b) Residual section dimensions

Figure 4.2 Section dimensions of a box beam

The residual width of the flange, $w_{f,i}$, is calculated using Equation 4.7.

$$w_{f,i} = w_{f,0} - 2c_i \quad 4.7$$

Where: $w_{f,i}$ = Residual width of flanges at time i (mm)
$w_{f,0}$ = Initial width of flanges (mm)

Equations 4.8 and 4.9 are used to calculate the residual thickness and internal depth of the webs, $t_{w,i}$ and $d_{w,i}$, respectively.

$$t_{w,i} = t_{w,0} - c_i \quad 4.8$$

$$d_{w,i} = d_{w,0} \quad 4.9$$

Where: $t_{w,i}$ = Residual thickness of webs at time i (mm)
$t_{w,0}$ = Initial thickness of webs (mm)
$d_{w,i}$ = Residual internal depth of webs at time i (mm)
$d_{w,0}$ = Initial internal depth of webs (mm)

The residual depth of the section, D_i, is calculated using Equation 4.10.

$$D_i = D_0 - c_i \quad 4.10$$

Where: D_i = Residual depth of the section at time i (mm)
D_0 = Initial depth of the section (mm)

The residual cross sectional and shear areas are calculated using Equations 4.11 and 4.12, A_i and $A_{s,i}$, respectively.

$$A_i = 2t_{w,i}d_{w,i} + w_{f,i}\left(t_{f,top,i} + t_{f,bot,i}\right) \quad 4.11$$

$$A_{s,i} = \frac{2t_{w,i}I_i}{Q_i} \quad 4.12$$

Where: A_i = Residual cross sectional area of the section at time i (mm^2)
$A_{s,i}$ = Residual shear area of the section at time i (mm^2)
I_i = Residual second moment of area of the section at time i (mm^4)
Q_i = Residual first moment of area of the section at time i (mm^3)

The residual first moment of area, Q_i, is calculated using Equation 4.13.

$$Q_i = t_{f,top,i}w_{f,i}\left(\bar{y}_i - \frac{t_{f,top,i}}{2}\right) + t_{w,i}\left(\bar{y}_i - t_{f,top,i}\right)^2 \quad 4.13$$

Where: $\bar{y}_i$ = Residual neutral axis depth of the section at time i (mm)

The box beam is divided into individual rectangular sections in order to calculate the residual neutral axis depth and second moment of area. These individual sections are shown in Figure 4.3.

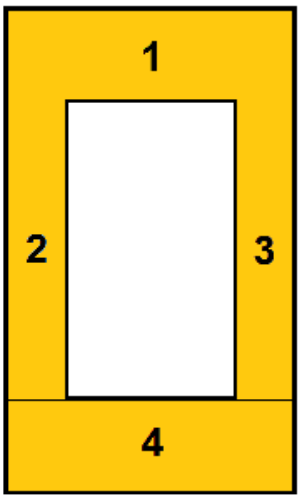

Figure 4.3 Individual sections used for neutral axis depth and second moment of area calculations

The residual neutral axis depth, $\bar{y}_i$, is calculated by dividing the sum product of the area and neutral axis depth of individual sections by the sum of the area of the individual sections, as shown in Equation 4.14. Equation 4.15 is the specific form of Equation 4.14 used for a box beam.

$$\bar{y}_i = \frac{\Sigma A_{x,i}\,\bar{y}_{x,i}}{\Sigma A_{x,i}} \qquad 4.14$$

Where: $A_{x,i}$ = Area of individual sections at time i (mm^2)

$\bar{y}_{x,i}$ = Neutral axis depth of individual sections at time i (mm)

$$\bar{y}_i = \frac{(t_{f,top,i}w_{f,i})\left(\frac{t_{f,top,i}}{2}\right)+2(t_{w,i}d_{w,i})\left(t_{f,top,i}+\frac{d_{w,i}}{2}\right)+(t_{f,bot,i}w_{f,i})\left(D_i-\frac{t_{f,bot,i}}{2}\right)}{(t_{f,top,i}w_{f,i})+2(t_{w,i}d_{w,i})+(t_{f,bot,i}w_{f,i})} \qquad 4.15$$

Due to the complexity of the beam's shape, the residual second moment of area, I_i, is calculated using the parallel axis theorem whereby the local second moment of area is calculated for each of the webs and flanges about their centroids and then the centroid of the entire section, as shown in Equation 4.16.

$$I_i = \Sigma I_{cc,x,i} + \Sigma A_{x,i}\left(\bar{y}_i - \bar{y}_{x,i}\right)^2 \qquad 4.16$$

Where: $\Sigma I_{cc,x,i}$ = Second moment of area of individual sections at time i (mm^4)

The residual section modulus, Z_i, is calculated using Equation 4.17.

$$Z_i = \Sigma A_{x,i}\left(\bar{y}_i - \bar{y}_{x,i}\right) \quad 4.17$$

Where: Z_i = Residual section modulus of the section at time i (mm^3)

The residual bending, $\varphi M_{n,i}$, and shear, $\varphi V_{n,i}$, capacities of the beam are then calculated using Equations 4.18 and 4.19.

$$\varphi M_{n,i} = \varphi k_1 k_8 k_{24} f_b Z_i \quad 4.18$$

$$\varphi V_{n,i} = \varphi k_1 f_s A_{s,i} \quad 4.19$$

Where:
$\varphi M_{n,i}$ = Residual bending capacity of the section at time i (kNm)
φ = Strength reduction factor
k_1 = Duration of load factor
k_8 = Stability factor
k_{24} = Size factor
f_b = Characteristic bending strength (MPa)
$\varphi V_{n,i}$ = Residual shear capacity of the section at time i (kN)
f_s = Characteristic shear strength (MPa)

An important property of LVL is the size factor, k_{24}. This factor is required as nominal bending and tension strengths are given for a member that was tested at a specific depth. The bending and tension strength of members larger than the test depth will be reduced. The size factor is used to quantify this reduction. Equation 4.20 is used to determine the value of the size factor.

$$k_{24} = \left(\frac{d_{test}}{d}\right)^{0.167} \quad 4.20$$

Where:
k_{24} = Size factor
d_{test} = k_{24} test depth (mm)
d = Individual component depth (mm)

NZS3603:1993 states that the test depth used in Equation 4.20 shall be 300 mm for both bending and tension. However, for NelsonPine LVL13 the test depth for tension and bending are 150 mm and 95 mm, respectively. The NelsonPine LVL13 values were used in the calculations for this research.

The individual component depth is the depth of the member being exposed to the loading action. That is, for bending, the entire member is undergoing bending so the individual component depth is

the depth of the beam. However, for tension in a box beam only the bottom flange will be acting in tension. As such, the individual component depth is only the largest dimension of the flange, i.e. the width of the flange.

Now the bending and shear demands on the beam are calculated. First the applied loads are determined using an appropriate loading standard. Equation 4.21 from AS/NZS 1170.1:2002 (Standards New Zealand, 2002b) is used for New Zealand structures.

$$q = G + \psi_l Q \tag{4.21}$$

Where: q = Applied loads (kPa)
G = Permanent actions (kPa)
ψ_l = Long-term load factor
Q = Imposed actions (kPa)

The uniformly distributed load acting on the beam is calculated by multiplying the applied loads by the tributary width of the beam. This is shown in Equation 4.22.

$$w = qW_{trib} \tag{4.22}$$

Where: w = Uniformly distributed load (kN/m)
q = Applied actions (kPa)
W_{trib} = Tributary width (m)

Equations 4.23 and 4.24 are then used to calculate the maximum bending, M^*, and shear, V^*, demands on the beam at mid-span and at supports respectively. As the post-tensioning system is not considered using this strategy the residual timber resists the entire load.

$$M^* = \frac{wL^2}{8} \quad 4.23$$

$$V^* = \frac{wL}{2} \quad 4.24$$

Where: M^* = Bending moment demand at mid-span (kNm)
L = Span of beam (m)
V^* = Shear force demand at supports (kN)

Equations 4.25 and 4.26 are used to check that the residual bending and shear capacities of the beam are greater than the respective demands.

$$M^* \leq \varphi M_{n,i} \quad 4.25$$

$$V^* \leq \varphi V_{n,i} \quad 4.26$$

Where: $\varphi M_{n,i}$ = Bending moment capacity at mid-span at time i (kNm)
$\varphi V_{n,i}$ = Shear force capacity at supports at time i (kN)

Assuming that beams act as solid members undergoing flexural bending may be non-conservative as they are constructed as hollow box beams so stresses in the flanges may exceed the strength in these smaller components of the beam. Therefore, it should be assumed that the top and bottom flanges act as individual compression and tension members respectively, and the stresses are checked to ensure that the strength of the flanges are greater than the respective applied stresses. This is especially important for small residual sections as crushing failures may occur in the top flange while failure may also occur when the bottom flange becomes too thin to carry the maximum tension stresses.

There are four design checks that are required to be completed to ensure the applied stress is not greater than the flange strength at any point, as explained in Section 4.1. These checks are undertaken for:

1. Compressive stress at centroid of top flange

$$\sigma_{f,c,i} \leq f_{c,i}$$

2. Tensile stress at centroid of bottom flange

$$\sigma_{f,t,i} \leq f_{t,i}$$

3. Compressive bending stress at extreme fibre of top flange

$$\sigma_{f,c,max,i} \leq f_{b,i}$$

4. Tensile bending stress at extreme fibre of bottom flange

$$\sigma_{f,t,max,i} \leq f_{b,i}$$

These checks are detailed in Equations 4.27 to 4.38. The concept of these checks is based on EN 1995-1-1:2004 (European Commission, 2004a), as illustrated in Figure 4.4. However, NZS3603:1993 (Standards New Zealand, 1993) is used to calculate the individual stresses used in these checks.

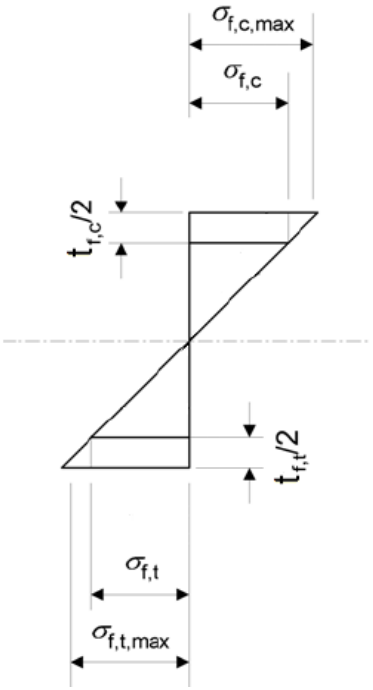

Figure 4.4 Basis of stress checks for box beams (European Commission, 2004a)

The mean flange compressive stress, which occurs at the centroid of the top flange, is checked to ensure that it is less than the residual compressive strength of the top flange. The mean flange compressive stress, $\sigma_{f,c,i}$, is calculated using Equation 4.27.

$$\sigma_{f,c,i} = \frac{M^* \left(\bar{y}_i - t_{f,top,i}/2\right)}{I_i} \quad 4.27$$

Where: $\sigma_{f,c,i}$ = Mean flange compressive stress at time i (MPa)

The residual compressive strength, $f_{c,i}$, is calculated using Equation 4.28.

$$f_{c,i} = \varphi k_1 k_8 f_c \quad 4.28$$

Where: $f_{c,i}$ = Residual compressive strength at time i (MPa)
k_1 = Duration of load factor
k_8 = Stability factor
f_c = Characteristic compressive strength (MPa)

N.B. The k-factors need to be calculated at the time step being considered.

The mean flange compressive stress is then checked against the residual compressive strength using Equation 4.29.

$$\sigma_{f,c,i} \leq f_{c,i} \quad 4.29$$

The mean flange tensile stress, which occurs at the centroid of the bottom flange, is checked to ensure that it is less than the residual tensile strength of the bottom flange. The mean flange tensile stress, $\sigma_{f,t,i}$, is calculated using Equation 4.30.

$$\sigma_{f,t,i} = \frac{M^* \left(D_i - \bar{y}_i - t_{f,bot,i}/2\right)}{I_i} \quad 4.30$$

Where: $\sigma_{f,t,i}$ = Mean flange tensile stress at time i (MPa)

The residual tensile strength, $f_{t,i}$, is calculated using Equation 4.31.

$$f_{t,i} = \varphi k_1 k_4 k_{24} f_t \quad 4.31$$

Where: $f_{t,i}$ = Residual permissible tensile stress at time i (MPa)
k_4 = Parallel support factor
k_{24} = Size factor
f_t = Characteristic tensile strength (MPa)

The mean flange tensile stress is then checked against the residual strength using Equation 4.32.

$$\sigma_{f,t,i} \leq f_{t,i} \qquad 4.32$$

The maximum flange compressive bending stress, which occurs at the extreme fibre of the top flange, is checked to ensure that it is less than the residual bending strength of the top flange. The maximum flange compressive stress, $\sigma_{f,c,max,i}$, is calculated using Equation 4.33.

$$\sigma_{f,c,max,i} = \frac{M^* \bar{y}_i}{I_i} \qquad 4.33$$

Where: $\sigma_{f,c,max,i}$ = Maximum flange compressive stress at time i (MPa)

The residual bending strength, $f_{b,i}$, is calculated using Equation 4.34.

$$f_{b,i} = \varphi k_1 k_4 k_5 k_8 k_{24} f_b \qquad 4.34$$

Where: $f_{b,i}$ = Residual compressive strength at time i (MPa)
k_5 = Grid system factor
f_b = Characteristic bending strength (MPa)

The maximum flange compressive stress is then checked against the residual bending strength using Equation 4.35.

$$\sigma_{f,c,max,i} \leq f_{b,i} \qquad 4.35$$

The maximum flange tensile stress, which occurs at the extreme fibre of the bottom flange, is checked to ensure that it is less than the residual bending strength of the bottom flange. The maximum tensile stress, $\sigma_{f,t,max,i}$, is calculated using Equation 4.36.

$$\sigma_{f,t,max,i} = \frac{M^* (D_i - \bar{y}_i)}{I_i} \qquad 4.36$$

Where: $\sigma_{f,t,max,i}$ = Maximum tensile stress at time i (MPa)

The residual bending strength, $f_{b,i}$, is again calculated using Equation 4.34.

Finally, the maximum flange tensile stress is then checked against the residual bending strength using Equation 4.37.

$$\sigma_{f,t,max,i} \leq f_{b,i} \qquad 4.37$$

The proximity of failure occurring due to the different loading actions, i.e. bending, shear, compressive stress and tensile stress, can easily be determined by dividing the demand by the respective residual capacity for each of the loading actions. Clearly, if any of the normalised demands are greater than 1.0 failure is predicted to occur. It is also useful to graphically represent the normalised demands. An example of the graph produced using normalised demands is shown in Figure 5.15. This is easily achieved if the residual section properties and capacity has been determined at each timestep, i.e. the second approach has been followed.

4.3 Calculation Method for Strategy 2: Fire Protected Post-Tensioning System

As well as assuming that second order effects are negligible and considering only a simply supported beam with a straight tendon initially, as shown in Figure 4.1, it is assumed the tendon remains at ambient temperature throughout the time period being considered. Further explanation of this assumption is provided in Section 7.3.

The same process is used to determine the residual section properties and bending and shear capacities of a timber box beam with a fire protected post-tensioning system, i.e. Equations 4.2 – 4.19 are repeated. However, the residual axial capacity of the beam, $\varphi N_{n,i}$, must also be calculated. This is achieved using Equation 4.38.

$$\varphi N_{n,i} = \varphi k_1 k_8 f_c A_i \qquad 4.38$$

Where:

$\varphi N_{n,i}$	=	Axial capacity at time i (kN)
φ	=	Strength reduction factor
k_1	=	Duration of load factor
k_8	=	Stability factor
f_c	=	Characteristic compressive strength (MPa)
A_i	=	Residual cross sectional area of the section at time i (mm^2)

Unlike in the design process for Strategy 1, the bending moment demand is resisted by both the timber and the post-tensioning system, as it has been protected from fire. As such, the bending moment acting on the timber cannot simply be determined using Equation 4.23.

The bending moment acting on the timber at mid-span, M_i^*, taking into account the resistance provided by the post-tensioning system, is calculated using Equation 4.39. This value is then used in the subsequent strength calculations.

$$M_i^* = M_q - M_{PT,i} \quad 4.39$$

Where: M_i^* = Bending moment acting on the timber at mid-span at time i (kNm)
M_q = Bending moment demand at mid-span (kNm)
$M_{PT,i}$ = Bending moment due to post-tensioning at time i (kNm)

The bending moment that results from the uniformly distributed load, M_q, is calculated in the same manner as Equation 4.23, as shown in Equation 4.40.

$$M_q = \frac{wL^2}{8} \quad 4.40$$

Where: w = Uniformly distributed load (kN/m)
L = Span of beam (m)

The bending moment due to the post-tensioning system, $M_{PT,i}$, is calculated using Equation 4.41. The post-tensioning force will be determined during the structural design.

$$M_{PT,i} = e_i F_{PT} \quad 4.41$$

Where: e_i = Eccentricity of the tendon at time i (mm)
F_{PT} = Post-tensioning force (kN)

The eccentricity of the tendon is the distance between the centroid of the section and the centroid of the tendon. The eccentricity of the tendon, e_i, is calculated using Equation 4.42, which is based on Figure 4.5. The initial eccentricity of the tendon will be determined during the structural design.

$$e_i = e_0 + \Delta\bar{y}_i - \delta_i \quad 4.42$$

Where: e_0 = Initial eccentricity of the tendon (mm)
$\Delta\bar{y}_i$ = Change in neutral axis depth at mid-span at time i (mm)
δ_i = Deflection of beam at mid-span at time i (mm)

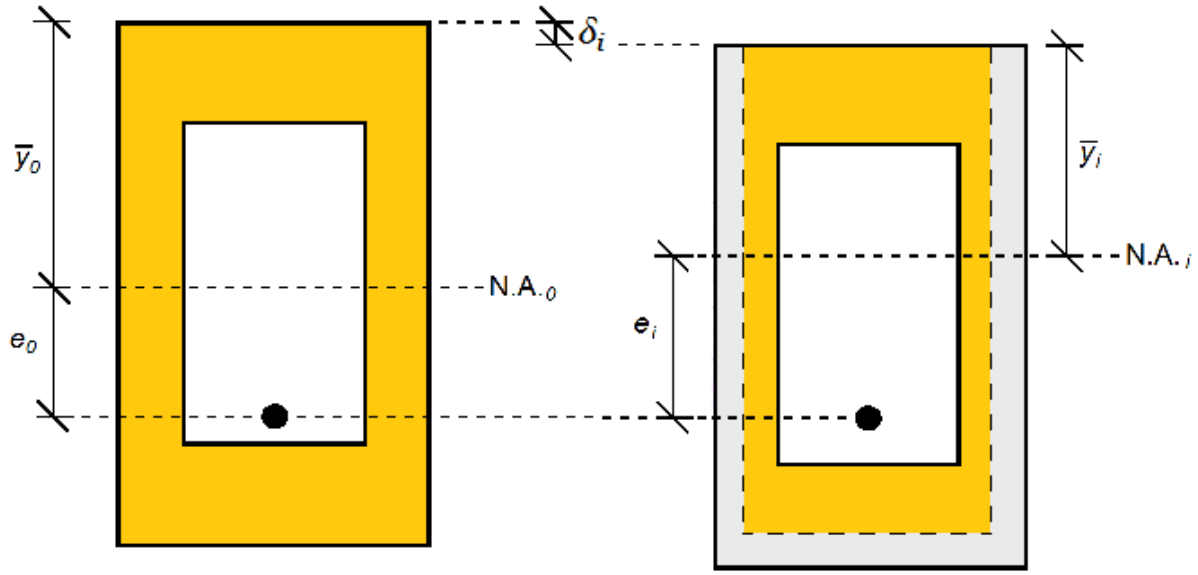

Figure 4.5 Tendon eccentricity for a full cross section and a deflected charred cross section

As the beam chars the neutral axis depth of the section changes because the beam is no longer symmetrical about the horizontal axis. This changes the eccentricity between the tendon and the neutral axis. The change in neutral axis depth, $\Delta\bar{y}_i$, is taken into account in Equation 4.43. The neutral axis depth is measured from the top fibre.

$$\Delta\bar{y}_i = \bar{y}_0 - \bar{y}_i \qquad 4.43$$

Where: $\bar{y}_0$ = Initial neutral axis depth (mm)

$\bar{y}_i$ = Neutral axis depth at time i (mm)

When the beam deflects during the fire exposure the straight tendon remains in its original position as it is unbonded along its span. As such, the mid-span deflection must be considered when calculating the eccentricity. The mid-span deflection of the beam is caused by the elastic gravity and shear deflections, which both deflect the beam downwards, and the hogging deflection from the post-tensioning system. These components of the mid-span deflection are shown in Figure 4.6.

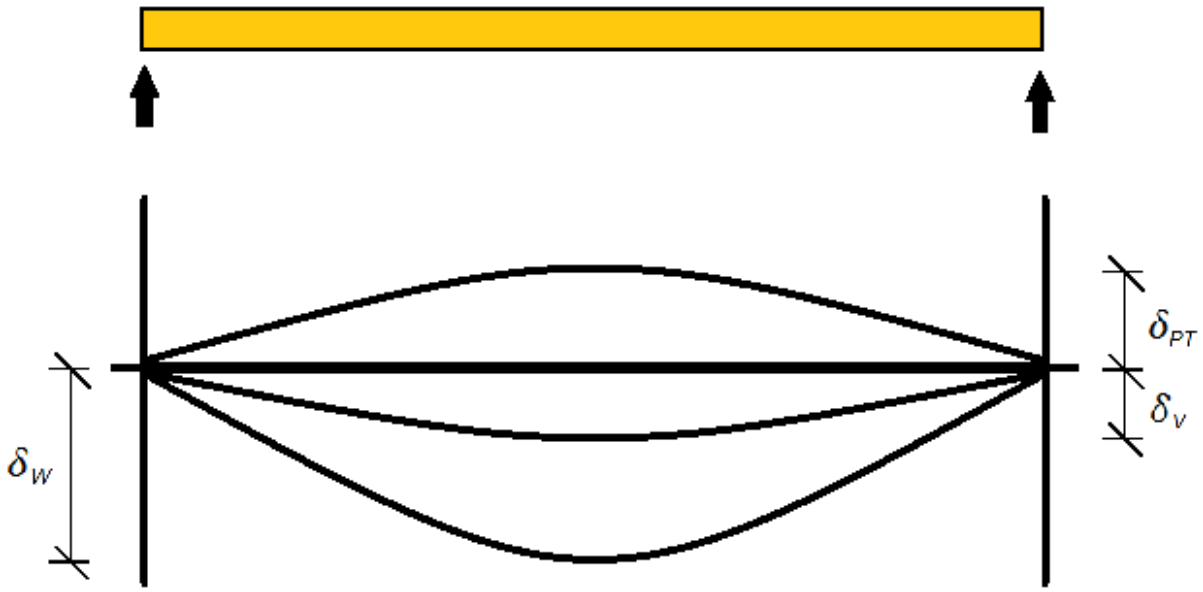

Figure 4.6 Deflection components of a post-tensioned beam

The mid-span deflection of the beam, δ_i, is calculated using Equation 4.44.

$$\delta_i = \delta_{w,i} + \delta_{V,i} - \delta_{PT,i} \qquad 4.44$$

Where: $\delta_{w,i}$ = Elastic gravity deflection at mid-span at time i (mm)
$\delta_{V,i}$ = Elastic shear deflection at mid-span at time i (mm)
$\delta_{PT,i}$ = Post-tensioning hogging deflection at mid-span at time i (mm)

The calculation method considers the elastic deflection caused by gravity loads, $\delta_{w,i}$, elastic shear deflection, $\delta_{V,i}$, and the hogging deflection due to the post-tensioning system, $\delta_{PT,i}$. All deflections are calculated for the residual section at mid-span.

Equation 4.45 is used to calculate the elastic deflection caused by gravity loads.

$$\delta_{w,i} = \frac{5\mathrm{w}L^4}{384EI_i} \qquad 4.45$$

Where: E = Elastic modulus of the section (GPa)
I_i = Second moment of area at mid-span at time i (mm^4)

Equation 4.46 (Blodgett, 1966) is used to calculate the elastic shear deflection.

$$\delta_{V,i} = \frac{wL^2}{8GA_{s,i}} \quad 4.46$$

Where: G = Shear modulus of the section (GPa)

$A_{s,i}$ = Residual shear area of the section at time i (mm^2)

Equation 4.47 (STIC, 2013) is used to calculate the hogging deflection due to the post-tensioning system. As Equation 4.47 requires the eccentricity to be known and deflection is a dependent variable used to calculate eccentricity in Equation 4.42 an iterative calculation is required.

$$\delta_{PT,i} = \frac{e_i F_{PT} L^2}{8EI_i} \quad 4.47$$

Equation 4.24 is again used to calculate the shear demand at the supports, i.e. the point of maximum shear force.

The axial demand on the beam, N^*, is taken from the post-tensioning force, as determined in the structural design of the beam. This is demonstrated in Equation 4.48.

$$N^* = F_{PT} \quad 4.48$$

Where: N^* = Axial demand (kN)

Next Equations 4.25 and 4.26 are used again to check that the residual bending and shear capacities of the beam are greater than the respective demands.

The residual axial capacity of the section is also checked using Equation 4.49.

$$N^* \leq \varphi N_n \quad 4.49$$

A combined bending-compression check is also performed. This is shown in Equation 4.50.

$$\frac{N^*}{\emptyset N_n} + \frac{M^*}{\emptyset M_n} \leq 1.0 \quad 4.50$$

Equations 4.27 to 4.37 are again used to check the stresses in the flanges. Again, the bending demand acting on the timber, i.e. allowing for the post-tensioning force, should be used.

As per Strategy 1, the normalised demands of each of the different loading actions, including compression and combined bending-compression, can easily be determined by dividing the demand by the residual capacity for each of the loading actions. Again failure is predicted to occur if any of the normalised demands are greater than 1.0, which can easily be displayed graphically if the residual section properties and capacities have been determined at each timestep. An example of the graph produced using normalised demands is shown in Figure 5.15.

4.4 Other Design Considerations

It has been assumed that the beams considered above are simply-supported with a straight tendon profile. However, it is likely that only a few post-tensioned timber box beams will fit into this category, with many more utilising either draped tendons or moment-resisting connections as part of a structural frame. The effects that these changes would have on the calculation method are described below.

4.4.1 Draped Tendons

The design of a beam with a draped tendon follows a similar methodology as to that detailed in Sections 4.2 and 4.3. Figure 4.7 shows a simply supported post-tensioned box beam with draped tendons.

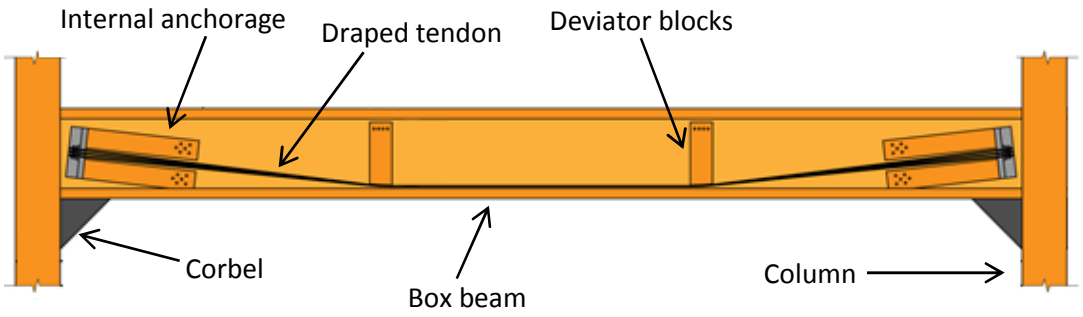

Figure 4.7 Post-tensioned box beam with a draped tendon (STIC, 2013)

The major difference that needs to be considered when designing a post-tensioned box beam with a draped tendon, rather than a straight tendon, is that the shear demand on the timber reduces over the length of the inclined tendon. The inclined tendon creates a vertical component of the post-tensioning force in the end regions of the beam. This decreases the shear demand on the timber in the areas where the tendon is inclined. This is demonstrated in the respective shear force diagrams for straight and draped tendons shown in Figure 4.8. These shear force diagrams display the post-tensioning forces only, with no applied loads on the beam.

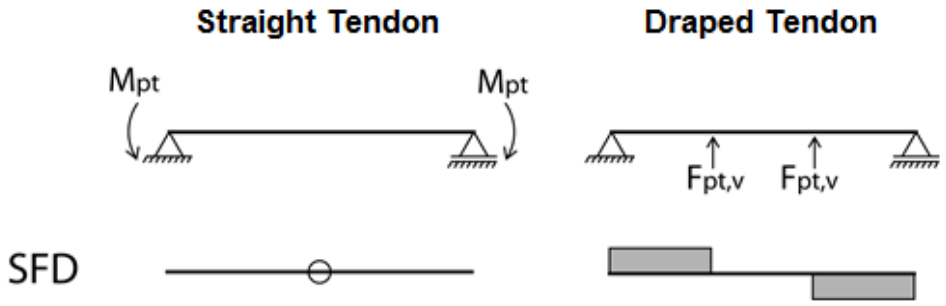

Figure 4.8 Shear force diagram for straight and draped post-tensioned beams (STIC, 2013)

Additional calculations can be completed to include the effect of the draped tendon profile, which may produce a more efficient design. This is achieved by calculating the shear demand on the timber in the region where the tendon is inclined, $V^*_{inclined}$, by subtracting the vertical component of the post-tensioning force from the total shear demand, as shown in Equation 4.51. For simplicity the designer can choose to conservatively ignore the effect of the draped tendons and the calculations detailed in Sections 4.2 and 4.3 can be followed.

$$V^*_{inclined} = \frac{wL}{2} - \mathrm{F}_{PT} \sin\theta \qquad 4.51$$

Where:
$V^*_{inclined}$ = Shear force acting on the timber with an inclined tendon (kN)
w = Uniformly distributed load (kN/m)
L = Span of beam (m)
F_{PT} = Post-tensioning force (kN)
θ = Angle between the tendon and horizontal

The calculation to determine the eccentricity of the tendon at mid-span will also change for a draped tendon. As the tendon is fixed in place by deviators the tendon will deflect with the beam.

Therefore, the deflection component, δ_i, of Equation 4.42 can be ignored, as shown in Equation 4.52.

$$e_i = e_0 + \Delta\bar{y}_i \qquad 4.52$$

Where: e_i = Eccentricity of the tendon at time i (mm)
e_0 = Initial eccentricity of the tendon (mm)
$\Delta\bar{y}_i$ = Change in neutral axis depth at mid-span at time i (mm)

The bending moment created by a draped tendon is different to that caused by a straight tendon, as shown in Figure 4.9.

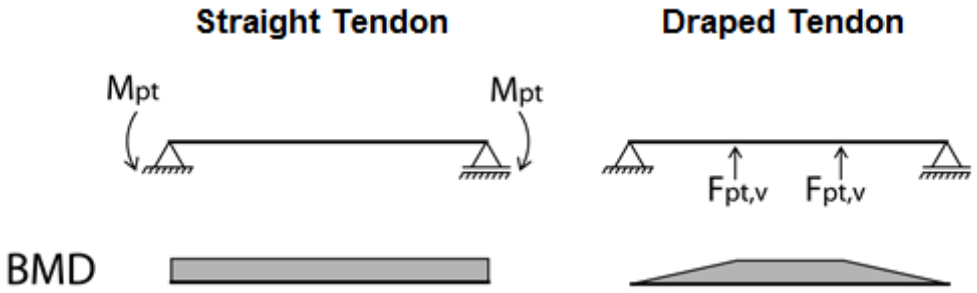

Figure 4.9 Bending moment diagram for straight and draped post-tensioned beams (STIC, 2013)

Clearly, the bending moment is reduced for the length of the tendon inclination. This reduction is caused by two principles. Firstly, the horizontal tendon force, which creates the resisting bending moment, will be reduced as the tendon acts at an angle to the horizontal. Much more significantly, the eccentricity between the tendon and centroid decreases.

As the post-tensioning system is used to resist the applied actions on the beams, which reduces the bending demand on the timber, the post-tensioning bending moment in the area of the inclined tendon, $M_{PT,inclined}$, needs to be calculated. This can be achieved using Equation 4.53.

$$M_{PT,inclined,i} = e_{inclined,i} \cdot F_{PT} \sin\theta \qquad 4.53$$

Where: $M_{PT,inclined,i}$ = Bending moment due to post-tensioning at time i (kNm)
$e_{inclined,i}$ = Eccentricity of inclined tendon at time i (mm)

N.B. The tendon height changes along the length of the inclined tendon so the eccentricity of the inclined tendon is dependent on the position along the beam being considered.

As the maximum bending demand will occur at mid-span of a member, i.e. outside the region where the tendon is inclined, it is unlikely that the reduced resistance provided by the post-tensioning system in the inclined region will be significant. As such, it is recommended that designers do not consider the reduction in the bending resistance provided by the post-tensioning system unless the actions on the beam are not uniformly distributed. Furthermore, if the first strategy is used in the design, i.e. the post-tensioning system is not specifically fire protected, the post-tensioning system is not considered so there is no difference between the design processes for straight or draped tendons.

4.4.2 Moment Resisting Frame Systems

Many post-tensioned timber buildings will utilise a moment resisting frame system. A moment resisting frame is shown in Figure 4.10. As described in Section 3.1, the maximum bending demand of a beam is reduced when incorporated in a moment resisting frame.

Figure 4.10 Moment resisting frame in a post-tensioned timber building

The negative moments at the ends of the beams, and corresponding reduced maximum bending demand, are ignored when the beams are assumed to be simply supported. This assumption was applied in the calculations detailed in Sections 4.2 and 4.3. If the beam is shown to be satisfactory when the beam is assumed to be simply supported it will also be satisfactory if the beam is part of a moment-resisting frame. However, a more efficient design may be produced if the effect of the frame is included, depending on the height of the tendon where it passes through the column. This can be achieved by using demands determined during the structural design, rather than calculating the demand on the beam for a simply supported beam, as shown in Equations 4.23, 4.24 and 4.38.

4.4.3 Columns and Walls

While the simplified calculation method proposed in this Chapter focuses on beams only, either as simply supported members or as part of a moment resisting frame, the same design approach used above can be used for other structural members, such as columns and walls. For post-tensioned timber buildings the same two design strategies outlined in Section 3.3.1 can be used to determine the fire resistance of columns and walls; the post-tensioning system is either unprotected or protected from fire exposure.

For both design strategies the design process is the same, albeit with additional equations and considerations as the post-tensioning system is to be protected. As per the fire resistance calculations for beams, the residual section dimensions of the member are determined at the FRR being considered, and are used to calculate the strength of the member. The demands acting on the members for fire conditions are calculated using the same loading configuration as for beams as required in AS/NZS 1170.1:2002 (Standards New Zealand, 2002b). The strength of the member is again checked against the demand at the FRR being considered to determine whether the member has sufficient fire resistance.

There is a significant difference between the fire resistance design of beams, columns and walls when the post-tensioning system is to be protected from fire exposure. The main purpose of the post-tensioning system in a wall is to resist lateral loads, usually seismic loads, whereas the post-tensioning system in a beam may resist both gravity and lateral loads. A column may be in either category. AS/NZS 1170.1:2002 (Standards New Zealand, 2002b) only requires a building to resist a "normal" wind load, as described in Section 2.1.5. The lateral load resistance of the structure post-fire exposure is expected to be sufficient to resist this "normal" wind load without the inclusion of the post-tensioning system. As such, it is expected the post-tensioning system in columns and walls is not required for these elements to achieve the required fire resistance. This is different to beams as the post-tensioning system may be required to resist gravity loads so may be required to be protected.

5 Furnace Testing

This Chapter presents the background, conduct and results of the full scale furnace test of a post-tensioned LVL box beam conducted on 11 July 2013 at the BRANZ campus at Porirua City, New Zealand. The background to the test, including the objectives of the test and a description of the testing apparatus, is stated in Section 5.1. The testing apparatus used in this test is described in Section 5.2. A description of the materials and test specimen used in the test are given in Sections 5.3 and 5.4 respectively. The testing procedure used is described in Section 5.5. The predicted behaviour of the test specimen, determined using the simplified calculation method, is presented in Section 5.6. The results obtained from the test, including key observations, are presented in Section 5.7.

5.1 Background

As discussed in Section 3.2.1, Spellman (2012) concluded that shear failure in post-tensioned timber box beams needed to be investigated in detail. Spellman's conclusion was the catalyst that directly led to this test being conducted. Consequently, this test was designed so that a shear failure mode occurred.

The two objectives of the full scale furnace test of a post-tensioned LVL box beam were:

1. To investigate the behaviour of post-tensioned LVL box beams, specifically the shear performance.
2. To obtain data to validate the simplified calculation method presented in Chapter 4.

5.2 Testing Apparatus

The test was conducted in accordance with ISO 834 (ISO, 1975), which is widely used throughout the world to assess and compare the fire resistance of construction elements. The time-temperature curve used in the test, i.e. the temperature that the specimen is exposed to, is referred to as the "standard fire" (Buchanan, 2001). Equation 5.1 is the expression used to determine the furnace temperature.

$$T = 345\ log_{10}(8t + 1) + T_0 \qquad 5.1$$

Where: T = Furnace temperature (°C)
t = Time (min)
T_0 = Ambient temperature (°C)

There are three main components of the furnace used in the test, shown in Figure 5.1; the furnace body, test frame and loading frame. The furnace body has an interior span of 3 m by 4 m and can be orientated either vertically, to test walls, or horizontally, to test floors and beams. The furnace was heated using a series of diesel injection burners. The furnace temperature was dependent on the rate of injection of diesel fuel. The internal pressure of the furnace was controlled to follow the standard. Twelve independent thermocouples were installed within the furnace and were used to measure the furnace temperature at various locations throughout the test.

Figure 5.1 ISO 834 Furnace

The test frame is a steel frame that is used to house the test specimen. The internal surfaces of the steel frame are lined with concrete to significantly reduce heat transfer through the steel that would reduce the efficiency of the furnace and create a hazard for the operators if the steel was not lined. The test frame was placed on the top of the furnace body using an overhead crane and is bolted in place. Figure 5.2 shows the test frame being lifted prior to being placed on the furnace body. An enclosure to contain the fire and its products was built on the test frame. This consisted of a 500 mm high hebel block surround, concrete lids, and a gypsum plasterboard lined light timber frame lid. Each element of the enclosure, as well as the test specimen, is shown in Figure 5.2.

Figure 5.2 Test frame being lifted

The light timber frame lid used to enclose the furnace above the test specimen, shown in Figure 5.3, allowed load to be applied directly to the test specimen. The light timber frame was made up of eight individual 0.55 m by 1.2 m rectangles that were built with 40 mm by 100 mm sawn timber. These rectangles were placed adjacent to each other but were not physically connected so that the deflection of the beam was not inhibited. Three layers of 13 mm gypsum plaster board were screwed into the timber frame to physically enclose the furnace. Kaowool, a ceramic fibre that is widely used as insulation material (Forman, 2010), was used to seal the interface between the different components of the test frame, such as between the concrete lids and the light timber frame lid. This can be seen in Figure 5.3.

Figure 5.3 Light timber frame lined with gypsum plasterboard

The loading frame, shown in Figure 5.4, was used to apply load to the specimen during the test. It was also lifted by an overhead crane and was bolted to the test frame. The load was applied using a 500 kN jack which was connected to a strong beam. The jack was able to apply the load through the use of a spreader beam, which created a four-point loading arrangement. Figure 5.5 shows a schematic of the bending moment and shear force diagrams for the LVL beam for this loading arrangement. A load cell measured the applied load and potentiometers were used to measure the mid-span deflection of the LVL beam. This data was recorded automatically in a laptop using "Universal Data Logging" (UDL) software.

Figure 5.4 Loading frame being lifted onto the furnace

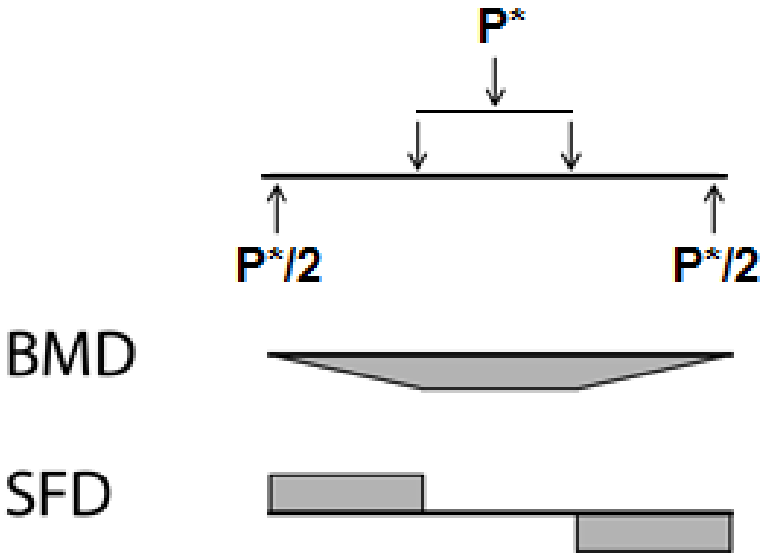

Figure 5.5 Loading arrangement for furnace test

5.3 Materials

The box beam tested was built from laminated veneer lumber (LVL). LVL is an engineered wood product that is made of multiple layers of approximately 3 mm thick timber veneers that are glued together to form a structural member. The grain of the timber runs parallel to the main axis of the member for increased strength in the main axis. Using multiple thin layers of timber distributes knots and other imperfections such that the strength and other properties of LVL are reliably higher than sawn timber. Radiata pine is the most commonly used species of timber used in the manufacture of LVL in New Zealand. (Buchanan, 2007)

NelsonPine LVL13 was the specific LVL type used to manufacture the test specimen. The properties of NelsonPine LVL13 are given in Table 5.1. Full product specification of NelsonPine LVL13 are given in the LVL Specific Engineering Design Guide (Nelson Pine Industries Ltd, 2012).

Table 5.1 Properties of NelsonPine LVL13

Modulus of elasticity	E	13.2 GPa
Modulus of rigidity	G	660 MPa
Bending strength	f_b	48 MPa
Tension strength parallel to grain	f_t	33 MPa
Compression strength parallel to grain	f_c	38 MPa
Shear strength	f_s	5.3 MPa

The tendons used were 7-wire strands with a nominal diameter of 12.7 mm. High strength steel was the material used. The nominal properties of the tendons are given in Table 5.2 (STIC, 2013).

Table 5.2 Nominal properties of tendons

Nominal diameter	d_{PT}	12.7 mm
Nominal area	A_{PT}	99.9 mm
Modulus of elasticity	E_{PT}	200 GPa
Yield strength	f_y	1520 MPa
Yield force	F_y	152 kN
Maximum design force	$0.9F_y$	137 kN

The maximum design force is included in Table 5.2 as a tendon force greater than this value creates a safety hazard. This maximum force should not be exceed in the design or construction.

Figure 5.6 shows the tendon anchorage setup used in the furnace test. Mild steel end plates and "barrel and wedge" type tendon anchorages were used in the post-tensioning system. As the design and performance of the post-tensioning system itself was not being investigated a 26 mm thick plate with a nominal yield strength of 300 MPa was conservatively used. Detailed observations were not made regarding the performance of the post-tensioning system. The tendons were run through load cells, which were placed between the tendon anchorages and end plates, so that the tendon forces could be recorded. This data was also recorded using UDL software on a laptop.

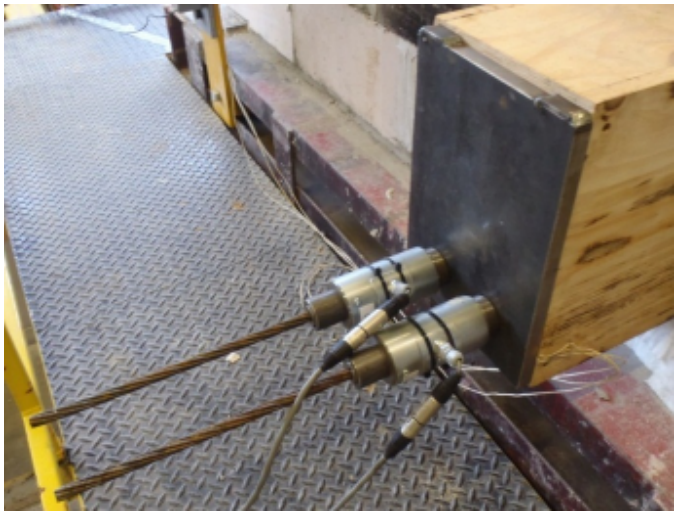

Figure 5.6 Tendon anchorage setup

K-type thermocouples were used to measure temperatures at different locations on the test specimen. A thermocouple attached to a tendon is shown in Figure 5.12. Thermocouples are an inexpensive and reliable device to measure a wide range of temperature, approximately –200°C to +1300°C. Thermocouples are able to measures temperature as a current is produced across dissimilar metals when a temperature difference occurs within the thermocouple. The sensitivity of K-type thermocouples is approximately 41 µV/°C (Park et al., 1993).

5.4 Specimen Details

A 5.0 m long LVL box beam was used in the furnace test, as shown in Figure 5.7. The span of the beam in the test frame was 4.2 m. The cross section of the beam is shown in Figure 5.8. This cross section, in conjunction with the loading arrangement, was designed for shear failure to occur prior to any other failure mode.

Figure 5.7 LVL beam used in furnace test

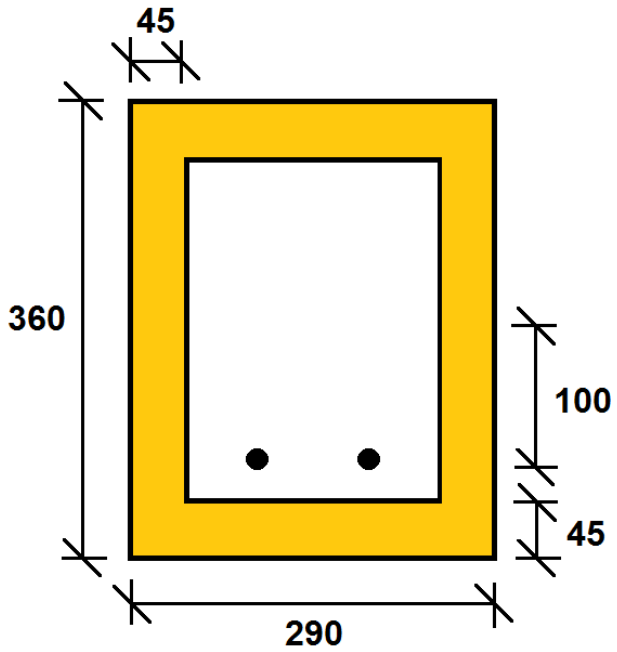

Figure 5.8 Cross section of box beam used in the furnace test

28 mm of timber was milled from the sides of the beam along the 250 mm closest to the ends of the beam, as shown in Figure 5.8. This section was milled to reduce the inherent shear reinforcement that would be provided by the timber that extended outside the beam, which is not exposed to fire and hence does not char away. This timber is undesirable as it may increase the shear strength of the beam and prevent shear failure, the desired failure mechanism, from occurring. A thickness of 28 mm was used as this represented the assumed char layer depth for a 30 minute fire, which was the expected failure time for the beam.

Figure 5.9 Milled timber at end of beam

N.B. The solid line running longitudinally on the top surface of the beam is a local defect and did not affect the performance of the beam.

Two 12.7 mm tendons were used in the test specimen. These were placed 100 mm below the centroid of the section, i.e. the initial tendon eccentricity was 100 mm. Two tendons were used to ensure the maximum design force was not exceeded. The tendons were offset 50 mm from the vertical centreline of the section to accommodate the load cells. The tensioning of the tendons was completed using a manual pneumatic jack, as shown in Figure 5.10. The tendon forces were 52 kN and 57 kN, which is significantly below the maximum design force, giving a total tendon force of 107 kN. The tendon forces were not equal due to constructability issues but this did not affect the performance of the beam. The tensioning of the tendons was completed after the test frame had been placed on top of the furnace body but prior to the loading frame being attached.

Figure 5.10 Tendon stressing jack

In order to achieve shear failure in the test specimen a spreader beam with a span of 2.5 m was used so that the maximum bending moment demand was relatively low compared to the shear demand.

The loading jack applied a 100 kN load to the spreader beam system, although the actual load applied varied between 98 kN and 101 kN. The load was transferred to the LVL beam through the spreader beam system. Holes were cut through the gypsum plasterboard so the loading points acted directly onto the LVL beam. Kaowool was used to seal any potential gaps around the loading points. This loading arrangement is shown in Figure 5.11.

Figure 5.11 Loading arrangement for furnace test

Three thermocouples were attached to each tendon to record the tendon temperature, as shown in Figure 5.12. These were located at mid-span and 1.5 m from the each end of the beam, which corresponded to 700 mm inside the furnace. Thermocouples were also attached to the inside surface of the beam 1.2 m from each end of the beam, i.e. 400 mm inside the furnace, to record the temperature of the inner layer of the timber.

Figure 5.12 Tendon with attached thermocouple

5.5 Testing Procedure

In accordance with ISO 834, the loading jack applied the 100 kN load to the LVL beam, through the spreader beams, 30 minutes prior to the start of the test. The furnace pressure, therefore the rate of diesel inflow and furnace temperature, was controlled by a BRANZ technician to ensure the temperature remained within the specified limits of the ISO 834 time-temperature curve. The furnace during the test is shown in Figure 5.13.

Figure 5.13 Furnace during test

After failure of the LVL beam occurred the applied load was removed and the test frame was unbolted and lifted from the furnace body. This was done to cool and safely lower the test frame and allow the test specimen to be inspected. Figure 5.14 shows the test frame shortly after being lifted from the furnace body. The combustion of the timber has ceased at this point but a hot smoke layer was formed at the interface between the bottom surface of the test frame and the surrounding atmosphere.

Figure 5.14 Testing frame after removal from furnace

Cooling of the specimen was achieved using hand held water hoses. This process of removing and cooling the beam was done as quickly as possible to minimise charring after failure of the LVL beam occurred. This process took four minutes.

5.6 Predicted Behaviour

The performance of the LVL beam was predicted using the simplified calculation method described in Chapter 4. The inputs used in the calculations were the known material properties and section dimensions, as described in Sections 5.3 and 5.4, respectively, and the applied load and total tendon force, as shown in Table 5.3.

Table 5.3 Input parameters for furnace test

Parameter	Symbol	Input value
Applied load	P^*	100 kN
Tendon force	F_{PT}	107 kN

An expected failure time of 29 minutes was calculated for this test. The parameters that describe the behaviour of the LVL beam at the predicted failure time, i.e. at 29 minutes, are presented in Table 5.4. As the shear capacity is lower than shear demand it is predicted that shear failure would occur.

Table 5.4 Behaviour parameters of furnace test at predicted failure time

Parameter	**Demand**	**Capacity**
Failure time	$T_{failure} = 29\ min$	–
Bending demand	$M_q = 43\ kNm$	–
Hogging bending moment	$M_{PT} = -14\ kNm$	–
Bending	$M^* = 29\ kNm$	$\emptyset M_n = 74\ kNm$
Shear	$V^* = 50\ kN$	$\emptyset V_n = 50\ kN$
Axial	$N^* = 107\ kN$	$\emptyset N_n = 915\ kN$
Top flange compressive stress	$\sigma_{f,c} = 9\ MPa$	$f_c = 38\ MPa$
Bottom flange tensile stress	$\sigma_{f,t} = 15\ MPa$	$f_t = 31\ MPa$
Maximum compressive stress	$\sigma_{f,c,max} = 11\ MPa$	$f_b = 39\ MPa$
Maximum tensile stress	$\sigma_{f,t,max} = 16\ MPa$	$f_b = 39\ MPa$
Mid-span deflection	$\delta = 16\ mm$	–

As suggested in Chapter 4, the normalised demand on the beam, i.e. the demand divided by the respective residual capacity for each of the loading actions, was calculated for the duration of the fire. This is graphically represented in Figure 5.15, showing that this beam is much more critical in shear than in bending or axial load.

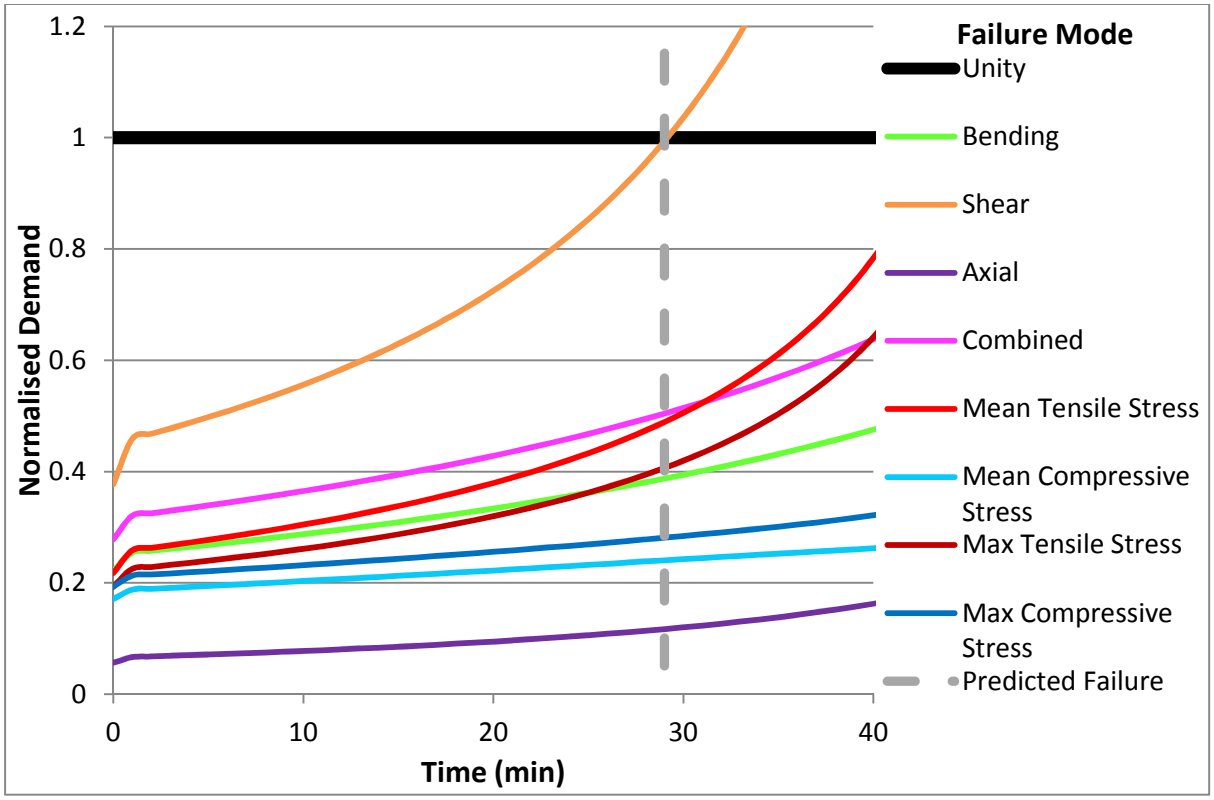

Figure 5.15 Normalised demand of LVL beam during furnace test

5.7 Experimental Results

5.7.1 General Observations

During the early stages of the test significant volumes of smoke unexpectedly leaked around the steel anchorage plates. Upon observing the smoke leakage, gaps between the LVL beam and the anchorage plate at both ends were sealed using a fire-resistant filler material. This is shown in Figure 5.16. Sealing these gaps blocked the flow path that allowed the ingress of hot smoke into the beam cavity and subsequently through the ends of the beams. Further discussion of the implications of this leakage is presented in Section 5.7.3.

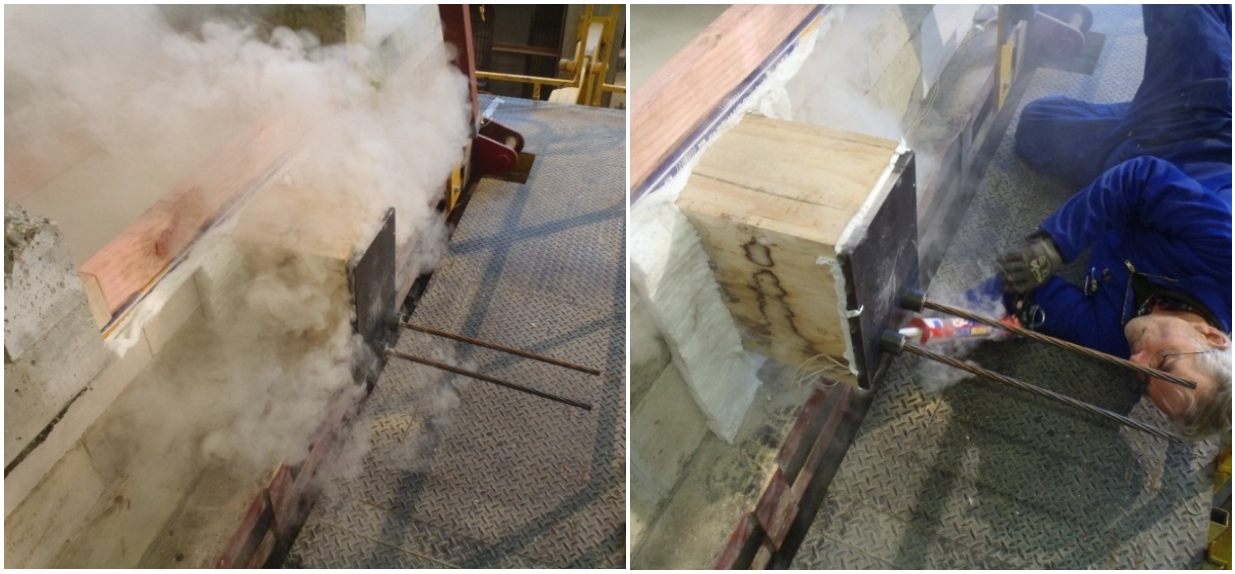

(a) Smoke leaking from tendon anchorage (b) Sealing gaps at tendon anchorage

Figure 5.16 Smoke leaking from ends of beam

The LVL beam could be seen to be charring throughout the test. This was observed through the furnace viewing window, as shown in Figure 5.17. However, after failure occurred and the testing frame was lifted combustion ceased, as seen in Figure 5.14. This was unexpected as previous full scale furnace tests of LVL specimens underwent flaming combustion after being lifted from the furnace until water was applied to the sample by the BRANZ technicians (O'Neill, 2008, Spellman, 2012).

Figure 5.17 View of charring LVL beam through furnace viewing window

The most important observation from the furnace test was that a shear failure mode occurred. The deflected shape of the failed beam, seen in Figure 5.18, illustrates that shear failure occurred in the region between the loading point and the beam support. Figure 5.19 provides a closer view of the region of failure. Six major horizontal cracks occurred across the entire depth of the beam at regular intervals of approximately 40 mm. The cracks were largest under the loading point, which also corresponded with the maximum localised deflection. The shear cracks were approximately 1000 mm in length. The shear cracks did not extend into the timber at the support, i.e. the timber that had been protected from fire exposure by the test frame was not charred. This timber was also not in the region of timber that had been milled so was 45 mm thick. It is this thicker timber that provided additional shear reinforcement that prevented the shear cracks from propagating to the end of the beam. This is further discussed in Section 7.4.

Figure 5.18 LVL beam after shear failure

Figure 5.19 Region of failure

N.B. The beam is shown upside down in Figure 5.19

Failure of the LVL beam occurred 29 minutes after the start of the test. The failure time was determined through observations of loud noises of timber breaking suddenly and obvious movement of the test specimen and loading frame. These observations were strongly supported by a large increase in recorded downwards deflection, shown in Figure 5.26, a reduction in recorded applied load and recorded tendon force, shown in Figure 5.23, each of which occurred after approximately 29 minutes.

The actual failure time was the same as the predicted failure time of 29 minutes. This provides very good validation of the proposed simplified calculation method, which was used to determine the predicted failure time. Further discussion of the validity of the simplified calculation method is presented in Section 7.3.

The residual cross section of the beam is shown in Figure 5.20. The char depth for both webs and bottom flange was approximately 25 mm. This corresponds to a char rate of 0.86 mm/min, which is greater than the assumed char rate of 0.70 mm/min. However, after adding the zero strength layer to the assumed char rate the actual char depth is less than the predicted char depth, which was 28 mm. Therefore, the assumed char rate with the zero strength layer included was conservative for this test. This result supports the use of the assumed char rate as stated in Section 4.2.

Figure 5.20 Residual cross section of LVL beam

5.7.2 Furnace Temperature

The furnace temperature during the test is presented in Figure 5.21. The ISO 834 time-temperature curve and limits that must be adhered to are also displayed in Figure 5.21. The furnace temperature closely followed the ISO 834 time-temperature curve and remained within the limits for the duration of the test. As such, this test adhered to the ISO 834 standard so the results obtained are valid to be used in comparison with the FRR of other construction elements.

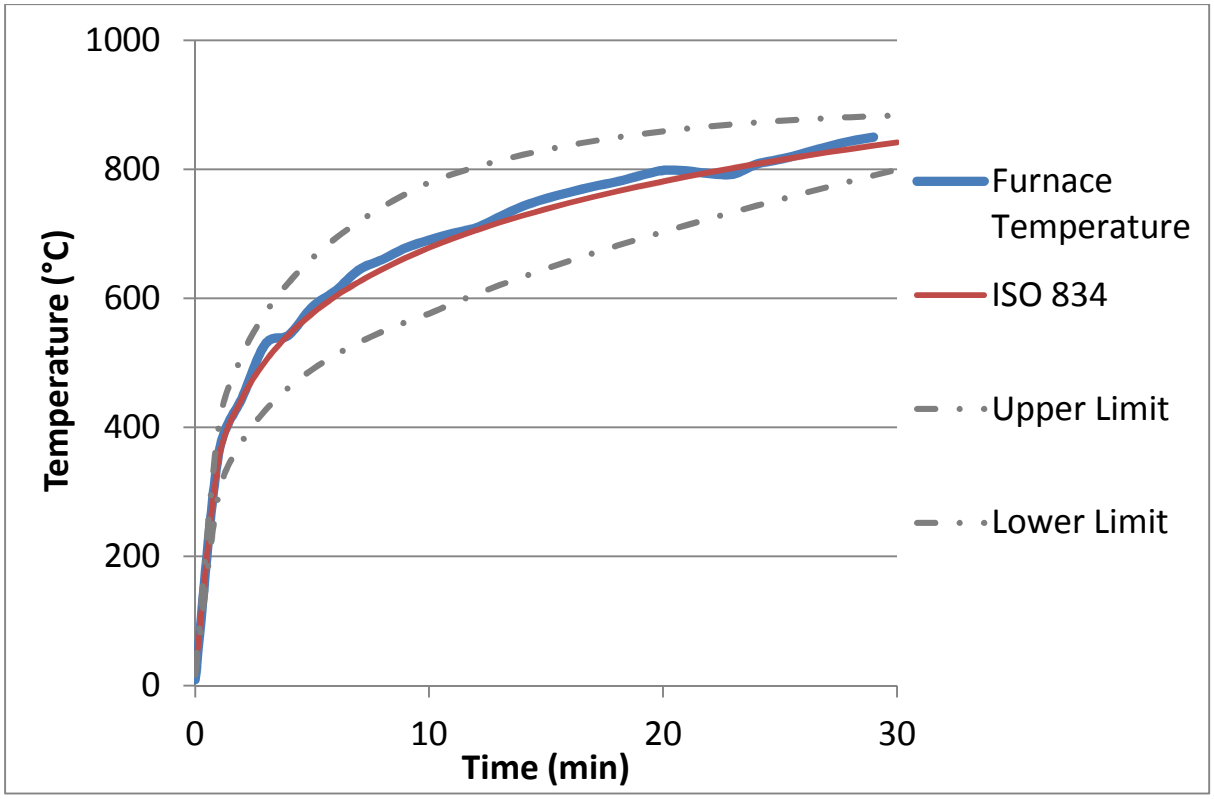

Figure 5.21 Time-temperature graph for the furnace test

5.7.3 Tendon Temperature

The temperature profiles of the tendons during the furnace test are presented in Figure 5.22. As three thermocouples were attached to each tendon three temperature profiles are presented for each tendon.

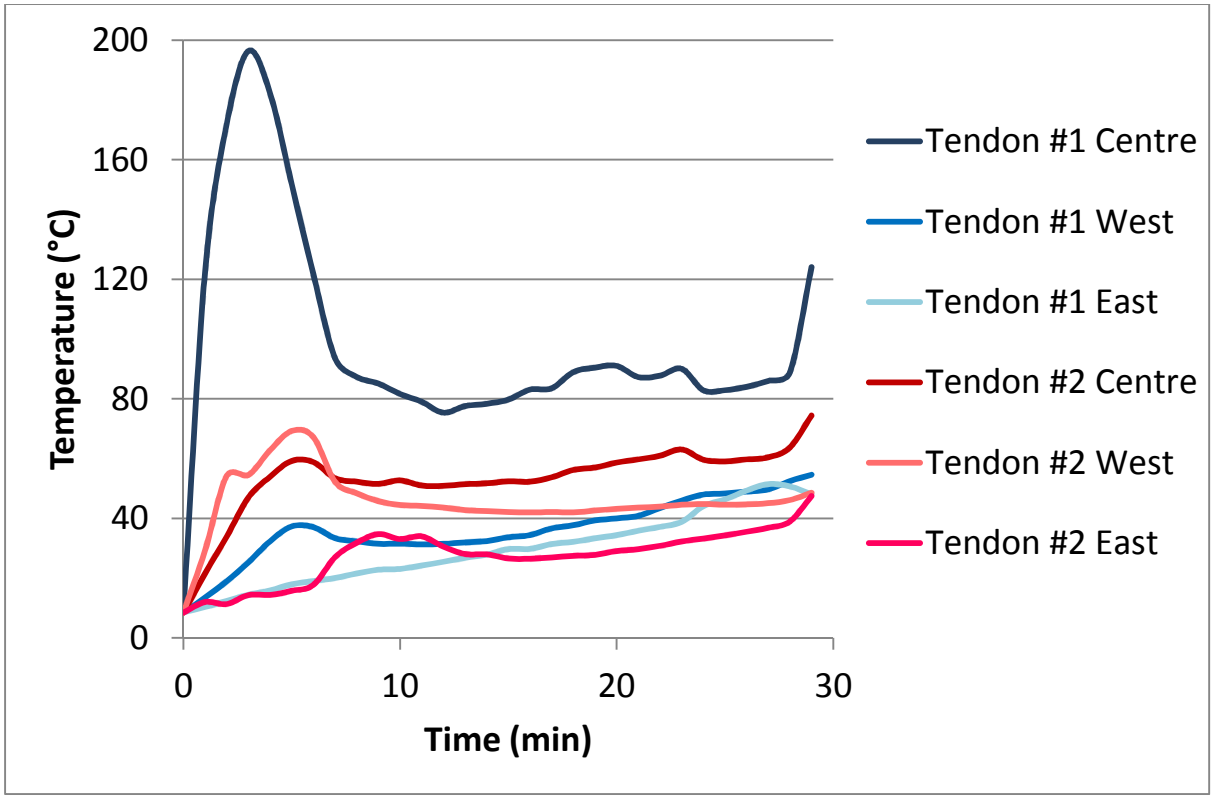

Figure 5.22 Tendon temperature

The tendon temperature quickly increased and peak values were recorded approximately five minutes after the start of the test for the majority of the thermocouples. The centre thermocouple on tendon #1 experienced the greatest temperature rise, peaking at 196°C. After the recorded peaks the tendon temperature decreased, but it did not drop back to ambient.

It is believed that the rapid increase in tendon temperature was caused by a hole in the beam which allowed hot smoke to enter the cavity of the box beam. It is assumed that the centre thermocouple of tendon #1 was in line with the hole and a jet of hot gases impinged directly on the thermocouple resulting in high levels of convective heat transfer. This theory is supported by the large volumes of smoke that leaked from the ends of the beams, as described in Section 5.7.1. Furthermore, the decrease in tendon temperature corresponds to the sealing of the gaps around the anchorage plates.

The temperature increase at all locations was relatively minor after the end plates had been sealed and the temperature did not exceed 90°C until failure occurred. This is considerably less than 150°C, which is the temperature at which the strength of prestressing steel is affected (Buchanan, 2001). Therefore, the strength of the tendon will be unaffected by a minor increase in temperature. This supports the assumptions used in the design strategy that tendon temperature remains at ambient temperature during a fire.

5.7.4 Tendon Force

The tendon force for each tendon and a total tendon force are shown in Figure 5.23. A decrease of approximately 3 kN occurred in each tendon in the first five minutes of the test. It is believed that this was again caused by the ingress of hot gas into the beam cavity as the tendon force ceased to drop after the anchorage plates were sealed.

During the time from the sealing of the end plates until failure occurring the tendon force increased slightly, approximately 2 kN in total. This is believed to be caused by the deflection of the beam, which elongated the tendon, increasing its strain and therefore increasing the tendon force, albeit to a small degree.

The fact that there was very little change in the tendon force for the majority of the test, rather than a continued decrease, demonstrates that second order effects have a negligible effect on the performance of a post-tensioned timber beam. This validates the assumption used in the simplified calculation method to not include second order effects. Furthermore, it is likely that the tendon force would not have decreased until failure occurred if the ingress of smoke did not occur. This demonstrates that for a beam with a protected post-tensioning system the assumption to use the ambient temperature tendon force is valid.

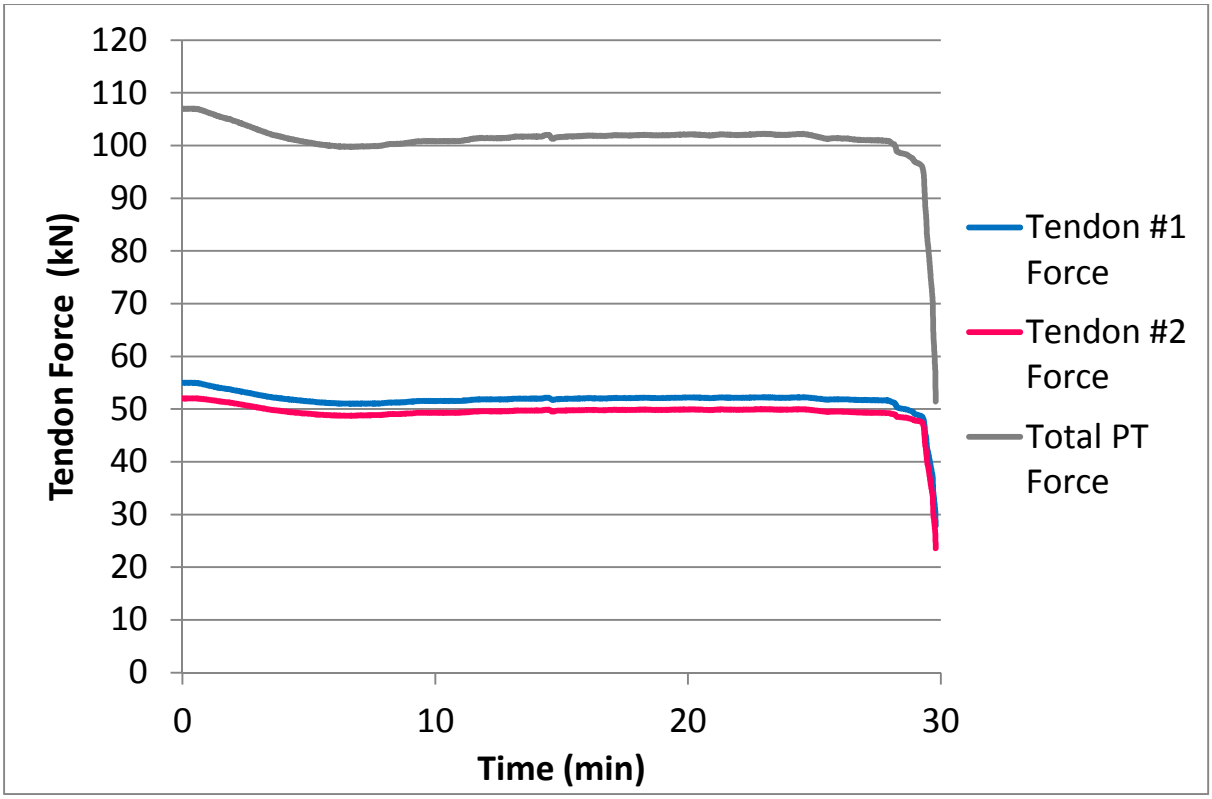

Figure 5.23 Tendon force

5.7.5 Tendon Temperature and Force

Figure 5.24 superimposes the mean tendon temperature and the tendon force for each tendon. This highlights that the slight decrease in tendon force corresponds to the tendon temperature increase during the early stages of the test. The gradual increase in tendon temperature during the majority of the test can be seen to have a negligible impact on the tendon force.

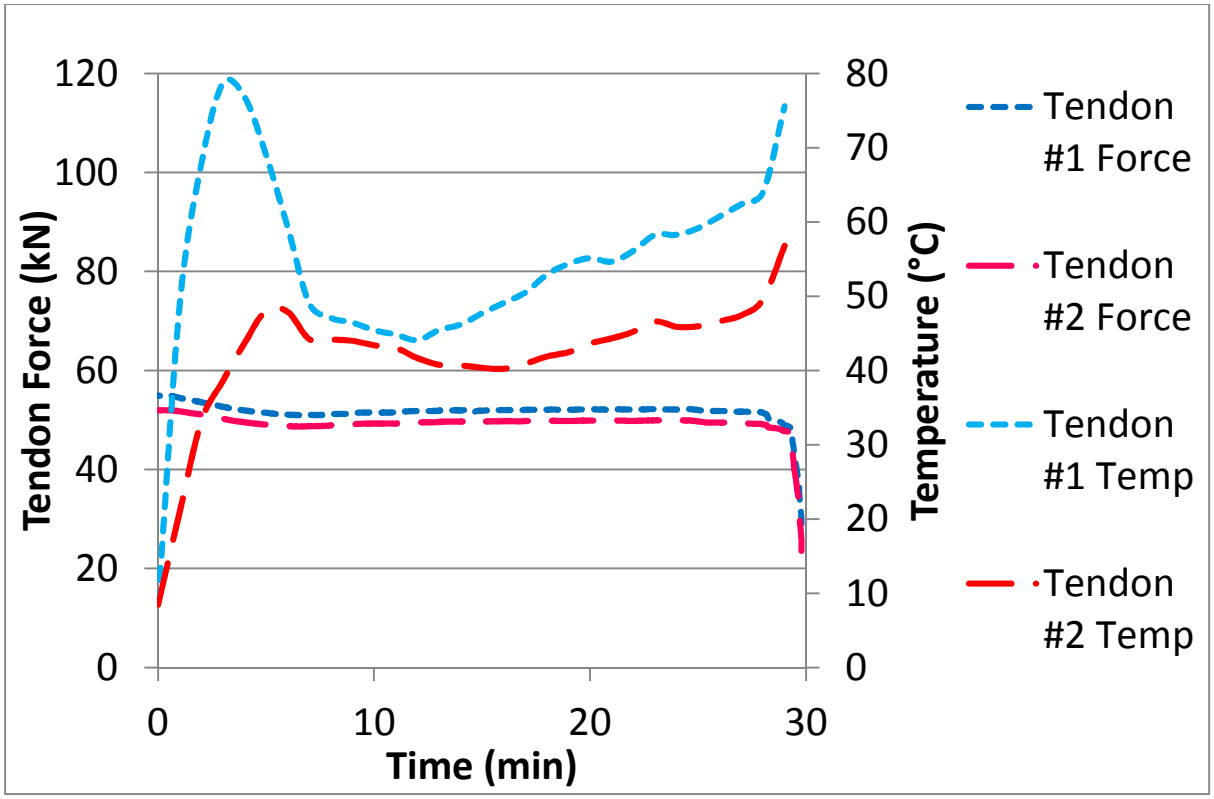

Figure 5.24 Tendon temperatures and forces

5.7.6 LVL Beam Temperature

The temperature of the inside surface of the LVL beam is shown in Figure 5.25. The temperature gradually increased during the test and reached a maximum value of less than 50°C. The increase in timber temperature appears to demonstrate that the depth of the heat affected zone of timber is greater than 45 mm, as the temperature increased immediately. This does not agree with Janssens and White (1994) or Lache (1992). However, it is believed that the increase in temperature was not caused by conductive heat transfer through the wood but was instead caused by the ingress of hot smoke into the beam cavity. This is supported by the presence of fluctuations in the temperature recorded using the west thermocouple during the first five minutes of the test, i.e. prior to the end plates being sealed.

The relatively small increase in timber temperature would not have been sufficient to cause more than negligible changes in the properties of the LVL. This supports the assumption that the ambient temperature properties of any timber below the char layer can be used.

The small increase in timber temperature also supports the assumption used in the simplified calculation method that the tendon remains at ambient temperature. Disregarding the ingress of hot smoke into the beam cavity, heat transfer through the timber beam must occur prior to heat being transferred to the tendon. The timber temperatures recorded in this test, even when considering the hot smoke ingress, were not sufficient for heat transfer to the tendon from the timber to be more than negligible, hence the assumption that the tendon temperature remains ambient is valid.

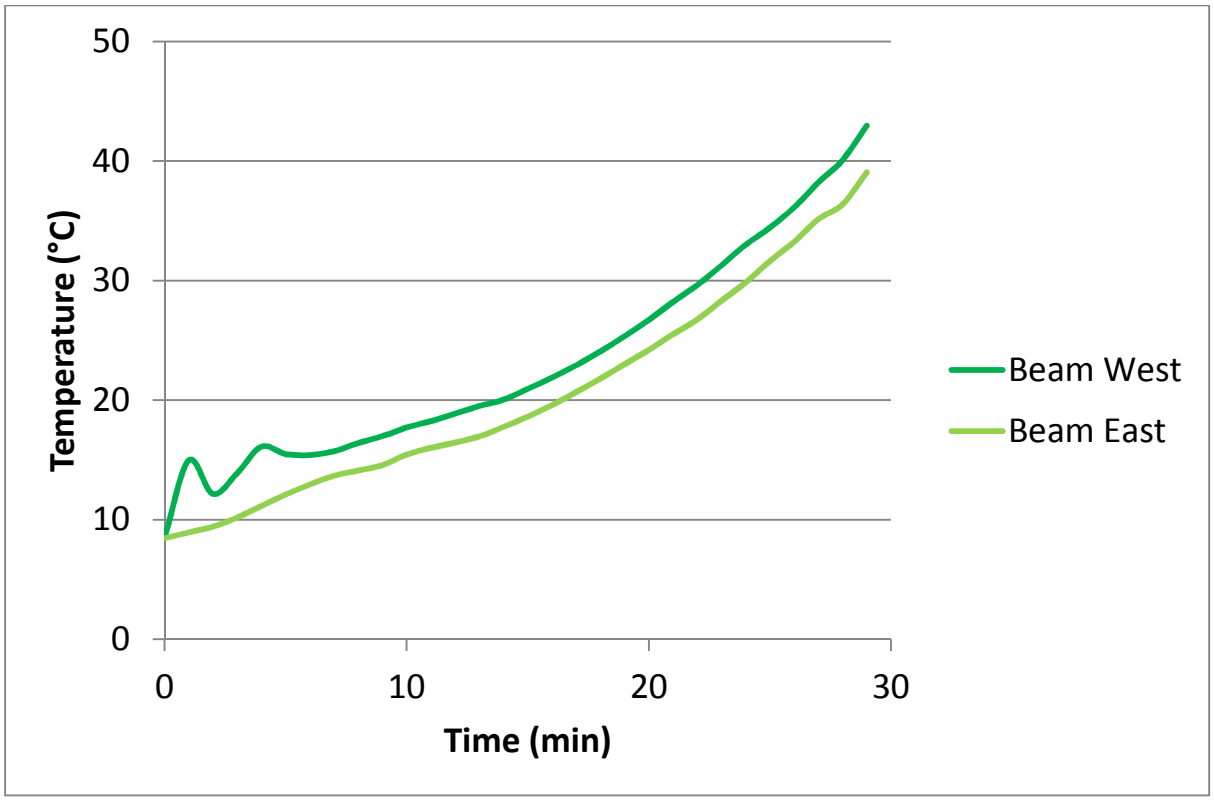

Figure 5.25 Timber temperature

5.7.7 Mid-span Deflection

The mid-span deflection of the LVL beam during the furnace test is shown in Figure 5.26. The predicted mid-span deflection of the LVL beam, 8 mm at 27 minutes, was significantly less than the actual mid-span deflection, approximately 20 mm at 27 minutes. As deflection is not a criterion for fire resistance this result, although not desirable, does not have a significant impact on the validity of the simplified calculation method. The under-predicted mid-span deflection will affect the tendon eccentricity used when calculating the hogging bending moment caused by the tendon. However, the magnitude of the difference between the actual and predicted mid-span deflections is small enough when compared to the initial tendon eccentricity that the hogging bending moment will be sufficiently accurate for the simplified calculation method. Future research, including further investigation of mid-span deflections and numerical modelling of post-tensioned timber box beams, should be conducted. This is discussed further in Section 7.3.

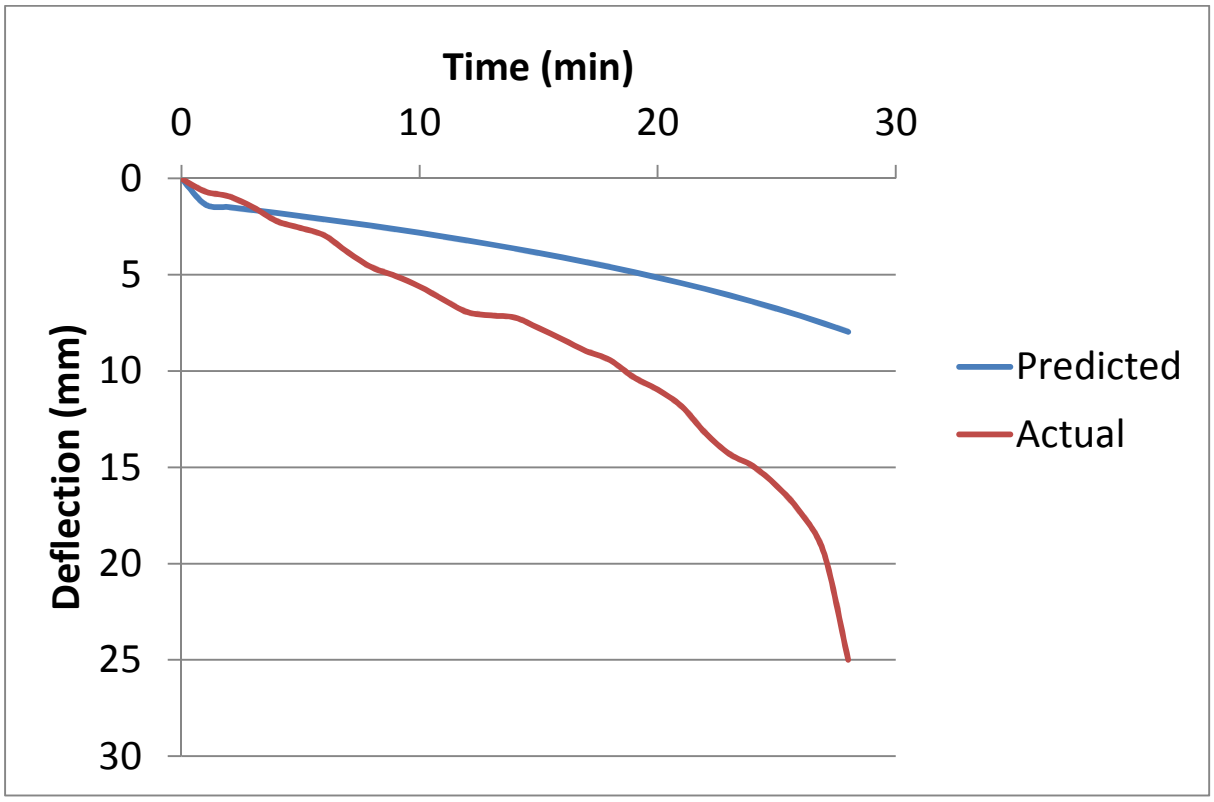

Figure 5.26 Mid-span deflection

6 Ambient Temperature Testing

This Chapter presents the background, conduct and results of four full scale tests of LVL box beams conducted in August and September 2013 and at the University of Canterbury Structures Laboratory. The background to the tests, including the objectives of the tests and a description of the testing apparatus, is stated in Section 6.1. The testing apparatus used in these tests is described in Section 6.2. A description of the materials and test specimens used in the tests are given in Sections 6.3 and 6.4, respectively. The testing procedure used is described in Section 6.5. The predicted behaviour of the test specimens, determined using the simplified calculation method, is presented in Section 6.6. The results obtained from the tests, including key observations, are presented in Section 6.7.

6.1 Background

The ambient temperature tests were also conducted on the basis of Spellman's conclusion that shear failure in post-tensioned timber box beams needed to be investigated in detail. The ambient temperature tests were conducted, rather than multiple full scale furnace tests, as the cost of conducting multiple full scale furnace tests was prohibitive. Each of the ambient temperature tests were designed so that a shear failure mode occurred.

The two objectives of the full scale ambient temperature tests of LVL box beams were:

1. To investigate the behaviour of LVL box beams, specifically the shear performance.
2. To obtain data to validate the simplified calculation method presented in Chapter 4.

6.2 Testing Apparatus

The tests were conducted in an Avery Universal Testing machine, commonly referred to as "The Avery". The Avery, shown in Figure 6.1, has a capacity of 1000 kN. The main elements of The Avery are the hydraulic loading platform, strong floor, strong frame and control station.

Figure 6.1 Avery Universal Testing machine

The hydraulic loading platform is cast into the floor and moves upwards to apply loads. As such, the applied loads act in the direction opposite to gravity. This loading arrangement is shown in Figure 6.2. The self-weight of the LVL beam is negligible relative to the forces applied so the effect of loading the LVL beam "upside down" is not considered in any further detail during this research.

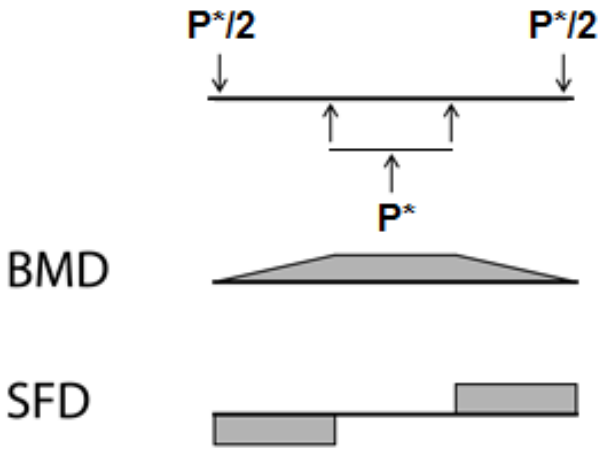

Figure 6.2 Loading arrangement for ambient temperature tests

A 3.0 m long steel spreader beam with two loading points was placed on the loading platform to achieve four-point loading. Two 300 mm x 300 mm x 18 mm steel plates, which were pinned to allow rotation to occur as the beam deflected, were used as the loading points. The loading points were bolted to the spreader beam at the spacing required for each test.

The strong floor was used to restrain the test specimen during the test in conjunction with a series of steel elements, including two 50 mm diameter threaded steel rods, rectangular hollow sections, a parallel flange channel and a 20 mm thick steel plate. This restraint system is shown in Figure 6.3. The steel plate was used to distribute the applied load so crushing of the LVL, which was loaded perpendicular to the grain across the flange, was minimised.

Figure 6.3 Restraint of LVL beam

The strong frame of the Avery was used as a stationary point to which a potentiometer could use as a reference point in order to record mid-span deflection, as shown in Figure 6.4. The deflection data was recorded automatically in a laptop using UDL software.

Figure 6.4 Potentiometer measuring mid-span deflection against stationary strong frame

The control station, seen on the right of Figure 6.1, houses the manually operated, analogue control mechanism that is used to set the applied load. This includes both the rate at which loading occurs and the magnitude of the applied load. The applied load was also recorded automatically using UDL software.

6.3 Materials

The materials used in the ambient temperature tests were the same as those used in the furnace test, i.e. NelsonPine LVL13, 7-wire high strength steel tendons, mild steel plates and barrel and wedge anchorages. A full description of these materials is given in Section 5.3.

6.4 Specimen Details

The dimensions of the each of the four LVL beams tested are shown in Figure 6.5. The first ambient temperature test was called Test 2 to prevent confusion with the full scale furnace test.

Post-tensioning was only used in Test 2. The initial tendon eccentricity was 100 mm and a tendon force of 94 kN was used.

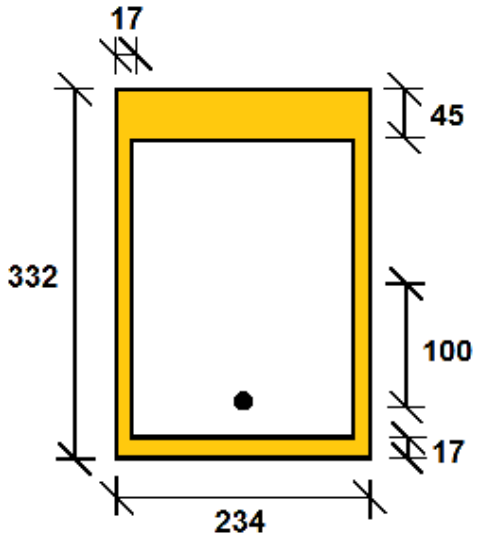

(a) Test 2

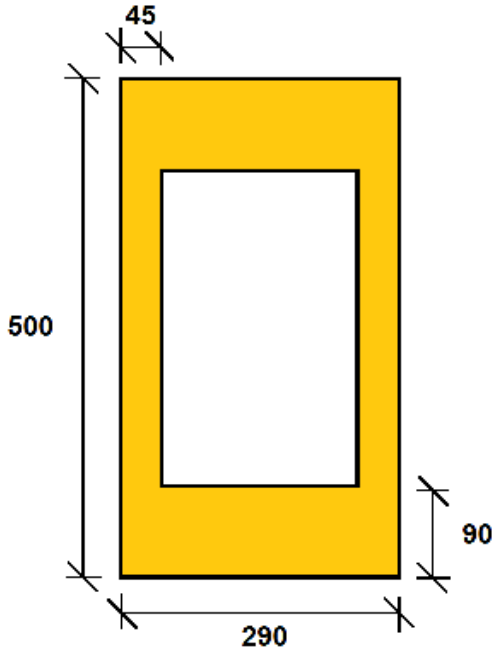

(b) Test 3

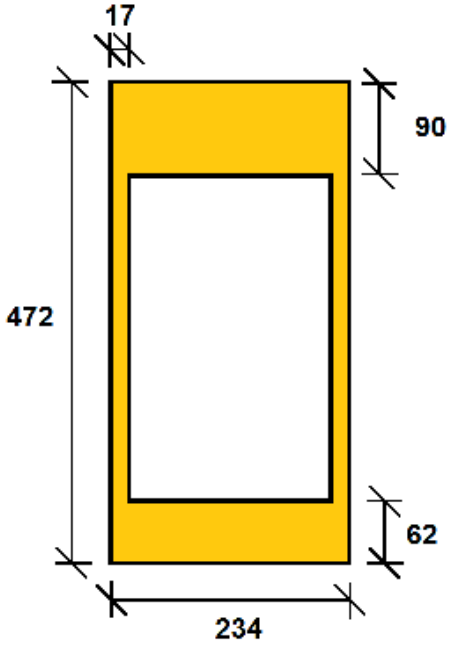

(c) Test 4

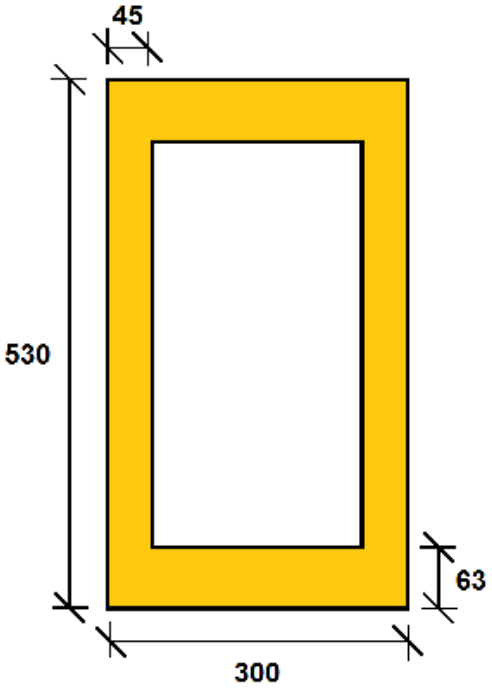

(d) Test 4

Figure 6.5 Cross section of LVL beams used in ambient temperature tests

N.B. Tension side shown at bottom

The webs and bottom flanges of the LVL beams used in Tests 2 and 4 were milled along the length of the beams. An LVL beam during the milling process is shown in Figure 6.6. Milling the webs and bottom flange simulated three sided charring that would occur in a fire if the top surface of the beam is not exposed to fire, e.g. protected by the floor above. The depth of the milling was 28 mm, which corresponds to the char layer depth for a 30 minute fire using an assumed char rate of 0.7 mm/min plus a zero strength layer of 7.0 mm.

Figure 6.6 Milling of LVL beams to simulate charring

Timber blocks were inserted into the beam cavity at each end of the beam to prevent web buckling, shown in Figure 6.7. These blocks were 90 mm thick and were fixed in place using timber screws through the webs. A hole was drilled in the timber insert to allow the tendon used in Test 2 to pass through. As the timber insert was outside the region being loaded it is not believed it impacted significantly on the behaviour of the beams and the results obtained, other than to prevent an undesirable and premature failure mode occurring.

Figure 6.7 Timber insert to prevent web buckling

The loading parameters used for each of the ambient temperature tests are shown in Table 6.1. These were specified so that a shear failure mode would occur for each test.

Table 6.1 Loading parameters for ambient temperature tests

Test	LVL Beam Span (m)	Spreader Beam Span (m)	Tendon Force (kN)
2	3.64	2.48	94
3	3.64	1.71	0
4	3.64	1.71	0
5	2.82	1.25	0

6.5 Testing Procedure

The LVL beams were placed on the spreader beam and secured to the strong floor using the steel restraint system. Load was applied to the LVL beam as the hydraulic loading platform was raised. A linear loading rate was set by the laboratory technician so the predicted failure load was reached after five minutes.

The load was applied until failure occurred. The point at which failure occurred was determined by observing loud cracking noises, large cracks forming in the LVL beam, rapid increase in mid-span deflection and an immediate drop in applied load. After all observations had been made the LVL beam was removed and the next test was prepared.

6.6 Predicted Behaviour

The performance of the LVL beams were again predicted using the simplified calculation method described in Chapter 4. The inputs used in the calculations were the known material properties, section dimensions and loading arrangements previously described.

The parameters that describe the behaviour of the LVL beam at the predicted failure load are presented in Tables 6.2 to 6.5 for the four tests. As the shear capacity is lower than shear demand for each test it is predicted that shear failure would occur.

Table 6.2 Behaviour parameters of Test 2 at predicted failure load

Parameter	**Demand**	**Capacity**
Failure load	$P^* = 106\ kN$	–
Bending demand	$M_q = 31\ kNm$	–
Hogging bending moment	$M_{PT} = -9\ kNm$	–
Bending	$M^* = 22\ kNm$	$\emptyset M_n = 80\ kNm$
Shear	$V^* = 53\ kN$	$\emptyset V_n = 52\ kN$
Axial	$N^* = 94\ kN$	$\emptyset N_n = 937\ kN$
Top flange compressive stress	$\sigma_{f,c} = 6\ MPa$	$f_c = 38\ MPa$
Bottom flange tensile stress	$\sigma_{f,t} = 11\ MPa$	$f_t = 31\ MPa$
Maximum compressive stress	$\sigma_{f,c,max} = 8\ MPa$	$f_b = 38\ MPa$
Maximum tensile stress	$\sigma_{f,t,max} = 11\ MPa$	$f_b = 38\ MPa$
Mid-span deflection	$\delta = 9\ mm$	–

Table 6.3 Behaviour parameters of Test 3 at predicted failure load

Parameter	Demand	Capacity
Failure load	$P^* = 364\ kN$	–
Bending demand	$M_q = 176\ kNm$	–
Hogging bending moment	$M_{PT} = 0\ kNm$	–
Bending	$M^* = 176\ kNm$	$\emptyset M_n = 315\ kNm$
Shear	$V^* = 182\ kN$	$\emptyset V_n = 182\ kN$
Axial	$N^* = 0\ kN$	$\emptyset N_n = 3078\ kN$
Top flange compressive stress	$\sigma_{f,c} = 15\ MPa$	$f_c = 38\ MPa$
Bottom flange tensile stress	$\sigma_{f,t} = 15\ MPa$	$f_t = 30\ MPa$
Maximum compressive stress	$\sigma_{f,c,max} = 18\ MPa$	$f_b = 36\ MPa$
Maximum tensile stress	$\sigma_{f,t,max} = 18\ MPa$	$f_b = 36\ MPa$
Mid-span deflection	$\delta = 13\ mm$	–

Table 6.4 Behaviour parameters of Test 4 at predicted failure load

Parameter	Demand	Capacity
Failure load	$P^* = 146\ kN$	–
Bending demand	$M_q = 70\ kNm$	–
Hogging bending moment	$M_{PT} = 0\ kNm$	–
Bending	$M^* = 70\ kNm$	$\emptyset M_n = 208\ kNm$
Shear	$V^* = 73\ kN$	$\emptyset V_n = 73\ kN$
Axial	$N^* = 0\ kN$	$\emptyset N_n = 1801\ kN$
Top flange compressive stress	$\sigma_{f,c} = 8\ MPa$	$f_c = 38\ MPa$
Bottom flange tensile stress	$\sigma_{f,t} = 10\ MPa$	$f_t = 31\ MPa$
Maximum compressive stress	$\sigma_{f,c,max} = 9\ MPa$	$f_b = 36\ MPa$
Maximum tensile stress	$\sigma_{f,t,max} = 11\ MPa$	$f_b = 36\ MPa$
Mid-span deflection	$\delta = 9\ mm$	–

Table 6.5 Behaviour parameters of Test 5 at predicted failure load

Parameter	**Demand**	**Capacity**
Failure load	$P^* = 392\ kN$	–
Bending demand	$M_q = 154\ kNm$	–
Hogging bending moment	$M_{PT} = 0\ kNm$	–
Bending	$M^* = 154\ kNm$	$\emptyset M_n = 300\ kNm$
Shear	$V^* = 196\ kN$	$\emptyset V_n = 196\ kN$
Axial	$N^* = 0\ kN$	$\emptyset N_n = 2818\ kN$
Top flange compressive stress	$\sigma_{f,c} = 14\ MPa$	$f_c = 38\ MPa$
Bottom flange tensile stress	$\sigma_{f,t} = 14\ MPa$	$f_t = 29\ MPa$
Maximum compressive stress	$\sigma_{f,c,max} = 16\ MPa$	$f_b = 36\ MPa$
Maximum tensile stress	$\sigma_{f,t,max} = 16\ MPa$	$f_b = 36\ MPa$
Mid-span deflection	$\delta = 8\ mm$	–

6.7 Experimental Results

6.7.1 Failure Modes and Crack Propagation

Shear failure occurred in each test, as demonstrated by the crack locations shown in Figures 6.8 to 6.11. The largest cracks in each test propagated from the end of the beam, which corresponds with shear failure occurring. The width and length of the cracks observed were proportional to the failure load of the beam, i.e. larger and longer cracks were observed in beams with higher failure loads.

(a) Crack locations observed in Test 2

(b) Major cracks observed in Test 2

Figure 6.8 Test 2 crack locations

(a) Crack locations observed in Test 3

(b) Major cracks observed in Test 3

Figure 6.9 Test 3 crack locations

(a) Crack locations observed for Test 4

(b) Major cracks observed in Test 4

Figure 6.10 Test 4 crack locations

(a) Crack locations observed for Test 5

(b) Major cracks observed in Test 5

Figure 6.11 Test 5 crack locations

6.7.2 Force–Deflection Behaviour

The force–deflection behaviour of each of the four tests is shown in Figures 6.12 to 6.15. Table 6.6 summarises the predicted elastic and actual mid-span deflection at failure and failure loads for each of the tests. Except for Test 4, the actual failure load was approximately 30% greater than what was predicted in the ambient temperature tests. This corresponded to a shear stress of approximately 7.0 MPa for these three tests, which is significantly higher than the characteristic value of 5.3 MPa. This is further discussed in Section 7.5. Similarly, the actual mid-span deflection at failure was significantly under predicted in all four tests, by as much as 170%. This is also further discussed in Section 7.5.

Table 6.6 Predicted and actual failure parameters

Test	Predicted Mid-span Deflection	Actual Mid-span Deflection	Predicted Failure Load	Actual Failure Load	Actual Failure Shear Stress
2	9 mm	22 mm	106 kN	138 kN	7.0 MPa
3	13 mm	24 mm	364 kN	473 kN	6.9 MPa
4	9 mm	16 mm	146 kN	147 kN	5.3 MPa
5	8 mm	21 mm	392 kN	515 kN	7.0 MPa

The predicted mid-span deflection at failure and failure load were both significantly under predicted in Test 2.

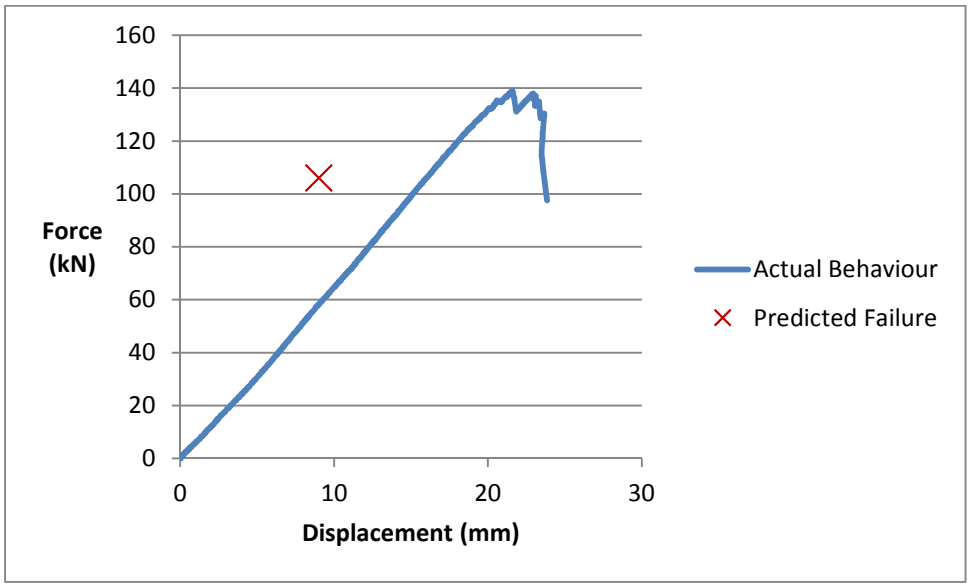

Figure 6.12 Force-deflection plot for Test 2

Again, the predicted mid-span deflection at failure and failure load were both significantly under predicted in Test 3. Once the applied load reached failure at 473kN the potentiometer became dislodged and no longer recorded the true displacement.

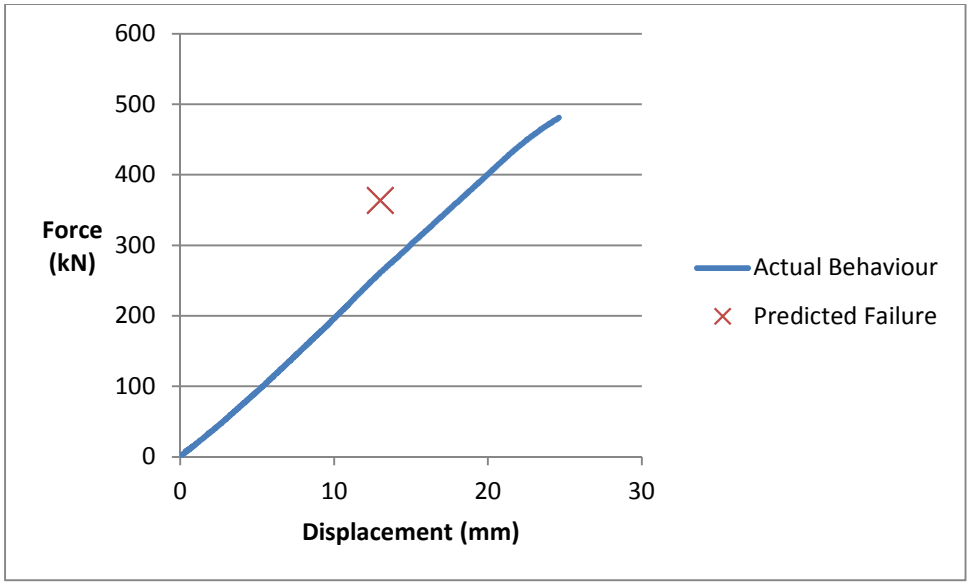

Figure 6.13 Force-deflection plot for Test 3

The predicted failure load for Test 4 was very close to the actual failure load. However, predicted mid-span deflection at failure was again significantly under predicted.

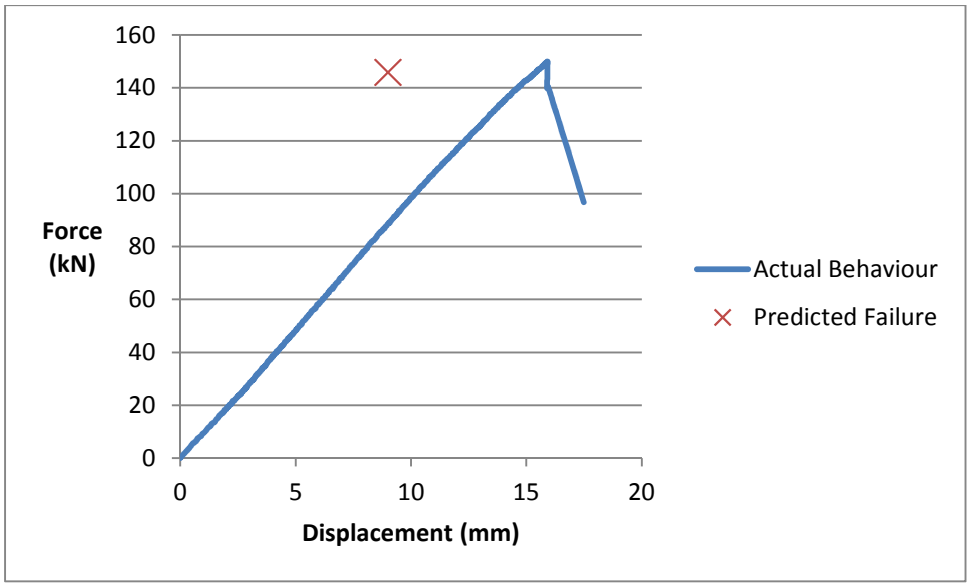

Figure 6.14 Force-deflection plot for Test 4

Similarly to Tests 2 and 3 the predicted mid-span deflection at failure and failure load were both significantly under predicted in Test 5.

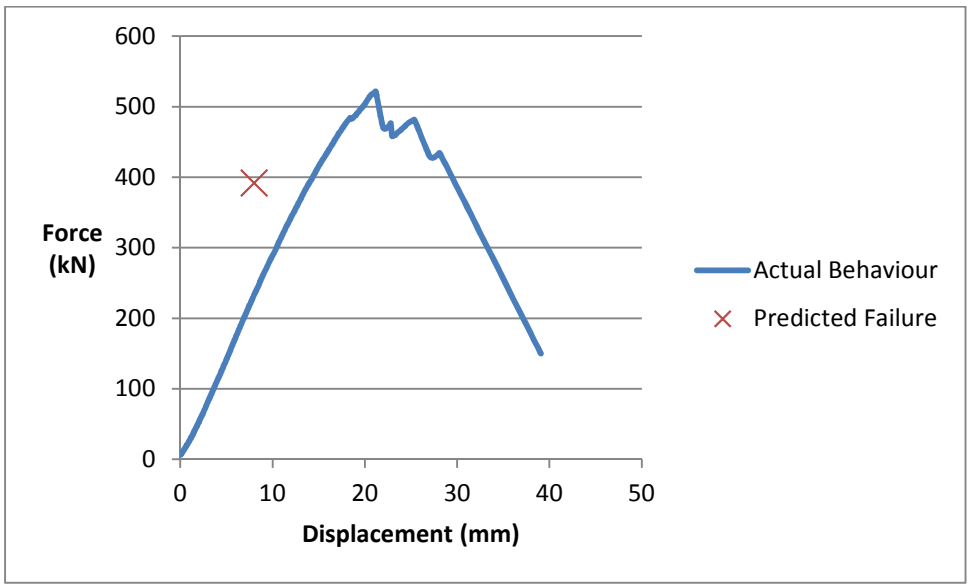

Figure 6.15 Force-deflection plot for Test 5

7 Discussion

Discussions of the key sections of this thesis are presented in this Chapter. Section 7.1 addresses the previous research completed on the fire performance of post-tensioned timber buildings. The fire resistance design of existing post-tensioned timber buildings is discussed in Section 7.2. The key assumptions and limitations of the simplified calculation method are discussed in Section 7.3. The furnace test and ambient temperature tests are discussed in Sections 7.4 and 7.5. Future research that is recommended to be undertaken is discussed in Section 0.

7.1 Previous Research

There is only limited previous research that has been conducted relating to the fire performance of post-tensioned timber buildings. Spellman (2012) has contributed the majority of published research in this area. An overview of his research is provided in Section 3.2.1.

The research conducted during this project used Spellman's work as a starting point and built on his findings. Spellman also proposed a calculation method for the fire performance of post-tensioned box beams. While both the simplified calculation method proposed in this thesis and Spellman's calculation method is based on the same calculation methodology, adopted from NZS3603:1992 (Standards New Zealand, 1993), the two methods vary in a number of key aspects. These aspects are discussed below.

Spellman's proposed design methodology is not presented in a way that can quickly and easily be adopted by a designer for use in practice. The inclusion of second order effects, such as axial bowing and beam end rotations, require a skill set and familiarity with structural mechanics that are greater than that of a typical practicing Fire Engineer. This is despite the fact that these effects have negligible effect on performance of the member so are not required to be used in practice. The unnecessary complexity of Spellman's method will only deter Fire Engineers from including the potential benefits of the post-tensioning system in a fire resistance design.

N.B. Further discussion of why the second order effects have a negligible effect on the performance of post-tensioned timber members is presented in Section 7.3.

Corner rounding was explicitly included in Spellman's calculation method. While this is valid and will provide a more accurate model of the actual behaviour of a timber member when exposed to fire, the assumed one-dimensional char rate in EN1995-1-2:2004 (European Commission, 2004b), which is used in the simplified calculation method proposed in this thesis, implicitly allows for corner rounding. Therefore, the inclusion of corner rounding is another complication that is not required in a simplified calculation method for use in practice so has not been included in the method proposed in this thesis.

The eccentricity of the tendon does not consider the deflection of the beam in Spellman's calculation method. This is not an accurate representation of the actual behaviour of a post-tensioned timber beam with a straight tendon. As the tendon is unbonded along its length it will remain stationary while the centroid of the timber beam changes, thus affecting the tendon eccentricity. Neglecting the beam deflection may have a significant impact on the predicted behaviour of a post-tensioned timber beam and should be included in a simplified calculation method.

Spellman did not consider tensile or compressive stress capacity of the flanges in his method. This is inadequate as the flanges may act as individual tension or compression members, as outlined in EN1995-1-1:2004 (European Commission, 2004a), and these should be checked in addition to the bending stress capacity.

Spellman outlined that shear failure was an important issue which required further research. This was a key reason why this research project was undertaken. There are two key aspects relating to shear failure that Spellman highlighted.

The first aspect of shear failure that Spellman discussed was that a post-tensioning system utilising straight tendons may result in shear failure occurring. This research supports this conclusion. However, this conclusion is not as important as previously thought and will not adversely affect the fire resistance of the member as a post-tensioning system can only potentially increase the fire resistance of a beam.

The failure mode of a member may change if post-tensioning is present. However, this will only occur if the fire resistance of the member has increased. For a member using straight tendons, the tendons will not resist any shear demand so the time for shear failure to occur will not change while a portion of the flexural demand will be resisted by the post-tensioning system, increasing the failure time for flexural demands. Shear failure will occur if the resistance provided by the post-tensioning system is sufficient to increase the predicted failure time of all flexural demands so that they are greater than the predicted shear failure time. Clearly, the increased likelihood of shear failure occurring correlates to an increased fire resistance of the member. Therefore, the risk of an increased likelihood of shear failure is not a serious issue and does not need addressing further.

The second issue regarding shear failure is the potential for shear failure to occur at the lower corner of box beams due to corner rounding reducing the shear area at the lower corners. This issue is not addressed in the simplified calculation method proposed in this thesis as corner rounding is not explicitly considered so the shear area in this region will not be less than in other areas. As such, shear strength at the lower corners does not need to be checked as part of the method proposed in this thesis. This is supported by the full scale furnace test where shear failure occurred in the web and not at the lower corners, despite corner rounding occurring. It is believed that shear failure at the lower corner will be confirmed to not be an issue through the development of a numerical model and the conduct of additional full scale furnace tests, as recommended in Section 0.

7.2 Existing Buildings

The post-tensioning systems used in the Pres-Lam buildings described in Section 3.5 are not specifically protected from fire. As such, the fire resistance design of these structures do not utilise the potential of the post-tensioning systems. While this was a conscious decision by the designers a contributing factor for this decision was the lack of published design methodology that could be followed that would allow the potential of the post-tensioning system to be utilised. This thesis will allow designers to consider the use of the post-tensioning system in fire resistance design, which may lead to more efficient structures and further uptake of Pres-Lam buildings.

7.3 Simplified Calculation Method

7.3.1 Second Order Effects

The purpose of the proposed simplified calculation method is to provide designers with a detailed method that can easily be used to design post-tensioned timber members for fire resistance. The simplified calculation method proposed in this thesis does not include rotation of anchorages, additional axial compression of the beam, axial bowing of the beam due to the eccentric tendon and flexural deflection of the beam due to the eccentric tendon. Introducing these second order effects would increase the complexity of the method, which would likely limit the uptake of method by designers. Therefore, it was desired that second order effects were not included. As such, it was assumed that second order effects had a negligible effect on the behaviour of post-tensioned timber members and so they were not included in the proposed simplified calculation method. This assumption is justified as the proposed method predicts behaviour of post-tensioned box beams with relatively good accuracy, as demonstrated by the full scale tests conducted as part of this research.

7.3.2 Tendon Temperature

The assumption that the tendon remains at ambient temperature throughout a fire was made to simplify the proposed calculation method and increase the likelihood of it being used by designers. The three reasons used to justify this are detailed below.

The depth of heated timber below the char layer is approximately 35 – 40 mm (Buchanan, 2001, Janssens and White, 1994). Therefore, the inside surface of the box beam, and so the tendon temperature, will not increase in temperature until there is very little timber remaining. This is likely to only occur after or close to failure occurring. This demonstrates that the time for heat transfer to the tendon occur is short, which will minimise the magnitude of the tendon temperature rise.

In order for the tendon temperature to increase heat transfer must occur from the inside surface of the box beam to the tendon through the air inside the cavity. The multiple phases of heat transfer required for heating of the tendon to occur will minimise the temperature rise in the tendon. This demonstrates that the magnitude of any temperature rise in the tendon will be negligible.

The failure time of beams has a low dependence on the post-tensioning force. For the beam considered in Appendix A the post-tensioning force can be reduced to approximately 450 kN, from the initial post-tensioning force of 1100 kN, before the failure time of the beam is reduced. This loss of post-tensioning force, which is approximately 60% is greater than what is expected to occur due to the heating of the tendon. This demonstrates that the tendon temperature will have a negligible effect on the performance of the beam.

The increase in tendon temperature that occurred during the full scale furnace test was unexpected. However, it is believe that this would not occur in other post-tensioned timber box beams. The reasons discussed above demonstrate that the assumption that the tendon remain at ambient temperature during a fire is valid.

7.3.3 Limitations

The intent of the simplified calculation method, i.e. to provide designers a detailed method that can easily be used to design post-tensioned timber members for fire resistance, has led to a number of assumptions being used, as discussed previously. As such, the proposed method does not model the behaviour of post-tensioned timber members with total accuracy. However, obtaining total accuracy would add significant complexity that would likely prevent designers from using the method. Therefore, the limitations introduced, such as assuming a one dimensional char rate and that second order effects have a negligible effect on the behaviour of the member, are valid.

7.4 Furnace Testing

7.4.1 Milling of Timber

As described in Section 5.4, timber was milled from the sides of the LVL beam at the supports. This was done to reduce the shear reinforcement provided by the extra thickness of timber that is not exposed to fire. However, this milled region did not extend all the way to the exposed surface so there was a region where the webs were full thickness. Preventing the milled region from being exposed to fire was intentional as a milled section that was exposed to fire would cause premature failure in the milled region. Therefore, the desired shear failure mechanism would not have occurred and the objective of the research would not have been achieved.

The shear cracks that occurred during failure of the beam, as described in Section 5.7.1, closed at the edge of the region of full thickness and did not propagate to the end of the beam, as desired. The extra thickness of the timber provided additional shear strength that prevented the shear cracks from propagating to the end of the beam. Therefore, the milling of the timber at the supports did not achieve its aim to prevent additional shear reinforcement at the supports. The shear strength of the beam is likely to be greater than it would have been without the thicker timber. The magnitude of this increase is hard to quantify but it is believed that it was not significant.

If a riskier methodology was used, i.e. a larger region was milled at the supports, shear failure where the cracks propagate to the end of the beam may be possible. The size of this area and the thickness of timber milled must be carefully detailed to prevent undesirable premature failure occurring, as detailed above.

The approach to mill the webs at the supports was a good idea, and could be used in future research into the shear performance of timber beams. However, this technique did not significantly affect the results obtained in the full scale furnace test.

7.4.2 Smoke Leakage

The smoke leakage that occurred was unexpected, as the beam was thought to be fully sealed. This has also not occurred in previous full scale furnace tests of LVL members with cavities. The smoke leakage resulted in an increase in tendon temperature and caused a small decrease in tendon force. However, the performance of the LVL beam was not significantly affected by the smoke leakage.

Potential causes of the smoke leakage include screw holes in beams created during manufacturing and gaps between flange and webs. This occurrence highlights the need to carefully detail all members where the post-tensioning system is being protected from exposure to fire, i.e. Strategy 2 is used, so that all potential sources of fire and smoke exposure are isolated.

7.4.3 Tendon Temperature

The increased tendon temperatures measured in the furnace test, which were likely caused by the smoke leakage previously described. This temperature increase did not affect the post-tensioning force significantly. Furthermore, the slight loss of post-tensioning force that did occur did not have a more than negligible effect on the performance of the beam. This demonstrates that the tendon temperature does not need to be considered in the simplified calculation method.

7.4.4 Validity of Simplified Calculation Method

The failure time predicted using the simplified calculation method was within one minute of the actual failure time. The simplified calculation method also predicted the failure mode of the beam. This is a very good result that is hard to improve. This result demonstrates the validity of the simplified calculation method proposed in this thesis.

It should be noted that only a single full-scale furnace test was conducted and the reproducibility of testing may result in variations to the accuracy of the predictions. However, it is expected that any differences between the calculation method and additional test results will be small.

The only area that requires further investigation and improvement is the mid-span deflection of the beam, which was under predicted. The variation between the predicted and actual mid-span deflections is not a major issue as the mid-span deflection is not an explicit criterion for the fire resistance of a beam. However, mid-span deflection is used within the proposed method and so requires further refinement.

7.5 Ambient Temperature Testing

7.5.1 Milling of Timber

The technique of milling that was used to "char" the specimens used in the ambient temperature testing is an effective method to accurately simulate furnace tests. The tolerance of the milling process was within 1 mm, which allowed the shear strength of the member to be accurately calculated. However, this technique is labour and time intensive and requires a skilled operator in addition to access to an appropriate machine to complete the work. The cost savings achieved by simulating a charred section using a milling machine, compared to the relatively high cost of conducting a full scale furnace test, must be considered when choosing a testing methodology.

7.5.2 Shear Strength

There were significant variations in the shear strengths of the beams used in the tests. The shear strength of the beams used in three tests was approximately 7.0 MPa, which is significantly higher than the nominal shear strength of the LVL used (5.3 MPa). The fact that the actual shear strength was greater than the characteristic shear strength was expected as the nominal strength is a 5% characteristic value, derived with 75% confidence, so the mean strength of the member is very likely to be higher. However, the magnitude of the increased shear strength was unexpected. van Beerschoten (2013) found that the characteristic shear strength of 45 mm LVL samples is 6.0 MPa, which is also lower than the shear strength of the beams used in the ambient temperature tests. Further investigation of the shear strength of LVL should be conducted.

7.5.3 Validity of Simplified Calculation Method

The four ambient temperature tests were specifically designed using the proposed simplified calculation method so that the beams fail in a shear failure mode. A shear failure mode was achieved in each of the four tests. This demonstrates that the simplified calculation method is an accurate method of predicting the behaviour of LVL box beams, with and without post-tensioning.

The failure loads were under predicted in three of the tests. This was a result of the actual shear strength of the LVL being higher than the nominal shear strength, which had been used as an input in the simplified calculation method to predict the failure load. Also, similar to the furnace test, the mid-span deflection was under predicted in the four ambient temperature tests. As discussed in Section 7.4.4 this issue is not critical but it is recommended that further investigation is conducted.

Overall, the results of the ambient temperature tests validate the simplified calculation method, especially the assumptions regarding second order effects.

7.6 Future Work

A numerical model of the behaviour of post-tensioned timber structures in fire conditions should be the main focus of future research on this subject. It is suggested that the model will build on research completed by Spellman (2012), O'Neill (2013) and van Beerschoten (2013). This model will allow further investigation of the failure modes of post-tensioned LVL box beams, including shear failure. Further validation of the simplified calculation method will also be possible, including assumptions that second order effects and increases in tendon temperature are negligible for design purposes. It will also allow further investigation of the under prediction of mid-span deflections when using the simplified calculation method. The numerical model could also be extended to include other structural members, such as post-tensioned columns, walls and diaphragms.

It is recommended that additional full scale tests of post-tensioned box beams are conducted. This is especially important if a numerical model, as described above, is developed as there is limited data that could be used to validate the model. It is recommended that full scale furnace tests are the preferred testing method, however, if cost dictates, ambient temperature tests will still be useful.

Further research is needed to investigate the shear strength of LVL box beams. The full scale testing showed that the shear strength of LVL decreases for thin sections. This is very relevant for box beams exposed to fire, especially slender box beams that utilise deep sections and thin webs.

8 Conclusions and Recommendations

8.1 Design for Fire Performance of Post-Tensioned Timber Buildings

The first major objective of this research was to develop a design strategy for the fire performance of post-tensioned timber buildings. This was completed in Chapters 2 and 3. The main conclusions drawn from this work are outlined below.

- Specific design considerations for the fire safety design of timber buildings are construction fire safety, early fire hazard and structural adequacy of timber members.
- The surface area of timber structural elements, not including the underside of timber floors, is relatively small and does not present a significant early fire hazard.
- There are two design strategies that can be used for the fire resistance design of post-tensioned timber structures:
    1. Use residual timber only to achieve structural adequacy fire resistance.
    2. Fire protect the post-tensioning system and include it in the fire resistance design.
- The strategy needs to be selected early in the design process and must be used throughout the design.
- Other structural elements that provide support to primary structural members under gravity loads, e.g. corbels, must also be considered during the fire safety design.
- Currently designed post-tensioned timber buildings do not use the post-tensioning system in the fire resistance design, i.e. follow the second design strategy.

8.2 Design for Fire Resistance of Post-Tensioned Timber Structures

The second major objective of this research was to develop a simplified calculation method for the fire resistance of post-tensioned timber box beams. This was completed in Chapter 4. The main conclusions drawn from this work are outlined below.

- A simplified calculation method based on fundamental structural mechanics can be used to accurately predict the behaviour of post-tensioned box beams and is appropriate for use in design.
- Protecting the post-tensioning system from fire exposure can significantly increase the capacity of a beam.

- Conversely, a post-tensioning system may not be required to achieve the FRR required for the structure
- Protecting the post-tensioning system can change the predicted failure mode from a bending or tensile failure mode to a shear failure mode.
- The capacity of the beam is not very sensitive to the post-tensioning force when the post-tensioning system is protected.
- The eccentricity of the tendon has a significant impact on the magnitude of the resistance to applied loads provided by the post-tensioning system. For beams with no initial eccentricity there will be very little benefit to protect the post-tensioning system.
- Shear failure of post-tensioned timber box beams does not need to be specifically considered other than performing strength checks as for other design actions.

8.3 Full Scale Testing

The third objective of this research was to investigate the fire performance and failure behaviour of post-tensioned box beams. The work conducted for this objective is described in Chapters 5 and 6. As well as studying the behaviour of the beams, the full scale tests enabled the simplified calculation method to be validated. The major conclusions from this work are outlined below.

- A shear failure mode occurred in each of the five test specimens. These are the first known occurrences of shear failure in LVL box beams. The shear failures occurred in the webs of the beams.
- The failure loads predicted using the simplified calculation method were reasonably close to the actual failure loads. This accuracy was achieved despite not considering second order effects or an increase in tendon temperature during the furnace test.
- The increased tendon temperatures measured in the furnace test did not affect the post-tensioning force significantly so had a negligible effect on the performance of the beam.
- The char depth during the furnace test was 25 mm, which corresponds to a char rate of 0.86 mm/min. The predicted char depth using the assumed char rate and zero strength layer was 28 mm. Therefore, the assumed char rate, 0.7 mm/min, and zero strength layer, 7 mm, was conservative and is recommended to be used in design.
- The mid-span deflections measured during the full scale tests were under-predicted by the simplified calculation method.

- The predicted failure loads were approximately 30% lower than the actual failure loads in three of the four ambient temperature tests. Correspondingly, the average shear strength of the beams in these three tests was approximately 7.0 MPa, significantly higher than the characteristic shear strength of 5.3 MPa.
- The milling technique that was used to simulate charring of the LVL beams is an effective method to accurately simulate furnace tests, although it is labour intensive.

8.4 Future Work

A number of recommendations for future work that should be completed to further develop this research are outlined below.

- A numerical model of the behaviour of post-tensioned timber structures in fire conditions should be the main focus of future research on this subject.
- It is recommended that additional full scale tests of post-tensioned box beams are conducted. Full scale furnace tests are the preferred testing method. However, if cost dictates, ambient temperature tests are useful.
- Further research is needed to investigate the shear strength of LVL box beams. Full scale furnace testing of LVL box beams are recommended.

References

ARDALANY, M., DEAM, B. & FRAGIACOMO, M. 2010. Numerical investigation of the load carrying capacity of laminated veneer lumber joists with holes. *World Conference on Timber Engineering 2010.* Trentino, Italy.

ARDALANY, M., FRAGIACOMO, M., DEAM, B. & CARRADINE, D. M. 2012. Effect of hole location on the load-carrying capacity of laminated veneer lumber beams. *Australian Journal of Structural Engineering,* 13**,** 231-242.

BLODGETT, O. W. 1966. *Design of Welded Structures,* Ohio, USA, James F. Lincoln Arc Welding Foundation.

BUCHANAN, A. H. 2001. *Structural Design for Fire Safety,* Chichester, England, John Wiley & Sons Ltd.

BUCHANAN, A. H. 2007. *Timber Design Guide,* Wellington, New Zealand, New Zealand Timber Industry Federation Inc.

BUCHANAN, A. H., PALERMO, A., CARRADINE, D. M. & PAMPANIN, S. 2011. Post-tensioned timber frame buildings. *The Structural Engineer,* 89**,** 24-30.

CRAFT, S. T., DESJARDINS, R. & MEHAFFEY, J. R. Investigation of the behaviour of CLT panels exposed to fire. *Conference Proceedings - Fire and Materials, 12th International Conference and Exhibtion* 2011. Interscience Communications Ltd, 441-454.

CRAFT, S. T., ISGOR, B., MEHAFFEY, J. R. & HADJISOPHOCLEOUS, G. Modelling Heat and Mass Transfer in Wood-frame Floor Assemblies Exposed to Fire. *Fire Safety Science - Proceedings of the Ninth International Symposium*, 2008. International Association for Fire Safety Science, 1303-1314.

DEPARTMENT OF BUILDING AND HOUSING 2011. B1/VM1. *Compliance Document for New Zealand Building Code, Clause B1, Structure.* Wellington, New Zealand: Department of Building and Housing.

DEPARTMENT OF BUILDING AND HOUSING 2012a. C/AS2. *Acceptable Solution for Buildings with Sleeping (non institutional).* Wellington, New Zealand: Department of Building and Housing.

DEPARTMENT OF BUILDING AND HOUSING 2012b. Extract from the New Zealand Building Code. *Clauses C1-C6 Protection from Fire.* Wellington, New Zealand: Department of Building and Housing.

EUROPEAN COMMISSION 2004a. EN 1995-1-1:2004. *Eurocode 5: Design of Timber Structures. Part 1.1: General - Common Rules and Rules for Buildings.* Brussels, Belgiuum: European Committee for Standardization.

EUROPEAN COMMISSION 2004b. EN 1995-1-2:2004. *Eurocode 5: Design of Timber Structures. Part 1.2: General - Structural Fire Design.* Brussels, Belgiuum: European Committee for Standardization.

FORMAN. 2010. *Kaowool* [Online]. www.forman.co.nz/products/Thermal_Insulation: Forman Building Systems. [Accessed September 2013].

FRANGI, A. & FONTANA, M. 2003. Charring rates and temperature profiles of wood sections. *Fire and Materials,* 27**,** 91-102.

HARMATHY, T. Z. 1970. Thermal properties of concrete at elevated temepratures. *ASTM Journal of Materials,* 5**,** 47-74.

HOPKIN, D. J. 2011. *The Fire Performance of Engineered Timber Products and Systems.* EngD Thesis, Loughborough University.

ISO 1975. ISO 834-1975 *Fire resistance tests - elements of building construction.* International Organization for Standarization.

JANSSENS, M. L. & WHITE, R. H. 1994. Temperature profiles in wood members exposed to fire. *Fire and Materials,* 18**,** 263-265.

LACHE, M. 1992. *Studies on the burning rate of solid wood and fire resistance glulam beams subject to bending,* Munich, Germany, Institute for Wood Research, University of Munich.

LANE, W. P. 2005. *Ignition, Charring and Structural Performance of Laminated Veneer Lumber.* MEFE Thesis, University of Canterbury.

MIKKOLA, E. 1990. Charring of Wood. *Research Report 689.* Helsinki, Finland: Technical Research Centre of Finland.

NELSON PINE INDUSTRIES LTD 2012. LVL Specific Engineering Design Guide Nelson, New Zealand.

NEWCOMBE, M. 2007. *Seismic Design of Multistory Post-Tensioned Timber Buildings.* ME Thesis, University of Pavia.

O'NEILL, J. 2008. *The Fire Performance of Timber-Concrete Composite Floors.* MEFE Thesis, University of Canterbury.

O'NEILL, J. 2013. *The Fire Performance of Timber Floors in Multi-Storey Buildings.* PhD Thesis, University of Canterbury.

PALERMO, A., PAMPANIN, S., BUCHANAN, A. H. & NEWCOMBE, M. Seismic Design of Multi-Storey Buildings using Laminated Veneer Lumber *New Zealand Society of Earthquake Engineering Conference*, 2005 Wairaki, New Zealand. 11-13.

PAMPANIN, S. 2005. Emerging Solutions for High Seismic Performance of Precast/Prestressed Concrete Buildings. *Journal of Advanced Concrete Technology,* 3**,** 207-223.

PARK, R. M., CARROLL, R. M., BLISS, P., BURNS, G. W., DESMARIS, R., HALL, F. B., HERZKOVITZ, M. B., MACKENZIE, D., MCGUIRE, E. F., REED, R. P., SPARKS, L. L. & WANG, T. P. 1993. *Manual on the use of thermocouples in temperature measurement*, ASTM.

PENG, L. 2010. *Performance of heavy timber connections in fire.* PhD Thesis. Carleton University.

PRIESTLEY, M. J. N., SRITHARAN, S., CONLEY, J. R. & PAMPANIN, S. 1999. Preliminary Results and Conclusions from the PRESSS Five-story Precast Concrete Test-Building. *PCI Journal,* 44**,** 42-67.

SP TECHNICAL RESEARCH INSTITUTE OF SWEDEN 2010. Fire safety in timber buildings. Technical guideline for Europe. Stockholm, Sweden: SP Technical Research Institute of Sweden.

SPEARPOINT, M. J. 2008. *Fire Engineering Design Guide,* Christchurch, New Zealand, New Zealand Centre For Advanced Engineering.

SPELLMAN, P. M. 2012. *The Fire Performance of Post-Tensioned Timber Beams.* MEFE Thesis, University of Canterbury.

SPELLMAN, P. M., ABU, A. K., CARRADINE, D. M., MOSS, P. J. & BUCHANAN, A. H. Design of Post-Tensioned Timber Beams for Fire Resistance. *In:* FONTANA, M., FRANGI, A. & KNOBLOCH, M., eds. *7th International Conference on Structures in Fire*, June 2012 2012 Zurich, Switzerland. ETH Zurich, 427-436.

STANDARDS NEW ZEALAND 1993. NZS 3603:1993 *Timber Structures Standard.* Wellington, New Zealand: Standards New Zealand.

STANDARDS NEW ZEALAND 2002a. AS/NZS 1170.0:2002 *Structural Design Actions Part 0: General principles.* Wellington, New Zealand: Standards New Zealand.

STANDARDS NEW ZEALAND 2002b. AS/NZS 1170.1:2002 *Structural Design Actions Part 1: Permanent, imposed and other actions.* Wellington, New Zealand: Standards New Zealand.

STANDARDS NEW ZEALAND 2007. NZS 4541:2007 *Automatic Fire Sprinkler Systems* Wellington, New Zealand: Standards New Zealand.

STANTON, J. F., STONE, W. C. & CHEOK, G. S. 1997. A hybrid reinforced precast frame for seismic regions. *PCI Journal,* 42**,** 20-32.

STIC. 2009. *Our Programme* [Online]. www.stic.co.nz/programme: Structural Timber Innovation Company. [Accessed September 2013].

STIC 2012a. *Technical Bulletin No. 1: Guidelines for Fire Safety on EXPAN Construction Sites,* Christchurch, New Zealand, Structural Timber Innovation Company.

STIC 2012b. *Technical Bulletin No. 2: Requirements Regarding Reaction-to-Fire Properties of Timber Used in the Construction and Finishing of Multi-Storey Timber Buildings in New Zealand,* Christchurch, New Zealand, Structural Timber Innovation Company.

STIC 2013. *Post-Tensioned Timber Buildings Design Guide,* Christchurch, New Zealand, Structural Timber Innovation Company.

TSAI, W. H. 2010. *Charring Rates for Different Cross Sections of Laminated Veneer Lumber (LVL).* MEFE Thesis, University of Canterbury.

VAN BEERSCHOTEN, W. 2013. *Structural Performance of Post-tensioned Timber Frames under Gravity Loading.* PhD Thesis, University of Canterbury.

WINSTONE WALLBOARDS. 2013. *GIB FYRELINE* [Online]. http://gib.co.nz/products/plasterboard/gib-fyreline/. [Accessed October 2013].

Appendix A: Design Example

The fire resistance design of a simply supported post-tensioned beam with a straight tendon is detailed below. The tendon has an initial eccentricity, e_0, of 220 mm, and the tendon force, F_{PT}, is 1,100 kN. The span of this beam is 8.6 m with a tributary width of 8.0 m. The cross section of the beam used is shown in Figure A.1. The timber is NelsonPine LVL13. These parameters were determined during the structural design of the beam. The design objective is to achieve a Fire Resistance Rating (FRR) of 30 minutes.

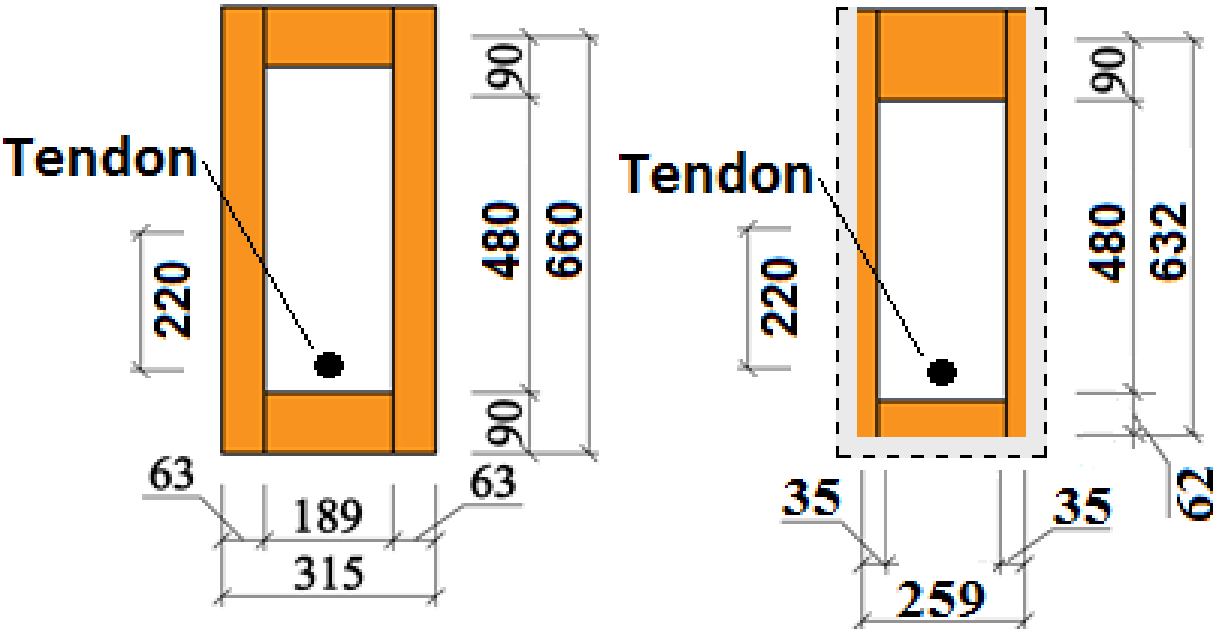

(a) Full section

(b) Residual cross section after 30 minute fire exposure

Figure A.1 Cross section of example post-tensioned timber box beam

Strategy 1: Residual Timber Only

The FRR will first be checked for a beam where the post-tensioning system is unprotected. Therefore, the post-tensioning system will not contribute to the strength of the beam.

First, the char depth, c_{30}, at 30 minutes is calculated.

$$c_i = \beta T_i + \gamma$$

$$c_{30} = 0.7 \times 30 + 7.0$$

$$c_{30} = 28\ mm$$

Next, the residual thickness of the top and bottom flanges, $t_{f,top,i}$ and $t_{f,bot,i}$, respectively, are calculated.

$$t_{f,top,i} = t_{f,top,0}$$

$$t_{f,top,30} = 90\ mm$$

$$t_{f,bot,i} = t_{f,bot,0} - c_i$$

$$t_{f,bot,30} = 90 - 28$$

$$t_{f,bot,30} = 62\ mm$$

Then the residual width of the flange, $w_{f,i}$, is calculated.

$$w_{f,i} = w_{f,0} - 2c_i$$

$$w_{f,30} = 315 - 2 \times 28$$

$$w_{f,30} = 259\ mm$$

Next, the residual thickness and internal depth of the webs, $t_{w,i}$ and $d_{w,i}$, respectively, are calculated.

$$t_{w,i} = t_{w,0} - c_i$$

$$t_{w,30} = 63 - 28$$

$$t_{w,30} = 35mm$$

$$d_{w,i} = d_{w,0}$$

$$d_{w,30} = 480\ mm$$

Following this, the residual depth of the section, D_i, is calculated.

$$D_i = D_0 - c_i$$

$$D_{30} = 660 - 28$$

$$D_{30} = 632\ mm$$

Next, the residual cross sectional and shear areas are calculated, A_i and $A_{s,i}$, respectively.

$$A_i = 2t_{w,i}d_{w,i} + w_{f,i}\left(t_{f,top,i} + t_{f,bot,i}\right)$$

$$A_{30} = 2 \times 35 \times 480 + 259(90 + 62)$$

$$A_{30} = 73.0 \times 10^3\ mm^2$$

$$A_{s,i} = \frac{2t_{w,i}I_i}{Q_i}$$

$$A_{s,30} = \frac{2 \times 35 \times I_{30}}{Q_{30}}$$

Then, the residual first moment of area, Q_i, is calculated.

$$Q_i = t_{f,top,i}w_{f,i}\left(\bar{y}_i - \frac{t_{f,top,i}}{2}\right) + t_{w,i}\left(\bar{y}_i - t_{f,top,i}\right)^2$$

$$Q_{30} = 90 \times 259\left(\bar{y}_i - \frac{90}{2}\right) + 35(\bar{y}_i - 90)^2$$

Next, the residual neutral axis depth, $\bar{y}_i$, is calculated.

$$\bar{y}_i = \frac{\left(t_{f,top,i}w_{f,i}\right)\left(\frac{t_{f,top,i}}{2}\right) + 2\left(t_{w,i}d_{w,i}\right)\left(t_{f,top,i} + \frac{d_{w,i}}{2}\right) + \left(t_{f,bot,i}w_{f,i}\right)\left(D_i - \frac{t_{f,bot,i}}{2}\right)}{\left(t_{f,top,i}w_{f,i}\right) + 2\left(t_{w,i}d_{w,i}\right) + \left(t_{f,bot,i}w_{f,i}\right)}$$

$$\bar{y}_{30} = \frac{(90 \times 259)\left(\frac{90}{2}\right) + 2(35 \times 480)\left(90 + \frac{480}{2}\right) + (62 \times 259)\left(632 - \frac{62}{2}\right)}{(90 \times 259) + 2(35 \times 480) + (62 \times 259)}$$

$$\bar{y}_{30} = 299\ mm$$

Next, the residual second moment of area, I_i, is calculated.

$$I_i = \Sigma I_{cc,x,i} + \Sigma A_{x,i}\left(\bar{y}_i - \bar{y}_{x,i}\right)^2$$

$$I_{30} = 3.66 \times 10^9\ mm^4$$

Now the residual first moment of area can be calculated.

$$Q_{30} = 90 \times 259\left(299 - \frac{90}{2}\right) + 35(299 - 90)^2$$

$$Q_{30} = 7.43 \times 10^6\ mm^3$$

$$A_{s,30} = \frac{2 \times 35 \times 3.66 \times 10^9}{7.43 \times 10^6}$$

$$A_{s,30} = 34.5 \times 10^3\ mm^2$$

This is followed by calculating, the residual section modulus, Z_i.

$$Z_i = \frac{W_i D_i^2}{6} - \frac{w_h d_h^2}{6}$$

$$Z_{30} = \frac{259 \times 632^2}{6} - \frac{189 \times 480^2}{6}$$

$$Z_{30} = 9.98 \times 10^6\ mm^3$$

Next, the residual bending, $\varphi M_{n,i}$, and shear, $\varphi V_{n,i}$, capacities of the beam are then calculated.

$$\varphi M_{n,i} = \varphi k_1 k_8 k_{24} f_b Z_i$$

$$\varphi M_{n,30} = 1.0 \times 1.0 \times 1.0 \times \left(\frac{95}{632}\right)^{0.167} \times 48.0 \times 9.98 \times 10^6$$

$$\varphi M_{n,30} = 349\ kNm$$

$$\varphi V_{n,i} = \varphi k_1 f_s A_{s,i}$$

$$\varphi V_{n,30} = 1.0 \times 1.0 \times 5.3 \times 34.5 \times 10^3$$

$$\varphi V_{n,30} = 183\ kN$$

Now the bending and shear demands on the beam are calculated. First the applied loads are determined.

$$q = G + \psi_l Q$$

$$q = 3.7 + 0.4 \times 3$$

$$q = 4.9\ kN/m^2$$

Next, the uniformly distributed load acting on the beam is calculated by multiplying the applied loads by the tributary width of the beam.

$$w = qW_{trib}$$

$$w = 4.9 \times 8.0$$

$$w = 39.2\ kN/m$$

Next, the maximum bending, M^*, and shear, V^*, demands on the beam at mid-span and at supports, respectively, are calculated.

$$M^* = \frac{wL^2}{8}$$

$$M^* = \frac{39.2 \times 8.6^2}{8}$$

$$M^* = 362\ kNm$$

$$V^* = \frac{wL}{2}$$

$$V^* = \frac{39.2 \times 8.6}{2}$$

$$V^* = 169\ kN$$

Following this, the residual bending and shear capacities of the beam are checked against the respective demands.

$$M^* \leq \varphi M_{n,30}$$

$$362\ kNm > 349\ kNm \qquad \textbf{NOT OK}$$

$$V^* \leq \varphi V_{n,30}$$

$$169\ kN \leq 183\ kN \qquad \textbf{OK}$$

Stress checks are completed next.

The mean flange compressive stress, $\sigma_{f,c,i}$, is calculated.

$$\sigma_{f,c,i} = \frac{M^* \left(\bar{y}_i\ -\ t_{f,top,i}/2\right)}{I_i}$$

$$\sigma_{f,c,30} = \frac{362 \times 10^6\ (299\ -\ 90/2)}{3.66 \times 10^9}$$

$$\sigma_{f,c,30} = 25.1\ MPa$$

Next, the residual compressive strength, $f_{c,i}$, is calculated.

$$f_{c,i} = \varphi k_1 k_8 f_c$$

$$f_{c,30} = 1.0 \times 1.0 \times 1.0 \times 38.0$$

$$f_{c,30} = 38.0\ MPa$$

Next, the mean flange compressive stress is checked against the residual compressive strength.

$$\sigma_{f,c,30} \leq f_{c,30}$$

$$25.1\ MPa \leq 38.0\ MPa \qquad \textbf{OK}$$

Then, the mean flange tensile stress, $\sigma_{f,t,i}$, is calculated.

$$\sigma_{f,t,i} = \frac{M^* \left(D_i\ -\ \bar{y}_i\ -\ t_{f,bot,i}/2\right)}{I_i}$$

$$\sigma_{f,t,30} = \frac{362 \times 10^6\ (632\ -\ 299 -\ 62/2)}{3.66 \times 10^9}$$

$$\sigma_{f,t,i} = 29.9\ MPa$$

Next, the residual tensile strength, $f_{t,i}$, is calculated.

$$f_{t,i} = \varphi k_1 k_4 k_{24} f_t$$

$$f_{t,30} = 1.0 \times 1.0 \times 1.0 \times \left(\frac{150}{259}\right)^{0.167} \times 33.0$$

$$f_{t,30} = 30.1\ MPa$$

Next, the mean flange tensile stress is checked against the residual strength.

$$\sigma_{f,t,30} \leq f_{t,30}$$

$$29.9\ MPa > 30.1\ MPa \qquad \textbf{OK}$$

Then, the maximum flange compressive stress, $\sigma_{f,c,max,i}$, is calculated.

$$\sigma_{f,c,max,i} = \frac{M^* \bar{y}_i}{I_i}$$

$$\sigma_{f,c,max,30} = \frac{362 \times 10^6 \times 299}{3.66 \times 10^9}$$

$$\sigma_{f,c,max,30} = 29.5\ MPa$$

Next, the residual bending strength, $f_{b,i}$, is calculated.

$$f_{b,i} = \varphi k_1 k_4 k_5 k_8 k_{24} f_b$$

$$f_{b,30} = 1.0 \times 1.0 \times 1.0 \times 1.0 \times 1.0 \times \left(\frac{95}{632}\right)^{0.167} \times 48.0$$

$$f_{b,30} = 35.0\ MPa$$

Next, the maximum flange compressive stress is then checked against the residual bending strength.

$$\sigma_{f,c,max,30} \leq f_{b,30}$$

$$29.5\ MPa \leq 35.0\ MPa \qquad \textbf{OK}$$

Next, the maximum tensile stress, $\sigma_{f,t,max,i}$, is calculated.

$$\sigma_{f,t,max,i} = \frac{M^* \, (D_i \, - \, \bar{y}_i \,)}{I_i}$$

$$\sigma_{f,t,max,30} = \frac{362 \times 10^6 \, (632 \, - \, 299)}{3.66 \times 10^9}$$

$$\sigma_{f,t,max,30} = 33.0 \, MPa$$

The residual bending strength, $f_{b,i}$, is unchanged.

Finally, the maximum flange tensile stress is then checked against the residual bending strength.

$$\sigma_{f,t,max,30} \leq f_{b,30}$$

$$33.0 \, MPa > 35.0 \, MPa \qquad \textbf{OK}$$

The beam DOES NOT achieve an FRR of 30 minutes.

The normalised demands acting on the beam have also been calculated across a range of timesteps. This is graphically represented in Figure A.2. This clearly demonstrates that the required FRR is not achieved as bending failure is predicted to occur prior to the required FRR.

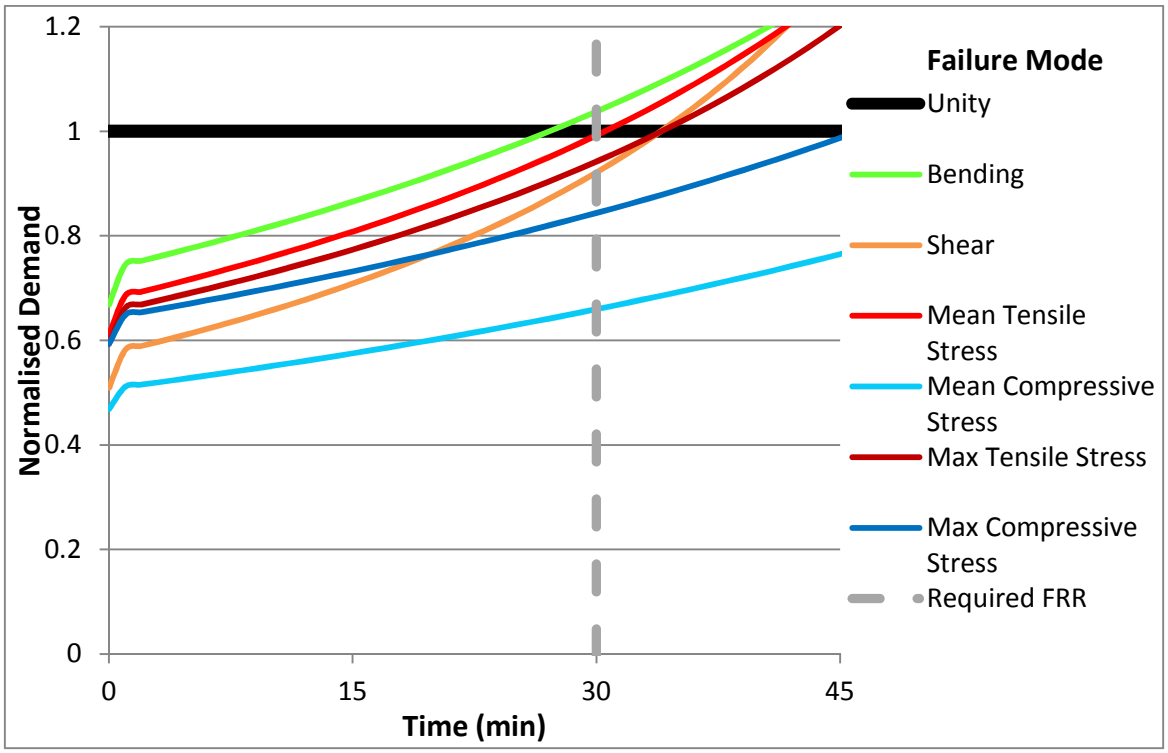

Figure A.2 Normalised demand for gravity beam with unprotected post-tensioning system

Strategy 2: Fire Protected Post-Tensioning System

The calculation process for Strategy 2 is largely similar to that used in Strategy 1. Again an FRR of 30 minutes is required so the calculations are performed at this time.

The shear and bending capacity of the member is unchanged at 30 minutes.

$$\varphi M_{n,30} = 349\ kNm$$

$$\varphi V_{n,30} = 183\ kN$$

The residual axial capacity of the beam, $\varphi N_{n,i}$, must also be calculated.

$$\varphi N_{n,i} = \varphi k_1 k_8 f_c A_i$$

$$\varphi N_{n,30} = 1.0 \times 1.0 \times 1.0 \times 38.0 \times 73.0 \times 10^3$$

$$\varphi N_{n,30} = 2{,}773\ kN$$

Next, the bending moment acting on the timber at mid-span, M_i^*, taking into account the resistance provided by the post-tensioning system, is calculated.

$$M_i^* = M_q - M_{PT,i}$$

This requires the bending moment that results from the uniformly distributed load, M_q, to be calculated.

$$M_q = \frac{wL^2}{8}$$

$$M_q = \frac{39.2 \times 8.6^2}{8}$$

$$M_q = 362\ kNm$$

Also, the bending moment due to the post-tensioning system, $M_{PT,i}$, is calculated.

$$M_{PT,i} = e_i F_{PT}$$

$$M_{PT,30} = e_{30} \times 1{,}100$$

This requires the eccentricity of the tendon, e_i, to be calculated.

$$e_i = e_0 + \Delta\bar{y}_i - \delta_i$$

$$e_{30} = 220 + \Delta\bar{y}_i - \delta_i$$

This requires the change in neutral axis depth, $\Delta\bar{y}_i$, to be calculated.

$$\Delta\bar{y}_i = \bar{y}_0 - \bar{y}_i$$

$$\Delta\bar{y}_{30} = 330 - 299$$

$$\Delta\bar{y}_{30} = 31\ mm$$

The mid-span deflection of the beam, δ_i, is also required and calculated.

$$\delta_i = \delta_{w,i} + \delta_{V,i} - \delta_{PT,i}$$

This requires the elastic deflection caused by gravity loads to be calculated.

$$\delta_{w,i} = \frac{5\mathrm{w}L^4}{384EI_i}$$

$$\delta_{w,30} = \frac{5 \times 39.2 \times 8{,}600^4}{384 \times 13.2 \times 10^3 \times 3.66 \times 10^9}$$

$$\delta_{w,30} = 58\ mm$$

The elastic shear deflection is also required and calculated.

$$\delta_{V,i} = \frac{wL^2}{8GA_{s,i}}$$

$$\delta_{V,30} = \frac{39.2 \times 8{,}600^2}{8 \times 660 \times 34.5 \times 10^3}$$

$$\delta_{V,30} = 16\ mm$$

The hogging deflection due to the post-tensioning system is also required and calculated.

$$\delta_{PT,i} = \frac{e_i F_{PT} L^2}{8EI_i}$$

$$\delta_{PT,30} = \frac{225 \times 1{,}100 \times 8{,}600^2}{8 \times 13.2 \times 10^3 \times 3.66 \times 10^9}$$

$$\delta_{PT,30} = 48\ mm$$

N.B. An iterative calculation is required to determine e_i and $\delta_{PT,i}$

Now the mid-span deflection can be calculated.

$$\delta_{30} = 58 + 16 - 48$$

$$\delta_{30} = 26\ mm$$

The eccentricity can also be calculated.

$$e_{30} = 220 + 31 - 26$$

$$e_{30} = 225\ mm$$

Consequently, the bending moment due to the post-tensioning system can also be calculated.

$$M_{PT,30} = 225 \times 1{,}100$$

$$M_{PT,30} = 248\ kNm$$

The bending moment acting on the timber at mid-span can then be calculated.

$$M_{30}^{*} = M_q - M_{PT,30}$$

$$M_{30}^{*} = 362 - 248$$

$$M_{30}^{*} = 114\ kNm$$

The shear strength at the supports, i.e. the point of maximum shear force, is unchanged from Strategy 1.

$$V^{*} = 169\ kN$$

Next, the axial demand on the beam, N^{*}, is determined.

$$N^{*} = F_{PT}$$

$$N^{*} = 1{,}100\ kN$$

Now, the residual bending and shear capacities of the beam are checked against the respective demands.

$$M^{*} \leq \varphi M_{n,30}$$

$$114\ kNm \leq 349\ kNm \qquad \textbf{OK}$$

$$V^{*} \leq \varphi V_{n,30}$$

$$169\ kN \leq 183\ kN \qquad \textbf{OK}$$

The residual axial capacity of the section is also checked.

$$N^* \leq \varphi N_n$$

$$1{,}100\ kN \leq 2{,}773\ kN \qquad \textbf{OK}$$

A combined bending-compression check is also performed.

$$\frac{N^*}{\emptyset N_n} + \frac{M^*}{\emptyset M_n} \leq 1.0$$

$$\frac{1{,}100}{2{,}773} + \frac{114}{349} \leq 1.0$$

$$0.40 + 0.33 \leq 1.0$$

$$0.72 \leq 1.0 \qquad \textbf{OK}$$

Stress checks are completed next.

The mean flange compressive stress, $\sigma_{f,c,i}$, is calculated.

$$\sigma_{f,c,i} = \frac{M^* \left(\bar{y}_i - t_{f,top,i}/2\right)}{I_i}$$

$$\sigma_{f,c,30} = \frac{114 \times 10^6\ (299 - 90/2)}{3.66 \times 10^9}$$

$$\sigma_{f,c,30} = 7.9\ MPa$$

The residual compressive strength, $f_{c,i}$, is unchanged from Strategy 1.

$$f_{c,30} = 38.0\ MPa$$

Next, the mean flange compressive stress is checked against the residual compressive strength.

$$\sigma_{f,c,30} \leq f_{c,30}$$

$$7.9\ MPa \leq 38.0\ MPa \qquad \textbf{OK}$$

Next, the mean flange tensile stress, $\sigma_{f,t,i}$, is calculated.

$$\sigma_{f,t,i} = \frac{M^* \left(D_i - \bar{y}_i - t_{f,bot,i}/2\right)}{I_i}$$

$$\sigma_{f,t,30} = \frac{114 \times 10^6 \ (632 - 299 - 62/2)}{3.66 \times 10^9}$$

$$\sigma_{f,t,i} = 9.5 \ MPa$$

The residual tensile strength, $f_{t,i}$, is unchanged from Strategy 1.

$$f_{t,30} = 30.1 \ MPa$$

Next, the mean flange tensile stress is then checked against the residual strength.

$$\sigma_{f,t,30} \leq f_{t,30}$$

$$9.5 \ MPa \leq 30.1 \ MPa \qquad \textbf{OK}$$

Next, the maximum flange compressive stress, $\sigma_{f,c,max,i}$, is calculated.

$$\sigma_{f,c,max,i} = \frac{M^* \ \bar{y}_i}{I_i}$$

$$\sigma_{f,c,max,30} = \frac{114 \times 10^6 \ \times 299}{3.66 \times 10^9}$$

$$\sigma_{f,c,max,30} = 9.4 \ MPa$$

The residual bending strength, $f_{b,i}$, is unchanged from Strategy 1.

$$f_{b,30} = 35.0 \ MPa$$

Next, the maximum flange compressive stress is then checked against the residual bending strength.

$$\sigma_{f,c,max,30} \leq f_{b,30}$$

$$9.4 \ MPa \leq 35.0 \ MPa \qquad \textbf{OK}$$

The maximum tensile stress, $\sigma_{f,t,max,i}$, is calculated.

$$\sigma_{f,t,max,i} = \frac{M^* \, (D_i \, - \, \bar{y}_i \,)}{I_i}$$

$$\sigma_{f,t,max,30} = \frac{114 \times 10^6 \, (632 \, - \, 299)}{3.66 \times 10^9}$$

$$\sigma_{f,t,max,30} = 10.4 \, MPa$$

The residual bending strength, $f_{b,i}$, is unchanged.

Finally, the maximum flange tensile stress is then checked against the residual bending strength.

$$\sigma_{f,t,max,30} \leq f_{b,30}$$

$$10.4 \, MPa \leq 35.0 \, MPa \qquad \textbf{OK}$$

Therefore, the beam achieves an FRR of 30 minutes.

Again, the normalised demands acting on the beam have also been calculated across a range of timesteps. This is graphically represented in Figure A.3. This clearly demonstrates that the required FRR is achieved.

It is also worth noting that the predicted failure mode has changed from bending failure to shear failure. This appears to be a bad result. However, the shear strength of the beam has not decreased. On the contrary, the FRR of the beam has increased from approximately 27 minutes to 34 minutes, a 26% increase in the FRR. This demonstrates that while the probability of shear failure occurring in a post-tensioned timber box beam may be increased compared to a timber box beam without a post-tensioning system, the shear strength of a post-tensioned timber box beam is not decreased. Furthermore, fire resistance can only be increased by the presence of a post-tensioning system.

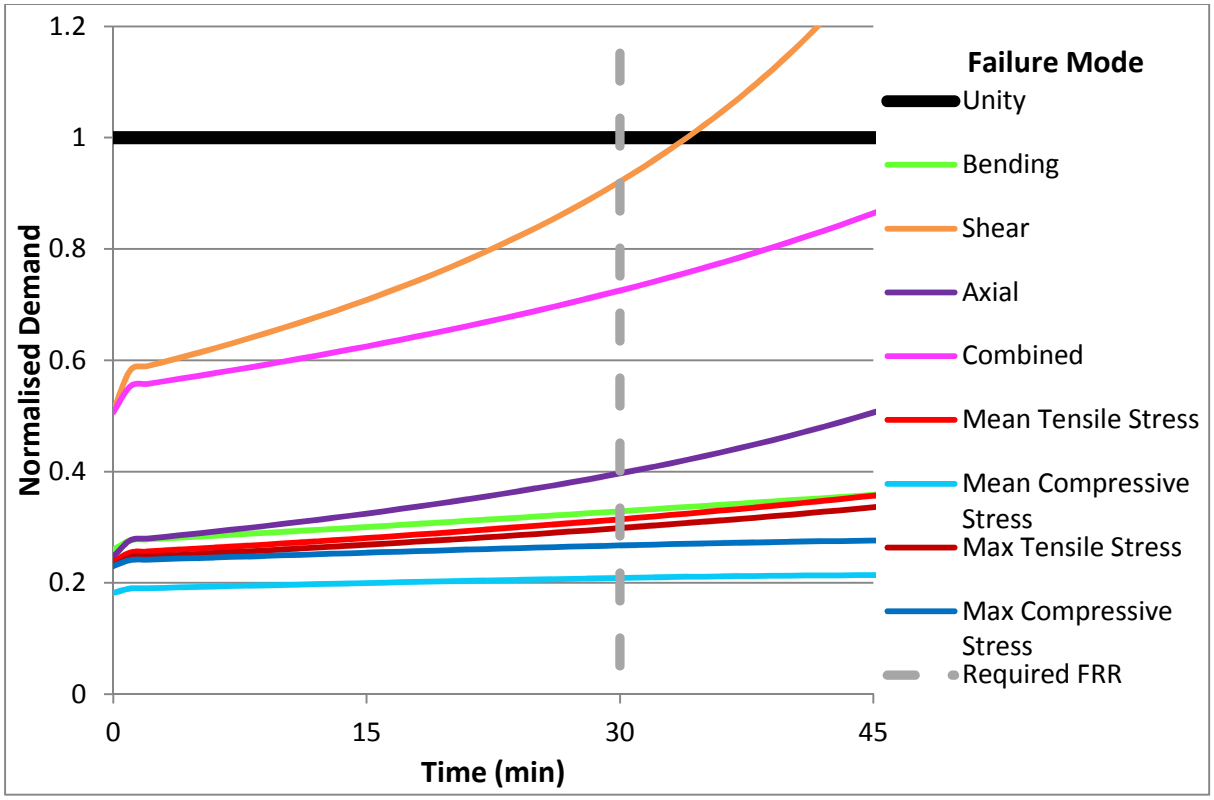

Figure A.3 Normalised demand for gravity beam with protected post-tensioning system